

**ISTANBUL TECHNICAL UNIVERSITY ★ INSTITUTE OF SCIENCE AND TECHNOLOGY**

**ALKYLATED POLY(ETHYLENEIMINE) LIGANDS IN HOMOGENEOUS  
ATOM TRANSFER RADICAL POLYMERIZATION**

**M. Sc. Thesis by**

**Artun ZORVARYAN**

**Department: Polymer Science and Technology**

**Programme: Polymer Science and Technology**

**Supervisor: Prof.Dr. Metin H. ACAR**

**JUNE 2008**

**ALKYLATED POLY(ETHYLENEIMINE) LIGANDS IN HOMOGENEOUS  
ATOM TRANSFER RADICAL POLYMERIZATION**

**M. Sc. Thesis by  
Artun ZORVARYAN  
(515061001)**

**Date of submission : 5 May 2008  
Date of Defence Examination : 10 June 2008**

**Supervisor : Prof. Dr. Metin H. ACAR**

**Members of Examining Committee : Prof. Dr. Ümit TUNCA (I.T.U.)**

**Assoc. Prof. Dr. A. Ersin ACAR (B.U.)**

**JUNE 2008**

**İSTANBUL TEKNİK ÜNİVERSİTESİ ★ FEN BİLİMLERİ ENSTİTÜSÜ**

**HOMOJEN ATOM TRANSFER RADİKAL POLİMERİZASYONU İÇİN  
ALKİLLENMİŞ POLİ(ETİLENİMİN) LİGANDLAR**

**YÜKSEK LİSANS TEZİ  
Artun ZORVARYAN  
(515061001)**

**Tezin Enstitüye Verildiği Tarih : 5 Mayıs 2008  
Tezin Savunulduğu Tarih : 10 Haziran 2008**

**Tez Danışmanı : Prof. Dr. Metin H. ACAR (İ.T.Ü.)**

**Diğer Jüri Üyeleri : Prof. Dr. Ümit TUNCA (İ.T.Ü)**

**Doç. Dr. A. Ersin ACAR (B.Ü.)**

**HAZİRAN 2008**

## **ACKNOWLEDGEMENT**

This master study has been carried out at Istanbul Technical University, Chemistry Department of Science & Letters Faculty.

I would like to express my gratitude to my supervisor Prof. Dr. Metin H. ACAR for his invaluable help, patience and helpful critics throughout in this research.

I especially thank to my colleagues RA&TA Şebnem İNCEOĞLU, M.Sc. Leyla BAYKAL, and Nergiz BOZOK for their tolerance and supportive attitudes during my laboratory study.

I am also grateful to my family for their moral support and understanding during all stages involved in the preparation of this research.

JUNE 2008

Artun ZORVARYAN

## TABLE OF CONTENTS

<b>ACKNOWLEDGEMENT</b>	<b>ii</b>
<b>LIST OF ABBREVIATIONS</b>	<b>v</b>
<b>LIST OF TABLES</b>	<b>vi</b>
<b>LIST OF FIGURES</b>	<b>vii</b>
<b>SUMMARY</b>	<b>xi</b>
<b>ÖZET</b>	<b>xii</b>
<b>1. INTRODUCTION</b>	<b>1</b>
<b>2. THEORETICAL SECTION</b>	<b>2</b>
2.1. Atom Transfer Radical Polymerization (ATRP)	2
2.1.1. Kinetics of ATRP	3
2.1.2. The function of components for ATRP and reaction conditions	6
2.1.3. Monomers	6
2.1.4. Initiators	6
2.1.5. Ligands	7
2.1.6. Transition metal complexes	9
2.1.7. Solvent	10
2.1.8. Temperature and reaction time	10
2.2. Poly(ethyleneimine)	10
<b>3. EXPERIMENTAL PART</b>	<b>12</b>
3.1. Chemicals	12
3.2. Synthesis of Alkylated Poly(ethyleneimine) (APEI)	12
3.2.1. Synthesis of ethylated poly(ethyleneimine) (EPEI)	12
3.2.2. Synthesis of butylated poly(ethyleneimine) (BPEI)	13
3.3. Polymerization of Styrene	13
3.4. Polymerization of Methyl Methacrylate	13
3.5. Characterization	14
<b>4. RESULTS AND DISCUSSION</b>	<b>15</b>
4.1. Synthesis of Ethylated Poly(ethyleneimine) (EPEI)	15
4.2. Synthesis of Butylated Poly(ethyleneimine) (BPEI)	16
4.3. ATRP of Styrene for Different APEI Ratios	17
4.3.1. Using ethylated poly(ethyleneimine) (EPEI)	17
4.3.2. Using butylated poly(ethyleneimine) (BPEI)	21
4.4. ATRP of Methyl Methacrylate for Different BPEI Ratios	25
<b>5. CONCLUSION AND RECOMMENDATIONS</b>	<b>30</b>

<b>REFERENCES</b>	<b>31</b>
<b>APPENDIX A</b>	<b>36</b>
<b>APPENDIX B</b>	<b>47</b>
<b>APPENDIX C</b>	<b>55</b>
<b>AUTOBIOGRAPHY</b>	<b>63</b>

## LIST OF ABBREVIATIONS

<b>ATRP</b>	: Atom Transfer Radical Polymerization
<b>St</b>	: Styrene
<b>MMA</b>	: Methyl Methacrylate
<b>PMDETA</b>	: N,N,N',N'',N'''-pentamethyldiethylenetriamine
<b>HMTETA</b>	: 1,1,4,7,10,10-hexamethyltriethylenetetramine
<b>ALAL</b>	: Alkylated linear amine ligand
<b>DMF</b>	: Dimethyl formamide
<b>EBrIB</b>	: Ethyl-2-bromoisobutyrate
<b>EBrP</b>	: Ethyl-2-bromopropionate
<b>EPEI</b>	: Ethylated polyethyleneimine
<b>BPEI</b>	: Butylated polyethyleneimine
<b>GC</b>	: Gas chromatography
<b>GPC</b>	: Gel permeation chromatography
<b>NMR</b>	: Nuclear magnetic resonance

## LIST OF TABLES

	<u>Page No</u>
<b>Table 2.1</b>	The most frequently used initiator types in ATRP systems .....
<b>Table 4.1</b>	ATRP of Styrene for different ligand (EPEI) ratios.....
<b>Table 4.2</b>	ATRP of Styrene for different ligand (BPEI) ratios.....
<b>Table 4.3</b>	ATRP of Styrene for Different Amine Ligand.....
<b>Table 4.4</b>	ATRP of Methyl Methacrylate for different ligand (BPEI) ratios
<b>Table 5.5</b>	ATRP of Methyl Methacrylate for Different Amine Ligands.....

## LIST of FIGURES

	<u>Page No</u>
<b>Figure 2.1</b> : Kinetic plot and conversion vs. time plot for ATRP.....	4
<b>Figure 4.1</b> : Synthesis of ethylated poly(ethyleneimine) (EPEI).....	15
<b>Figure 4.2</b> : $^1\text{H}$ NMR spectrum of EPEI in $\text{CDCl}_3$ .....	15
<b>Figure 4.3</b> : Synthesis of butylated poly(ethyleneimine) (BPEI).....	16
<b>Figure 4.4</b> : $^1\text{H}$ NMR spectrum of BPEI in $\text{CDCl}_3$ .....	16
<b>Figure 4.5</b> : ATRP of styrene by using APEI Ligands.....	17
<b>Figure 4.6</b> : $[\text{EPEI}]/[\text{CuBr}]$ versus $k_p^{app}$ for ATRP of Styrene $[\text{St}]: 5.70 \text{ mol L}^{-1}$ in anisole at $110^\circ\text{C}$ $[\text{St}]_0/[\text{EBrP}]_0/[\text{CuBr}]_0/[\text{EPEI}]_0 = 200/1/1/x$ . ....	19
<b>Figure 4.7</b> : $[\text{BPEI}]/[\text{CuBr}]$ versus $k_p^{app}$ for ATRP of Styrene $[\text{St}]: 5.7 \text{ mol L}^{-1}$ in toluene at $110^\circ\text{C}$ . $[\text{St}]_0/[\text{EBrP}]_0/[\text{CuBr}]_0/[\text{BPEI}]_0 = 200/1/1/x$ ....	22
<b>Figure 4.8</b> : ATRP of methyl methacrylate by using BPEI ligand.....	25
<b>Figure 4.9</b> : $[\text{BPEI}]/[\text{CuBr}]$ versus $k_p^{app}$ for ATRP of Methyl Methacrylate at $80^\circ\text{C}$ . $[\text{MMA}]: 4.60 \text{ mol L}^{-1}$ in anisole $[\text{MMA}]_0/[\text{EBrIB}]_0/[\text{CuBr}]_0/[\text{BPEI}]_0 = 200/1/1/x$ .....	27
<b>Figure A.1</b> : Kinetic plot of St by ATRP using EPEI at $110^\circ\text{C}$ $[\text{St}]: 5.7 \text{ mol L}^{-1}$ in anisole $[\text{St}]_0/[\text{EBrP}]_0/[\text{CuBr}]_0/[\text{EPEI}]_0 = 200/1/1/0.30$ .....	36
<b>Figure A.2</b> : Kinetic plot of St by ATRP using EPEI at $110^\circ\text{C}$ $[\text{St}]: 5.7 \text{ mol L}^{-1}$ in anisole $[\text{St}]_0/[\text{EBrP}]_0/[\text{CuBr}]_0/[\text{EPEI}]_0 = 200/1/1/0.45$ .....	36
<b>Figure A.3</b> : Kinetic plot of St by ATRP using EPEI at $110^\circ\text{C}$ $[\text{St}]: 5.7 \text{ mol L}^{-1}$ in anisole $[\text{St}]_0/[\text{EBrP}]_0/[\text{CuBr}]_0/[\text{EPEI}]_0 = 200/1/1/0.60$ .....	37
<b>Figure A.4</b> : Kinetic plot of St by ATRP using EPEI at $110^\circ\text{C}$ $[\text{St}]: 5.7 \text{ mol L}^{-1}$ in anisole $[\text{St}]_0/[\text{EBrP}]_0/[\text{CuBr}]_0/[\text{EPEI}]_0 = 200/1/1/0.75$ .....	37
<b>Figure A.5</b> : Kinetic plot of St by ATRP using EPEI at $110^\circ\text{C}$ $[\text{St}]: 5.7 \text{ mol L}^{-1}$ in anisole $[\text{St}]_0/[\text{EBrP}]_0/[\text{CuBr}]_0/[\text{EPEI}]_0 = 200/1/1/1.00$ .....	38
<b>Figure A.6</b> : Kinetic plot of St by ATRP using EPEI at $110^\circ\text{C}$ $[\text{St}]: 5.7 \text{ mol L}^{-1}$ in anisole $[\text{St}]_0/[\text{EBrP}]_0/[\text{CuBr}]_0/[\text{EPEI}]_0 = 200/1/1/1.25$ .....	38
<b>Figure A.7</b> : Kinetic plot of St by ATRP using BPEI at $110^\circ\text{C}$ $[\text{St}]: 5.7 \text{ mol L}^{-1}$ in toluene $[\text{St}]_0/[\text{EBrP}]_0/[\text{CuBr}]_0/[\text{BPEI}]_0 = 200/1/1/0.15$ .....	39
<b>Figure A.8</b> : Kinetic plot of St by ATRP using BPEI at $110^\circ\text{C}$ $[\text{St}]: 5.7 \text{ mol L}^{-1}$ in toluene $[\text{St}]_0/[\text{EBrP}]_0/[\text{CuBr}]_0/[\text{BPEI}]_0 = 200/1/1/0.30$ .....	39
<b>Figure A.9</b> : Kinetic plot of St by ATRP using BPEI at $110^\circ\text{C}$ $[\text{St}]: 5.7 \text{ mol L}^{-1}$ in toluene $[\text{St}]_0/[\text{EBrP}]_0/[\text{CuBr}]_0/[\text{BPEI}]_0 = 200/1/1/0.45$ .....	40
<b>Figure A.10</b> : Kinetic plot of St by ATRP using BPEI at $110^\circ\text{C}$ $[\text{St}]: 5.7 \text{ mol L}^{-1}$ in toluene $[\text{St}]_0/[\text{EBrP}]_0/[\text{CuBr}]_0/[\text{BPEI}]_0 = 200/1/1/0.60$ .....	40
<b>Figure A.11</b> : Kinetic plot of St by ATRP using BPEI at $110^\circ\text{C}$ $[\text{St}]: 5.7 \text{ mol L}^{-1}$ in toluene $[\text{St}]_0/[\text{EBrP}]_0/[\text{CuBr}]_0/[\text{BPEI}]_0 = 200/1/1/0.75$ .....	41
<b>Figure A.12</b> : Kinetic plot of St by ATRP using BPEI at $110^\circ\text{C}$ $[\text{St}]: 5.7 \text{ mol L}^{-1}$ in toluene $[\text{St}]_0/[\text{EBrP}]_0/[\text{CuBr}]_0/[\text{BPEI}]_0 = 200/1/1/1.00$ .....	41
<b>Figure A.13</b> : Kinetic plot of St by ATRP using BPEI at $110^\circ\text{C}$ $[\text{St}]: 5.7 \text{ mol L}^{-1}$ in toluene $[\text{St}]_0/[\text{EBrP}]_0/[\text{CuBr}]_0/[\text{BPEI}]_0 = 200/1/1/1.25$ .....	42

<b>Figure A.14</b> : Kinetic plot of St by ATRP using BPEI at 110 °C [St]: 5.7 mol L <sup>-1</sup> in toluene [St] <sub>o</sub> /[EBrP] <sub>o</sub> /[CuBr] <sub>o</sub> /[BPEI] <sub>o</sub> =200/1/1/2.00.....	42
<b>Figure A.15</b> : Kinetic plot of MMA by ATRP using BPEI at 80 °C. [MMA] <sub>o</sub> /[EBrIB] <sub>o</sub> /[CuBr] <sub>o</sub> /[BPEI] <sub>o</sub> =200/1/1/0.15 [MMA]:4.60 mol L <sup>-1</sup> in anisole.....	43
<b>Figure A.16</b> : Kinetic plot of MMA by ATRP using BPEI at 80 °C. [MMA] <sub>o</sub> /[EBrIB] <sub>o</sub> /[CuBr] <sub>o</sub> /[BPEI] <sub>o</sub> =200/1/1/0.30 [MMA]:4.60 mol L <sup>-1</sup> in anisole.....	43
<b>Figure A.17</b> : Kinetic plot of MMA by ATRP using BPEI at 80 °C. [MMA] <sub>o</sub> /[EBrIB] <sub>o</sub> /[CuBr] <sub>o</sub> /[BPEI] <sub>o</sub> =200/1/1/0.45 [MMA]:4.60 mol L <sup>-1</sup> in anisole.....	44
<b>Figure A.18</b> : Kinetic plot of MMA by ATRP using BPEI at 80 °C. [MMA] <sub>o</sub> /[EBrIB] <sub>o</sub> /[CuBr] <sub>o</sub> /[BPEI] <sub>o</sub> =200/1/1/0.60 [MMA]:4.60 mol L <sup>-1</sup> in anisole.....	44
<b>Figure A.19</b> : Kinetic plot of MMA by ATRP using BPEI at 80 °C. [MMA] <sub>o</sub> /[EBrIB] <sub>o</sub> /[CuBr] <sub>o</sub> /[BPEI] <sub>o</sub> =200/1/1/0.75 [MMA]:4.60 mol L <sup>-1</sup> in anisole.....	45
<b>Figure A.20</b> : Kinetic plot of MMA by ATRP using BPEI at 80 °C. [MMA] <sub>o</sub> /[EBrIB] <sub>o</sub> /[CuBr] <sub>o</sub> /[BPEI] <sub>o</sub> =200/1/1/1.00 [MMA]:4.60 mol L <sup>-1</sup> in anisole.....	45
<b>Figure A.21</b> : Kinetic plot of MMA by ATRP using BPEI at 80 °C. [MMA] <sub>o</sub> /[EBrIB] <sub>o</sub> /[CuBr] <sub>o</sub> /[BPEI] <sub>o</sub> =200/1/1/1.25 [MMA]:4.60 mol L <sup>-1</sup> in anisole.....	46
<b>Figure B.1</b> : $M_n$ versus conversion plot of St by ATRP using EPEI at 110 °C. [St] <sub>o</sub> /[EBrP] <sub>o</sub> /[CuBr] <sub>o</sub> /[EPEI] <sub>o</sub> =200/1/1/0.30 [St]: 5.7 mol L <sup>-1</sup> in anisole.....	47
<b>Figure B.2</b> : $M_n$ versus conversion plot of St by ATRP using EPEI at 110 °C. [St] <sub>o</sub> /[EBrP] <sub>o</sub> /[CuBr] <sub>o</sub> /[EPEI] <sub>o</sub> =200/1/1/0.45 [St]: 5.7 mol L <sup>-1</sup> in anisole.....	47
<b>Figure B.3</b> : $M_n$ versus conversion plot of St by ATRP using EPEI at 110 °C. [St] <sub>o</sub> /[EBrP] <sub>o</sub> /[CuBr] <sub>o</sub> /[EPEI] <sub>o</sub> =200/1/1/0.60 [St]: 5.7 mol L <sup>-1</sup> in anisole.....	48
<b>Figure B.4</b> : $M_n$ versus conversion plot of St by ATRP using EPEI at 110 °C. [St] <sub>o</sub> /[EBrP] <sub>o</sub> /[CuBr] <sub>o</sub> /[EPEI] <sub>o</sub> =200/1/1/0.75 [St]: 5.7 mol L <sup>-1</sup> in anisole.....	48
<b>Figure B.5</b> : $M_n$ versus conversion plot of St by ATRP using EPEI at 110 °C. [St] <sub>o</sub> /[EBrP] <sub>o</sub> /[CuBr] <sub>o</sub> /[EPEI] <sub>o</sub> =200/1/1/1.00 [St]: 5.7 mol L <sup>-1</sup> in anisole.....	49
<b>Figure B.6</b> : $M_n$ versus conversion plot of St by ATRP using EPEI at 110 °C. [St] <sub>o</sub> /[EBrP] <sub>o</sub> /[CuBr] <sub>o</sub> /[EPEI] <sub>o</sub> =200/1/1/1.25 [St]: 5.7 mol L <sup>-1</sup> in anisole.....	49
<b>Figure B.7</b> : $M_n$ versus conversion plot of St by ATRP using BPEI at 110 °C. [St] <sub>o</sub> /[EBrP] <sub>o</sub> /[CuBr] <sub>o</sub> /[BPEI] <sub>o</sub> =200/1/1/0.15 [St]: 5.7 mol L <sup>-1</sup> in toluene.....	50
<b>Figure B.8</b> : $M_n$ versus conversion plot of St by ATRP using BPEI at 110 °C. [St] <sub>o</sub> /[EBrP] <sub>o</sub> /[CuBr] <sub>o</sub> /[BPEI] <sub>o</sub> =200/1/1/0.30 [St]: 5.7 mol L <sup>-1</sup> in toluene.....	50
<b>Figure B.9</b> : $M_n$ versus conversion plot of St by ATRP using BPEI at 110 °C. [St] <sub>o</sub> /[EBrP] <sub>o</sub> /[CuBr] <sub>o</sub> /[BPEI] <sub>o</sub> =200/1/1/0.45 [St]: 5.7 mol L <sup>-1</sup> in toluene.....	51

<b>Figure B.10</b> : $M_n$ versus conversion plot of St by ATRP using BPEI at 110 °C. $[St]_0/[EBrP]_0/[CuBr]_0/[BPEI]_0=200/1/1/0.60$ [St]: 5.7 mol L <sup>-1</sup> in toluene.....	51
<b>Figure B.11</b> : $M_n$ versus conversion plot of St by ATRP using BPEI at 110 °C. $[St]_0/[EBrP]_0/[CuBr]_0/[BPEI]_0=200/1/1/0.75$ [St]: 5.7 mol L <sup>-1</sup> in toluene.....	52
<b>Figure B.12</b> : $M_n$ versus conversion plot of St by ATRP using BPEI at 110 °C. $[St]_0/[EBrP]_0/[CuBr]_0/[BPEI]_0=200/1/1/1.00$ [St]: 5.7 mol L <sup>-1</sup> in toluene.....	52
<b>Figure B.13</b> : $M_n$ versus conversion plot of St by ATRP using BPEI at 110 °C. $[St]_0/[EBrP]_0/[CuBr]_0/[BPEI]_0=200/1/1/1.25$ [St]: 5.7 mol L <sup>-1</sup> in toluene.....	53
<b>Figure B.14</b> : $M_n$ versus conversion plot of St by ATRP using BPEI at 110 °C. $[St]_0/[EBrP]_0/[CuBr]_0/[BPEI]_0=200/1/1/2.00$ [St]: 5.7 mol L <sup>-1</sup> in toluene.....	53
<b>Figure B.15</b> : $M_n$ versus conversion plot of MMA by ATRP using BPEI at 110 °C. $[MMA]_0/[EBrIB]_0/[CuBr]_0/[BPEI]_0=200/1/1/0.30$ [MMA]: 4.6 mol L <sup>-1</sup> in anisole.....	54
<b>Figure B.16</b> : $M_n$ versus conversion plot of MMA by ATRP using BPEI at 110 °C. $[MMA]_0/[EBrIB]_0/[CuBr]_0/[BPEI]_0=200/1/1/1.00$ [MMA]: 4.6 mol L <sup>-1</sup> in anisole.....	54
<b>Figure C.1</b> : GPC traces of St by ATRP using EPEI at 110 °C. [St]: 5.7 mol L <sup>-1</sup> in anisole $[St]_0/[EBrP]_0/[CuBr]_0/[EPEI]_0=200/1/1/0.3$ .....	55
<b>Figure C.2</b> : GPC traces of St by ATRP using EPEI at 110 °C. [St]: 5.7 mol L <sup>-1</sup> in anisole $[St]_0/[EBrP]_0/[CuBr]_0/[EPEI]_0=200/1/1/0.45$ .....	55
<b>Figure C.3</b> : GPC traces of St by ATRP using EPEI at 110 °C. [St]: 5.7 mol L <sup>-1</sup> in anisole $[St]_0/[EBrP]_0/[CuBr]_0/[EPEI]_0=200/1/1/0.60$ .....	56
<b>Figure C.4</b> : GPC traces of St by ATRP using EPEI at 110 °C. [St]: 5.7 mol L <sup>-1</sup> in anisole $[St]_0/[EBrP]_0/[CuBr]_0/[EPEI]_0=200/1/1/0.75$ .....	56
<b>Figure C.5</b> : GPC traces of St by ATRP using EPEI at 110 °C. [St]: 5.7 mol L <sup>-1</sup> in anisole $[St]_0/[EBrP]_0/[CuBr]_0/[EPEI]_0=200/1/1/1.00$ .....	57
<b>Figure C.6</b> : GPC traces of St by ATRP using EPEI at 110 °C. [St]: 5.7 mol L <sup>-1</sup> in anisole $[St]_0/[EBrP]_0/[CuBr]_0/[EPEI]_0=200/1/1/1.25$ .....	57
<b>Figure C.7</b> : GPC traces of St by ATRP using BPEI at 110 °C. [St]: 5.7 mol L <sup>-1</sup> in toluene $[St]_0/[EBrP]_0/[CuBr]_0/[BPEI]_0=200/1/1/0.15$ .....	58
<b>Figure C.8</b> : GPC traces of St by ATRP using BPEI at 110 °C. [St]: 5.7 mol L <sup>-1</sup> in toluene $[St]_0/[EBrP]_0/[CuBr]_0/[BPEI]_0=200/1/1/0.30$ .....	58
<b>Figure C.9</b> : GPC traces of St by ATRP using BPEI at 110 °C. [St]: 5.7 mol L <sup>-1</sup> in toluene $[St]_0/[EBrP]_0/[CuBr]_0/[BPEI]_0=200/1/1/0.45$ .....	59
<b>Figure C.10</b> : GPC traces of St by ATRP using BPEI at 110 °C. [St]: 5.7 mol L <sup>-1</sup> in toluene $[St]_0/[EBrP]_0/[CuBr]_0/[BPEI]_0=200/1/1/0.60$ .....	59
<b>Figure C.11</b> : GPC traces of St by ATRP using BPEI at 110 °C. [St]: 5.7 mol L <sup>-1</sup> in toluene $[St]_0/[EBrP]_0/[CuBr]_0/[BPEI]_0=200/1/1/0.75$ .....	60
<b>Figure C.12</b> : GPC traces of St by ATRP using BPEI at 110 °C. [St]: 5.7 mol L <sup>-1</sup> in toluene $[St]_0/[EBrP]_0/[CuBr]_0/[BPEI]_0=200/1/1/1.00$ .....	60
<b>Figure C.13</b> : GPC traces of St by ATRP using BPEI at 110 °C. [St]: 5.7 mol L <sup>-1</sup> in toluene $[St]_0/[EBrP]_0/[CuBr]_0/[BPEI]_0=200/1/1/1.25$ .....	61
<b>Figure C.14</b> : GPC traces of St by ATRP using BPEI at 110 °C. [St]: 5.7 mol L <sup>-1</sup> in toluene $[St]_0/[EBrP]_0/[CuBr]_0/[BPEI]_0=200/1/1/2.00$ .....	61

**Figure C.15**: GPC traces of MMA by ATRP using BPEI at 80 °C.  
[MMA]<sub>o</sub>/[EBrIB]<sub>o</sub>/[CuBr]<sub>o</sub>/[BPEI]<sub>o</sub>=200/1/1 /0.30 [MMA]: 4.60  
mol L<sup>-1</sup> in anisole..... 62

**Figure C.16**: GPC traces of MMA by ATRP using BPEI at 80 °C.  
[MMA]<sub>o</sub>/[EBrIB]<sub>o</sub>/[CuBr]<sub>o</sub>/[BPEI]<sub>o</sub>=200/1/1 /0.30 [MMA]: 4.60  
mol L<sup>-1</sup> in anisole..... 62

## ALKYLATED POLY(ETHYLENEIMINE) LIGANDS IN HOMOGENEOUS ATOM TRANSFER RADICAL POLYMERIZATION

### SUMMARY

Recently, metal-mediated radical polymerization, more generally known as atom transfer radical polymerization (ATRP), has become one of the most efficient controlled/living radical polymerization methods to obtain linear polymers and copolymers with different topologies. The catalyst–ligand complex in ATRP plays a key role in controlling the chain growth, polymerization rate, and polydispersity. The main effect of the ligand is to solubilize the transition-metal salt in the organic media and to regulate the proper reactivity and dynamic halogen exchange between the metal center and the dormant species or persistent radical.

Tridentate and tetradentate ligands generally provide faster polymerizations than bidentate ligands, while monodentate nitrogen ligands yield redox-initiated free radical polymerization. In addition, ligands with an ethylene linkage between the nitrogens are more efficient than those with a propylene or butylene linkage.

Solubility of the ligand and its Cu(I) and Cu(II) complexes in organic media has particular importance to attain homogeneous polymerization conditions. The ligand with a long aliphatic chain on the nitrogen atoms provides solubility of its metal complexes in organic solvents. However, the increasing length of the alkyl substituents induces steric effects and affects the electron transfer, the activation–deactivation equilibrium.

In this study, ethylated and butylated polydentate nitrogen ligands (alkylated poly(ethyleneimine)) are synthesized and used in ATRP of styrene and methyl methacrylate which was carried out in the presence of CuBr as co-catalyst and ethyl 2-bromopropionate and ethyl 2-isobutyrate as initiator. The concentration effect of those two ligands is examined on living and controlled radical polymerization.

## **HOMOJEN ATOM TRANSFER RADİKAL POLİMERİZASYONU İÇİN ALKİLLENMİŞ POLİ(ETİLENİMİN) LİGANDLARI**

### **ÖZET**

Son yıllarda, metal katalizörlü radikal polimerizasyonu, daha bilinen adı ile atom transfer radikal polimerizasyonu (ATRP), değişik topolojilerde doğrusal polimerler ve kopolimerler elde etmek için kullanılan en etkin kontrollü / “yaşayan” polimerizasyon metodu haline gelmiştir. Katalizör-ligand kompleksi ATRP de zincir büyümesi kontrolünde, polimerizasyon hızında ve molekül ağırlığı dağılımında anahtar rol oynamaktadır. Ligandın asıl etkisi, geçiş metali tuzunu organik ortamda çözünür hale getirerek, uygun reaktivite ve metal merkez ile aktif uç, deaktif uç arasındaki halojen yer değişimini düzenlemektir.

Üçdişli ve dörtdişli ligandlar genellikle çiftdişli ligandlara göre daha hızlı polimerizasyon sağlarken, tekdişli ligandlar redoks-başlatılmış serbest radikal polimerizasyonu reaksiyonu verirler. Bununla birlikte, nitrojen atomları arasında etilen köprülerine sahip ligandlar, propilen veya butilen köprüsüne sahip ligandlardan daha etkindir.

Ligand/Cu(I) ve ligand/Cu(II) komplekslerinin organik ortamda çözünürlüğü, homojen polimerizasyon koşullarını sağlamak için en önemli parametredir. Nitrojen atomlarına bağlı uzun alifatik zincirler, ligandların metal komplekslerinin organik ortamda çözünürlüğünü sağlarlar. Ancak, alifatik grubun uzunluğunun artması sterik etkiye neden olur ve elektron transferini, aktivasyon-deaktivasyon dengesini değiştirir.

Bu çalışmada, iki ve dört karbon içeren alkil gruplarına sahip çokdişli yeni amin ligandları (alkillenmiş poli(etilenimin)) sentezlenmiş ve ligand olarak, CuBr (katalizör), etil 2-bromopropionat ve etil 2-bromo izobutirat (başlatıcı) varlığında, stiren ve metil metakrilatin ATRP reaksiyonlarında kullanılmıştır.. Bu ligandların değişik konsantrasyonlarının kontrollü / “yaşayan” polimerizasyon üzerindeki etkileri incelenmiştir.

## 1. INTRODUCTION

The synthesis of polymers with well-defined compositions, architectures and functionalities has long been of great interest in polymer chemistry. Transition metal mediated atom transfer radical polymerization (ATRP); a controlled/ “living” radical polymerization technique is utilized to obtain linear polymers and copolymers with different topologies.

ATRP is based on reversible activation/deactivation equilibrium between the active and dormant species mediated by transition metal complexes. Ligands serve several purposes. In addition to primary roles of tuning atom transfer equilibrium constant and dynamics as well as selectivity, they control solubility in the reaction mixture and ensure stability of the complexes in different monomers, solvents and temperatures. Nitrogen ligands have been used in copper- and iron-mediated ATRP. For copper-mediated ATRP nitrogen base ligands work particularly well. In contrast, sulfur, oxygen or phosphorus ligands are less effective due to inappropriate electronic effects of unfavorable binding constants [1].

The aim of this research is to develop highly active catalyst, having fast activation rate, had high activity for ATRP. Besides it is proposed that linear multidendate amines combining alky amines might have high activation rate, and thus form highly active catalysts with copper halides [2].

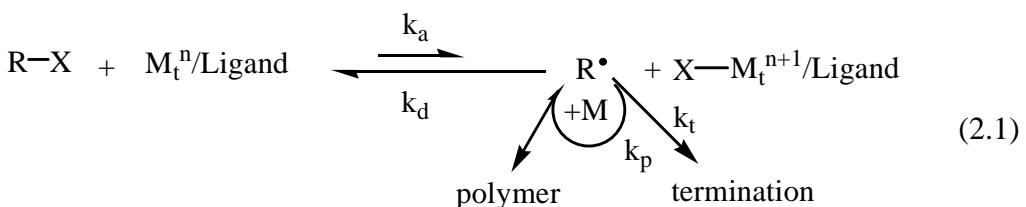
In this study, ethylated and butylated polydentate nitrogen ligands (alkylated poly(ethyleneimine)) are synthesized and used in ATRP of styrene and methyl methacrylate which was carried out in the presence of CuBr as co-catalyst and ethyl 2-bromopropionate and ethyl 2-isobutyrate as initiator. The concentration effect of those two ligands is examined on controlled / “living” radical polymerization.

Long chain ligand (multidendate) could be used for catalyst removable process by precipitation bulky catalyst-ligand complex properties of PEI, which can cause the retention of metal ions.

## 2. THEORETICAL SECTION

### 2.1 Atom Transfer Radical Polymerization (ATRP)

ATRP is one of the most versatile controlled radical polymerization methods [3-12]. This method utilizes a reversible halogen atom abstraction step in which a lower oxidation state metal complex ( $M_t^n$  complexed by ligand) reacts with an alkyl halide ( $R-X$ ) to generate a radical ( $R^\bullet$ ), with an activation rate constant ( $k_a$ ), and a higher oxidation state metal complex ( $X-M_t^{n+1}/\text{Ligand}$ ). This radical then adds to the monomer to generate the polymer chain ( $k_p$ ). The higher oxidation state metal can then deactivate the growing radical to generate a dormant chain and the lower oxidation state metal complex ( $k_d$ ) as seen in (2.1). The molecular weight is controlled because both initiation and deactivation are fast, allowing for all the chains to begin growing at approximately the same time while maintaining a low concentration of active species. Termination cannot be totally avoided; however, the proportion of chains terminated compared to the number of propagating chains is small [13]. Several metal/ligand systems have been used to catalyze this process and a variety of monomers including styrene, (meth)acrylates, and acrylonitrile have been successfully polymerized [8-10].



The rate of ATRP is internally first order in monomer, externally first order with respect to initiator and activator,  $M_t^n$ , and negative first order with respect to deactivator,  $X-M_t^{n+1}$ .

The actual kinetics depends on many factors including the solubility of activator and deactivator, their possible interactions, and variation of their structures and reactivities with concentrations and composition of the reaction medium.

One of the most important parameters in ATRP is the dynamics of exchange, especially the relative rate of deactivation. If the deactivation process is slow in comparison with propagation, then a classic redox initiation process operates leading to conventional, and not controlled, radical polymerization.

Polydispersities in ATRP decrease with conversion, with the rate constant of deactivation,  $k_d$ , and also with the concentration of deactivator,  $[X-M_t^{n+1}]$ . They, however, increase with the propagation rate constant,  $k_p$ , and the concentration of initiator,  $[R-X]_0$ . This means that more uniform polymers are obtained at higher conversion, when the concentration of deactivator in solution is high and the concentration of initiator is low. Also, more uniform polymers are formed when deactivator is very reactive and monomer propagates slowly (styrene rather than acrylate) [14].

### 2.1.1 Kinetics of ATRP

The rate of polymerization is first order with respect to monomer, alkyl halide (initiator), and transition metal complexed by ligand. The reaction is usually negative first order with respect to the deactivator ( $X-M_t^{n+1}/\text{Ligand}$ ). The rate equation of copper-based ATRP is formulated in discussed conditions and given in (2.2). The apparent propagation rate constant, where  $k_p$  and  $K_{eq}$  refer to the absolute rate constant of propagation and the atom transfer equilibrium constant for the propagating species, respectively.

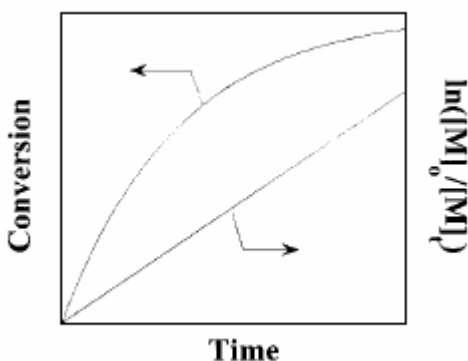
$$R_p = k_p^{app} [M] = k_p [R\cdot] [M] = k_p K_{eq} [I] ([CuX]/[CuX_2]) [M] \quad (2.2)$$

Figure 2.1 shows a typical linear variation of conversion with time in semi logarithmic coordinates (kinetic plot). Such a behavior indicates that there is a constant concentration of active species in the polymerization and first-order kinetics with respect to monomer.

However, since termination occurs continuously, the concentration of the Cu(II) species increases and deviation from linearity may be observed [1]. For the ideal case with chain length independent from termination, persistent radical effect [15,16] kinetics implies the semi logarithmic plot of monomer conversion vs. time to the 2/3 exponent should be linear. Nevertheless, a linear semi logarithmic plot is often observed.

This may be due to an excess of the Cu(II) species present initially, a chain length dependent termination rate coefficient, and heterogeneity of the reaction system due to limited solubility of the copper complexes.

It is also possible that self-initiation may continuously produce radicals and compensate for termination. Similarly, external orders with respect to initiator and the Cu(I) species may also be affected by the persistent radical effect [17].



**Figure 2.1.** Kinetic plot and conversion vs. time plot for ATRP

Results from kinetic studies of ATRP for styrene (S) [18], methyl acrylate (MA) [19] and methyl methacrylate (MMA) [20,21] under homogeneous conditions indicate that the rate of polymerization is first order with respect to monomer, initiator, and Cu(I) complex concentrations. These observations are all consistent with the derived rate law.

It should be noted that the optimum ratio can vary with regard to changes in the monomer, counter ion, ligand, temperature, and other factors [20,22,23]. The precise kinetic law for the deactivator  $\text{CuX}_2$  was more complex due to the spontaneous generation of Cu(II) via the persistent radical effect [15,17,18].

In the atom transfer step, a reactive organic radical is generated along with a stable Cu(II) species that can be regarded as a persistent metallo-radical. If the initial concentration of deactivator Cu(II) in the polymerization is not sufficiently large to ensure a fast rate of deactivation ( $k_d[\text{Cu(II)}]$ ), then coupling of the organic radicals will occur, leading to an increase in the Cu(II) concentration.

Radical termination occurs rapidly until a sufficient amount of deactivator Cu(II) is formed and the radical concentration is low. Under such conditions, the rate at which radicals combine ( $k_t$ ) will become much slower than the rate at which radicals react with the Cu(II) complex in a deactivation process and a controlled polymerization will proceed.

Typically, a small fraction (~5 %) of the total growing polymer chains will be terminated during the early stage of the polymerization, but the majority of the chains (>95 %) will continue to grow successfully.

The effect of Cu(II) on the polymerization may additionally be complicated by its poor solubility, by a slow reduction by reaction with monomers leading to 1,2-dihaloadducts, or from the self-initiated systems such as styrene and other monomers.

If the deactivation does not occur, or if it is too slow ( $k_p \gg k_d$ ), there will be no control and polymerization will become classical redox reaction therefore the termination and transfer reactions may be observed. To control the polymerization better, addition of one or a few monomers to the growing chain in each activation step is desirable. Molecular weight distribution for ATRP is given in (2.3).

$$M_w/M_n = 1 + ((k_d[\text{RX}]_0)/(k_p[\text{X}-\text{M}_t^{n+1}])) \times ((2/p)-1)$$

$p$  = polymerization yield

$[\text{RX}]_0$  = concentration of the functional polymer chain

(2.3)

$[\text{X}-\text{M}_t^{n+1}]$  = concentration of the deactivators

$k_d$  = rate constant of deactivation

$k_p$  = rate constant of activation

When a hundred percent of conversion is reached, in other words  $p=1$ , it can be concluded that;

a) For the smaller polymer chains, higher polydispersities are expected to be obtained because the smaller chains include little activation-deactivation steps and also the

chain length difference is higher for small polymer chains resulting in little control of the polymerization.

- b) For the higher ratios of  $k_p/k_d$ , higher polydispersities (molecular weight distributions) are usually obtained resulting in the little control of polymerization.
- c) Resulting molecular weight distribution decreases as the concentration of the deactivators increases [1].

### **2.1.2. The function of components for ATRP and reaction conditions**

#### **2.1.2.1. Monomers**

A variety of monomers have been successfully polymerized using ATRP. Typical monomers include styrene, (meth)acrylates, (meth)acrylamides, and acrylonitrile, which contain substituents that can stabilize the propagating radicals.

Even under the same conditions using the same catalyst, each monomer has its own unique atom transfer equilibrium constant for its active and dormant species. In the absence of any side reactions other than radical termination by coupling or disproportionation, the magnitude of the equilibrium constant ( $K_{eq}=k_a/k_d$ ) determines the polymerization rate [1].

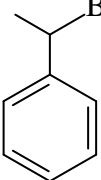
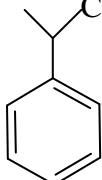
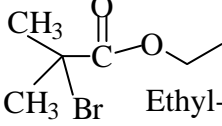
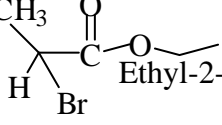
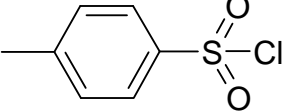
#### **2.1.2.2. Initiators**

The main role of the initiator is to determine the number of growing polymer chains. Two parameters are important for a successful ATRP initiating system. First, initiation should be fast in comparison with propagation. Second, the probability of the side reactions should be minimized.

In ATRP, alkyl halides (R-X) are typically used as initiator (Table 2.1.) and the rate of polymerization is first order with respect to the concentration of R-X.

To obtain well-defined polymers with narrow molecular weight distributions, the halide groups, X, must rapidly and selectively migrate between the growing chain and the transition metal complex. When X is either bromine or chlorine, the molecular weight control is the best. Fluorine is not used because the C-F bond is too strong to undergo homolytic cleavage. However, it has been demonstrated the first example using alkyl fluoride as macroinitiator to obtain graft copolymers for membrane applications [24,25].

**Table 2.1.** The most frequently used initiator types in ATRP systems

Initiator	Monomer
 1-Bromo-1-phenyl ethane	Styrene
 1-Chloro-1-phenyl ethane	Styrene
 Ethyl-2-bromo isobutyrate	Methyl methacrylate
 Ethyl-2-bromo propionate	Methyl acrylate and Styrene
 p-toluenesulphonyl chloride	Methyl methacrylate

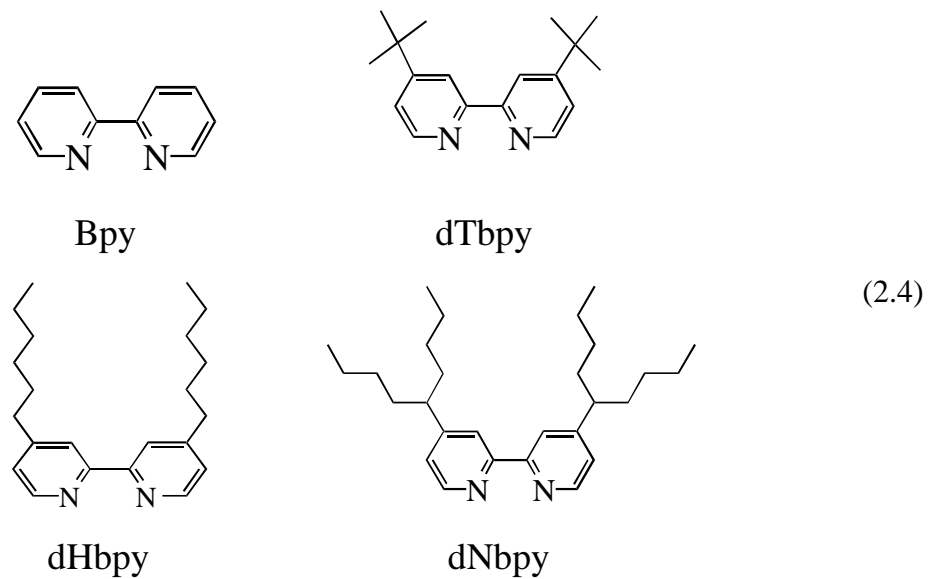
### 2.1.2.3. Ligands

Transition metal catalysts are the key to ATRP since they determine the position of the atom transfer equilibrium and the dynamics of exchange between the dormant and active species.

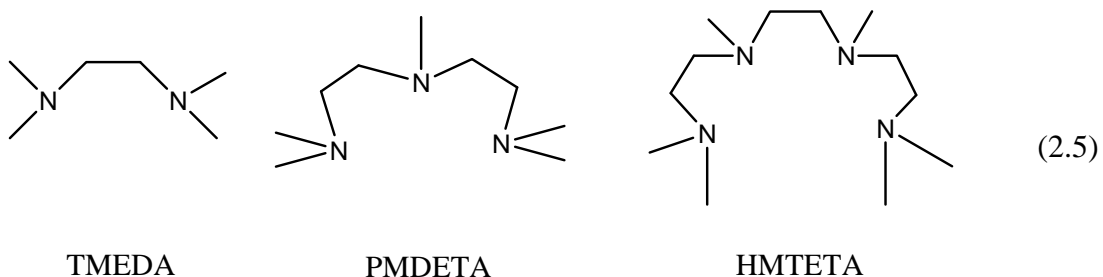
The main effect of the ligand is to solubilize the transition-metal salt in organic media and to regulate the proper reactivity and dynamic halogen exchange between the metal center and the dormant species or persistent radical.

Ligands, typically amines or phosphines, are used to increase the solubility of the complex transition metal salts in the solution and to tune the reactivity of the metal

towards halogen abstraction. So far, a range of multidentate neutral nitrogen ligands was developed as active and efficient complexing agents for copper-mediated ATRP, including, bipyridines [26,27,30] (2.4), terpyridines [28,29], phenantrolines [30], picolyl amines [29,31], pyridinemethinamines [32-36] and tri [26,29,37-39] or tetradentate aliphatic amines [40,41,42,43] including linear and branched amines (2.5). Tridentate and tetradentate ligands generally provide faster polymerizations than bidentate ligands, while monodentate nitrogen ligands yield redox-initiated free radical polymerization. In addition, ligands with an ethylene linkage between the nitrogens are more efficient than those with a propylene or butylene linkage [44].



Linear amines with ethylene linkage like 1,1,4,7,7-pentamethyldiethylenetriamine (PMDETA), and 1,1,4,7,10,10-hexamethyltriethylenetetramine (HMTETA) (2.5) were synthesized and examined for ATRP as ligands [26]. Reasons for examining of these type of ligands are, they have low price, due to the absence of the extensive  $\pi$ -bonding in the simple amines, the subsequent copper complexes are less colored and since the coordination complexes between copper and simple amines tend to have lower redox potentials than the copper-bpy complex, the employment of simple amines as the ligand in ATRP may lead to faster polymerization rates.



Solubility of the ligand and its metal complexes in organic media is of particular importance to attain homogeneous polymerization conditions. The rate of polymerization is also affected by the relative solubility of the activating and the deactivating species of the catalyst. In heterogeneous systems, a low stationary concentration of the catalyst species allows for a controlled polymerization, but the polymerization is much slower than in homogeneous systems [44]. The ligand with a long aliphatic chain on the nitrogen atoms provides solubility of its metal complexes in organic solvents. However, the increasing length of the alkyl substituents induces steric effects and can alter the redox potential of the metal center. Any shift in the redox potential affects the electron transfer and the activation–deactivation equilibrium [29]. Alkylated linear amine ligands (ALAL) [45-47] show a homogeneous and relatively fast polymerization reaction compared to most other atom transfer radical polymerization (ATRP) ligands.

#### 2.1.2.4. Transition Metal Complexes

Catalyst is the most important component of ATRP. It is the key to ATRP since it determines the position of the atom transfer equilibrium and the dynamics of exchange between the dormant and active species. There are several prerequisites for an efficient transition metal catalyst. First, the metal center must have at least two readily accessible oxidation states separated by one electron.

Second the metal center should have reasonable affinity toward a halogen. Third the coordination sphere around the metal should be expandable upon oxidation to selectively accommodate a (pseudo)-halogen. Fourth the ligand should complex the metal relatively strong. The most important catalysts used in ATRP are; Cu(I)Cl, Cu(I)Br, NiBr<sub>2</sub>(PPh<sub>3</sub>)<sub>2</sub>, FeCl<sub>2</sub>(PPh<sub>3</sub>)<sub>2</sub>, RuCl<sub>2</sub>(PPh<sub>3</sub>)<sub>3</sub>/ Al(OR)<sub>3</sub> [1].

#### **2.1.2.5. Solvents**

ATRP can be carried out either in bulk, in solution or in a heterogeneous system (e.g., emulsion, suspension). Various solvents such as benzene, toluene, anisole, diphenyl ether, ethyl acetate, acetone, dimethyl formamide (DMF), ethylene carbonate, alcohol, water, carbon dioxide and many others have been used for different monomers. A solvent is sometimes necessary especially when the obtained polymer is insoluble in its monomer [1].

#### **2.1.2.6. Temperature and reaction time**

The rate of the polymerization in ATRP increases with increasing temperature due to increase of both the radical propagation rate constant and the atom transfer equilibrium constant. As a result of the higher activation energy for the radical propagation than for the radical termination, higher  $k_p/k_t$  ratios and better control may be observed at higher temperature. However, chain transfer and other side reactions become more pronounced at higher temperature. In general, the solubility of the catalyst increases higher temperatures; however, catalyst decomposition may also occur with the temperature increase. The optimal temperature depends mostly on the monomer, the catalyst, and the target molecular weight.

At high monomer conversions, the rate of the propagation slows down considerably; however, the rate of the side reaction does not change significantly, as most of them are monomer concentration independent. Prolong reaction times leading to nearly complete monomer conversion may not increase the polydispersity of the final polymer but will induce loss of end groups [1].

### **2.2. Poly(ethyleneimine)**

Poly(ethyleneimine) is obtained by cationic polymerization. Its structure contains primary, secondary and tertiary amino groups due to transfer reactions. The ratio is approximately 1:2:1. Poly(ethyleneimine) PEI is the polycation with the highest charge density in the fully protonated form in aqueous solution. This high cationic activity opens a wide variety of applications to poly(ethyleneimine). One of the biggest markets world-wide is the paper industry, where PEI is used as retention aid. The polymer favors the flocculation of the negatively charged paper fibers and fillers. The flocculation properties of poly(ethyleneimine) are also utilized in the

cleaning of waste water. The fixing properties are advantageous for the printing of papers. Ink-jet paper is made by addition of PEI. The amino groups of PEI are chemically reactive. This property was utilized in cigarette-filters to remove aldehydes. Acidic gases can also be absorbed and neutralized on crosslinked poly(ethyleneimine)s. The complex-forming properties of PEI can cause the retention of metal ions and the catalysis of chemical reactions. [48]

The precipitation and microfiltration provide a practical means of purifying polymers produced by ATRP. The precipitation process uses reagents and procedures that can be easily procured and applied in common laboratories or industrially. Furthermore, the ligands used to form the ATRP catalyst (PMDETA and HMTETA) and to which the method applies are inexpensive, widely used, provide good control of polymer architecture, and form highly active catalysts. [49]

Hydrophobically modified poly(ethyleneimine)s can dispose the properties of the pure polymers having additionally amphiphilic properties. Epoxides of fatty alcohols can be reacted with poly(ethyleneimine) to yield products that are used as emulsifiers and dispersants. The amidation of fatty acids with PEI results in materials which can stabilize pigments [48].

### **3. EXPERIMENTAL PART**

#### **3.1. Chemicals**

Copper (I) bromide (CuBr, 99.99 %) , was purchased from the Aldrich Chemical Co. Methyl methacrylate (MMA, 99 %), styrene (St, 99 %), ethyl-2-bromo isobutyrate (EBrIB, used for MMA, 98 %), ethyl-2-bromopropionate (EBrP, used for S, 99%) were purchased from Acros Organics Co., poly(ethyleneimine) ( $M_w=423\text{ g mol}^{-1}$ ), potassium carbonate (99+ %), bromobutane (99 %) were purchased from the Aldrich Chemical Co, iodoethane (98 %) was purchased from Acros Organics Co., anhydrous sodium sulphate (99 %) tetrahydrofuran (THF), anisole, toluene, methanol, dichloromethane, ethyl acetate were purchased from J.T. Baker Co. All reagents were used without further purification. Ethylated poly(ethyleneimine) (EPEI) and butylated poly(ethyleneimine) (BPEI) were synthesized according to modified literature procedure [44-46].

#### **3.2. Synthesis of Alkylated Poly(ethyleneimine) (APEI)**

##### **3.2.1 Synthesis of ethylated poly(ethyleneimine) (EPEI)**

Iodoethane 93 mL (1.06 mol) was placed into 1 Ll round-bottom flask with 300 mL ethanol. While the solution was stirring at room temperature, 35 mL poly(ethyleneimine) (0.089 mol) ( $M_w=423\text{ g mol}^{-1}$ ) and 245 g (1.77 mol) potassium carbonate were added to the solution and the mixture was refluxed for 3 days. After refreshing potassium carbonate in same amount, it was refluxed for 3 more days. Then mixture was filtrated and ethanol was evaporated in rotavaporator. Product was extracted by distilled water and ethyl acetate. Organic phase was dried with anhydrous  $\text{Na}_2\text{SO}_4$ . After the filtration of sodium sulphate, ethyl acetate was evaporated in rotavaporator. Then the obtained product was dried in an oven under vacuum (conversion: 20%).

### 3.2.2 Synthesis of butylated poly(ethyleneimine) (BPEI)

Bromobutane 63 mL (0.56 mol) was placed into 1 L round-bottom flask with 300 mL ethanol. While the solution was stirring at room temperature, 18 mL (0.045 mol) poly(ethyleneimine) ( $M_n=423\text{g/mol}$ ) and 122.3 g (0.89 mol) potassium carbonate were added to the solution and the mixture was refluxed for 4 days. After refreshing potassium carbonate in same amount, it was refluxed for 5 more days. Then mixture was filtrated and ethanol was evaporated in rotavaporator. Distilled water, sodium chloride and dichloromethane were added in order to separate the organic phase. Organic phase was dried with anhydrous  $\text{Na}_2\text{SO}_4$ . After the filtration of sodium sulphate, dichloromethane was evaporated in rotavaporator. Then the obtained product was dried in a vacuum drier (conversion: 75%).

### 3.3. Polymerization of Styrene

A typical ATRP procedure was performed as follows. Catalyst,  $\text{CuBr}$  ( $3.9 \times 10^{-2} \text{ mol L}^{-1}$ ) was placed in a 48 ml of flask, which contained a side arm with a Teflon valve sealed with a Teflon stopper.

Then the flask was deoxygenated by vacuum-traw-nitrogen cycles three times. S ( $5.70 \text{ mol L}^{-1}$ ) in toluene and ligands APEI at different ratios were added to the flask, respectively.

Finally, initiator EBrP ( $2.9 \times 10^{-2} \text{ mol L}^{-1}$ ) was added then the flask was replaced in thermostatically controlled oil bath at  $110^\circ\text{C}$  and 400 rpm stirring rate. All liquid components were nitrogen bubbled prior to placement into the flask. Samples were taken periodically via an injector to follow the kinetics of the polymerization process. The adequate samples were precipitated in methanol, filtered and dried in order to have gravimetric measurements, or diluted in THF and methanol in order to have gas chromatography (GC) measurements. Obtained dried samples by gravimetrically were dissolved in THF containing 2,6-di-tert-butyl-4-methyl phenol (BHT) as internal standard, and filtered through micro filter (pore size 0.2 micron) in order to have gel permeation chromatography (GPC) measurements.

### **3.4. Polymerization of Methyl Methacrylate**

A typical ATRP procedure was performed as follows. Catalyst, CuBr ( $5.3 \times 10^{-2}$  mol L<sup>-1</sup>) was placed in a 48 mL of flask, which contained a side arm with a Teflon valve sealed with a Teflon stopper. Then the flask was deoxygenated by vacuum-thaw-nitrogen cycles three times. MMA (4.60 mol L<sup>-1</sup>) in anisole and ligand BPEI at different concentrations were added to the flask, respectively.

Finally, initiator EBrIB, ( $2.3 \times 10^{-2}$  mol L<sup>-1</sup>) was added then the flask was replaced in thermostatically controlled oil bath at 80°C and 400 rpm stirring rate. All liquid components were nitrogen bubbled prior to placement into the flask. Samples were taken periodically via an injector to follow the kinetics of the polymerization process. The samples were diluted in dichloromethane and methanol in order to have gas chromatography (GC) measurements. Obtained dried samples by gravimetrically were dissolved in THF containing BHT as internal standard, and filtered through micro filter (pore size 0.2 micron) in order to have GPC measurements.

### **3.5. Characterization**

The <sup>1</sup>H Nuclear Magnetic Resonance (NMR) spectrum was recorded on a Bruker spectrometer (250 MHz) in CDCl<sub>3</sub> solution using tetramethylsilane (TMS) as an internal standard for the characterization of APEI.

Monomer conversion was determined by gravimetrically and/or ATI Unicam gas chromatography (GC) equipped with a FID detector and a J&W scientific 15 m DB WAX widebore capillary column.

Molecular weight and molecular weight distributions were determined by a gel permeation chromatography (GPC) instrument. An Agilent Model 1200 consisting of a pump, a refractive index detector and two Waters Styragel columns HR 5E, HR 3; and THF was used as eluent at a flow rate of 1.0 mL/min at 30 °C. Molecular weights were calibrated using poly(methyl methacrylate) and polystyrene standards.

## 4. RESULTS AND DISCUSSIONS

### 4.1. Synthesis of Ethylated Poly(ethyleneimine) (EPEI)

Ethyl substituted poly(ethyleneimine) (EPEI) was synthesized according to Figure 4.1.

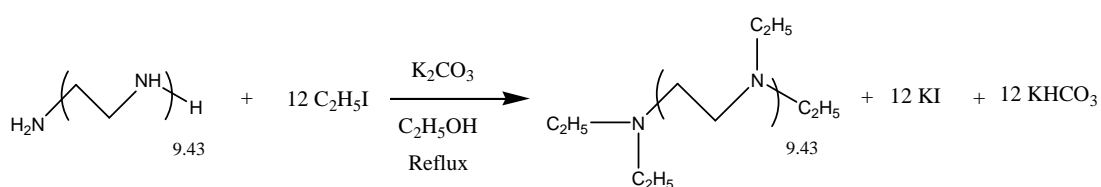


**Figure 4.1.** Synthesis of ethylated poly(ethyleneimine) EPEI.

The <sup>1</sup>H NMR spectrum was recorded on a Bruker spectrometer (250 MHz) in CDCl<sub>3</sub> solution using tetramethylsilane (TMS) as an internal standard for the characterization of EPEI. The structure of the ligand was assigned by the use of <sup>1</sup>H NMR spectrum that is given below.

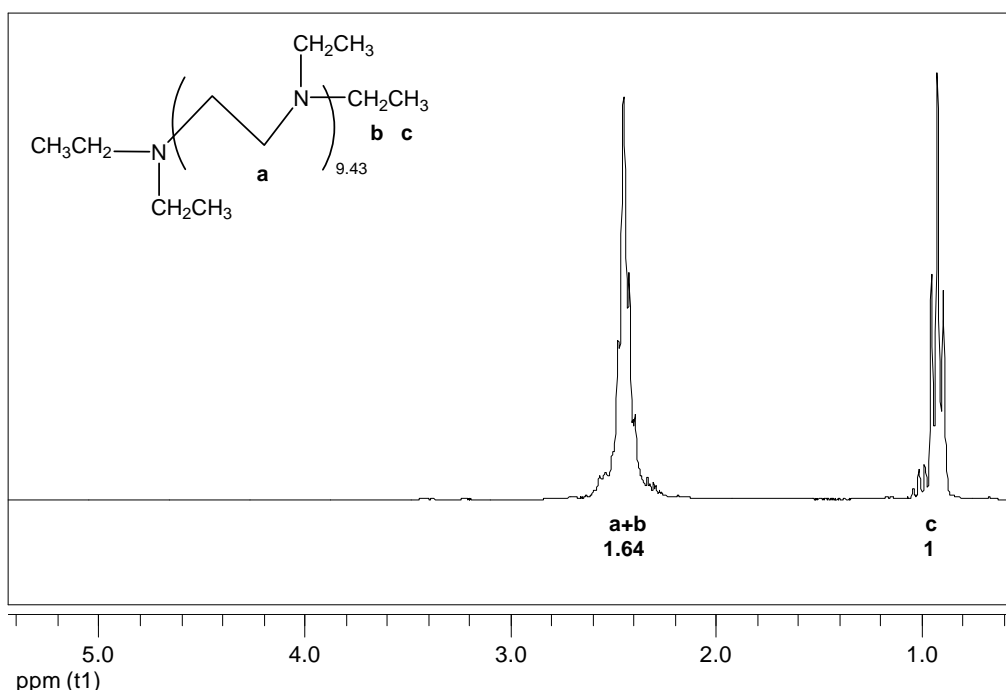


**Figure 4.2.** <sup>1</sup>H NMR Spectrum of EPEI in CDCl<sub>3</sub>

EPEI has two different types of hydrogen atoms, which are attached to the adjacent carbon atom of the nitrogen (represented as “a and b”) and the others are attached to the end carbon atom of alkyl substituents (represented as “c”). The ratio of integral value of those hydrogen atoms was found close to the theoretical ratio (1.68/1, a+b/c) as shown in Figure 4.2.

#### 4.2. Synthesis of Butylated Poly(ethyleneimine) (BPEI)

Butyl substituted poly(ethyleneimine) (BPEI) was synthesized according to Figure 4.3.

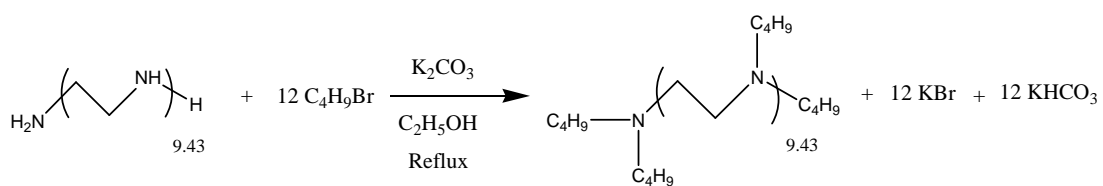


**Figure 4.3.** Synthesis of butylated poly(ethyleneimine) BPEI.

The  $^1\text{H}$  NMR spectrum was recorded on a Bruker spectrometer (250 MHz) in  $\text{CDCl}_3$  solution using tetramethylsilane (TMS) as an internal standard for the characterization of BPEI. The structure of the ligand was assigned by the use of  $^1\text{H}$  NMR spectrum that is given below.

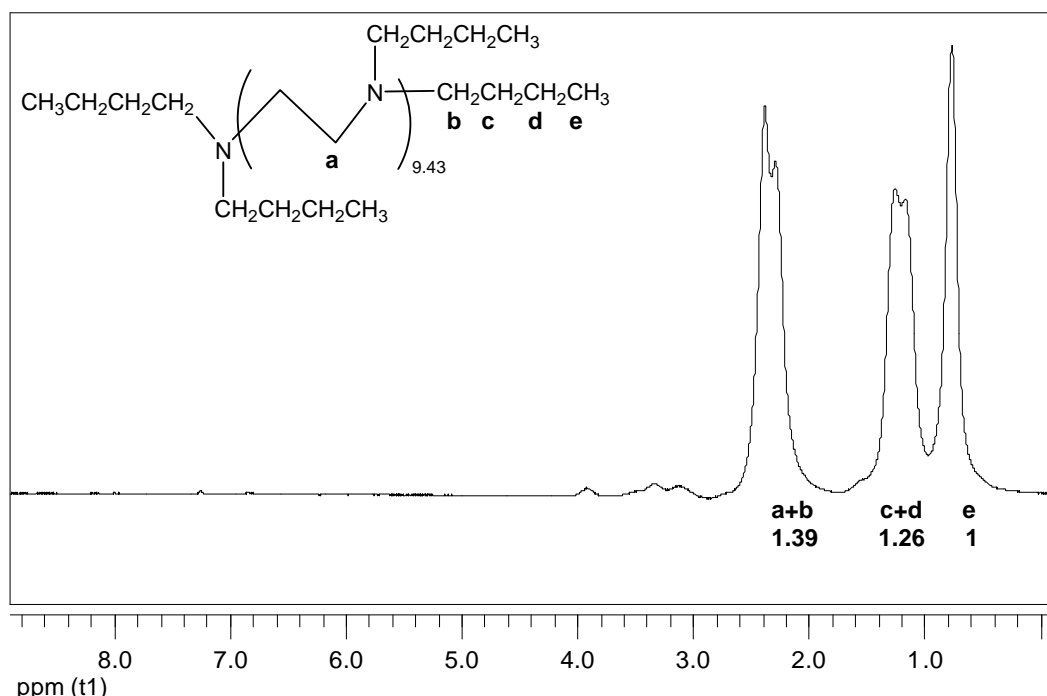


**Figure 4.4.**  $^1\text{H}$  NMR Spectrum of BPEI in  $\text{CDCl}_3$

BPEI has three different types of hydrogen atoms, which are attached to the adjacent carbon atom of the nitrogen (represented as “a and b”) and to the end carbon atom of alkyl substituents (represented as “e”) and to the carbon atom between them (represented as “c” and “d”). The ratio of integral value of those hydrogen atoms was found close to the theoretical ratio (1.67/1.33/1, a+b/c+d/e) as shown in Figure 4.4.

### 4.3. ATRP of Styrene for Different Ligand Ratios

ATRP of styrene was carried out with different ligands in similar conditions as follows. St (5.7 mol L<sup>-1</sup>), CuBr (3.9x10<sup>-2</sup> mol L<sup>-1</sup>), ethyl-2-bromopropionate (EBrP, 2.9x10<sup>-2</sup> mol L<sup>-1</sup>) in anisole for EPEI and in toluene for BPEI (50 % V/V), and different concentrations of two ligands were used in these ATRP reactions. Reaction temperature was set to 110 °C.  $[M]_0/[I]_0/[CuBr]_0/[ligand]_0 = 200/1/1/x$ . Reaction pathway is shown in Figure 4.5.

All the polymerization of St with both ligands were homogeneous and light green color were observed during the polymerization, which signified that Cu(I) salt and ligand complex was dominated the reaction medium.

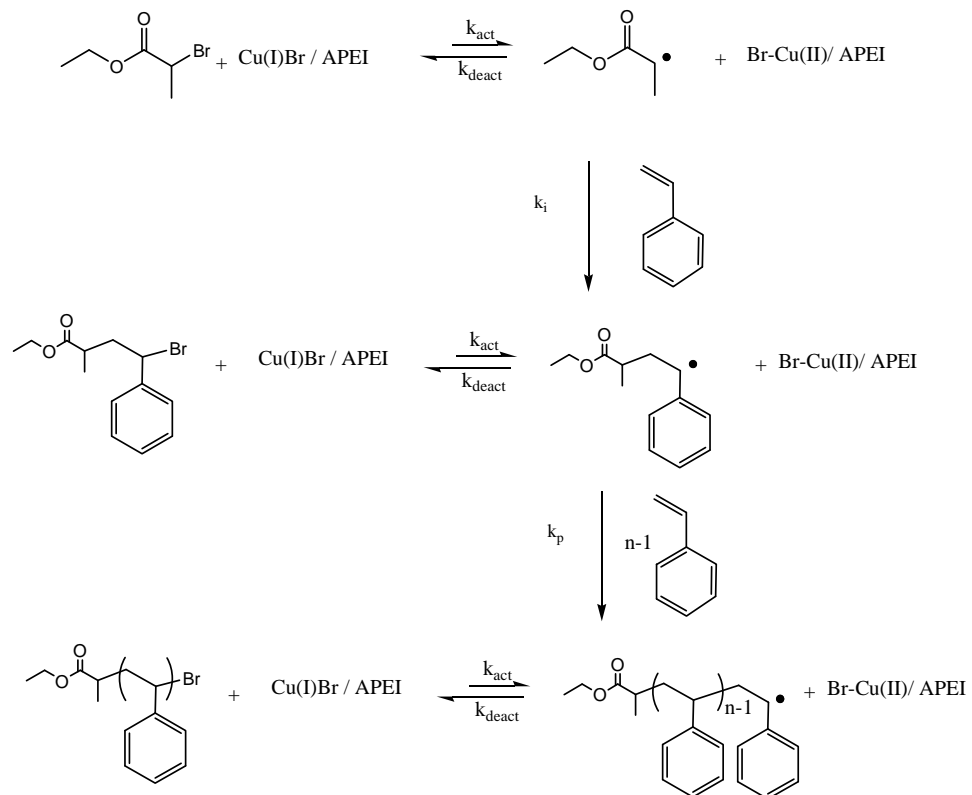


**Figure 4.5.** ATRP of Styrene by Using APEI Ligands.

### 4.3.1 Using Ethylated Poly(ethyleneimine) (EPEI)

The semi-logarithmic kinetic plots ( $\ln([M]_0/[M])$  vs time) of ATRP of St are shown in Appendix A, (Figures A.1-A.6) for different ligand (EPEI) ratios. Where,  $\ln([M]_0/[M])$  are determined from the conversion calculation of gravimetric measurements, which can be calculated as follows;

$$\% \text{ Conversion} = (W/M_o) \times 100$$

Where,  $W (=M_o - M)$  is the weight of the formed polymer and  $M_o$  represents the mass of the feed monomer. It is clearly seen that a straight line are observed, almost in all kinetic graphs, indicating that the first order kinetics with respect to the monomer concentration and demonstrates that active center concentration is constant during the polymerization. This result reveals that termination is negligible.

Molecular weight of polymer versus conversion plots were shown in Appendix B, (Figures B.1-B.6) for different ligand (EPEI) ratios. It is seen from figures, linear relationship indicates that transfer reactions are absent or insignificant. Measured molecular weights of the polymer are found close to the theoretical ones. Theoretical molecular weights were calculated by;

$$M_{n,th} = ([M]_0/[I]_0) \times (\% \text{ Conversion}/100) \times (M_w)_o + (M_w)_I$$

Where,  $(M_w)_o$  and  $(M_w)_I$  are the molecular weight of the monomer and initiator respectively,  $([M]_0/[I]_0)$  is the initial monomer, and initiator concentrations ratio.

Refractive index versus solvent elution plots in GPC traces shown in Appendix C, (Figures C.1-C.6) indicates that molecular weight increases by time.

The comparison of results of St polymerization for different EPEI ligand ratios are presented in Table 1. It is observed from Figure 4.6 that  $k_p^{app}$  is increasing by increase in  $[\text{EPEI}]/[\text{CuBr}]$  ratio, then reach plato value around  $[\text{EPEI}]/[\text{CuBr}] = 0.50$  ratio, which can be concluded that two copper salt molecules are ligated per ligand molecule.

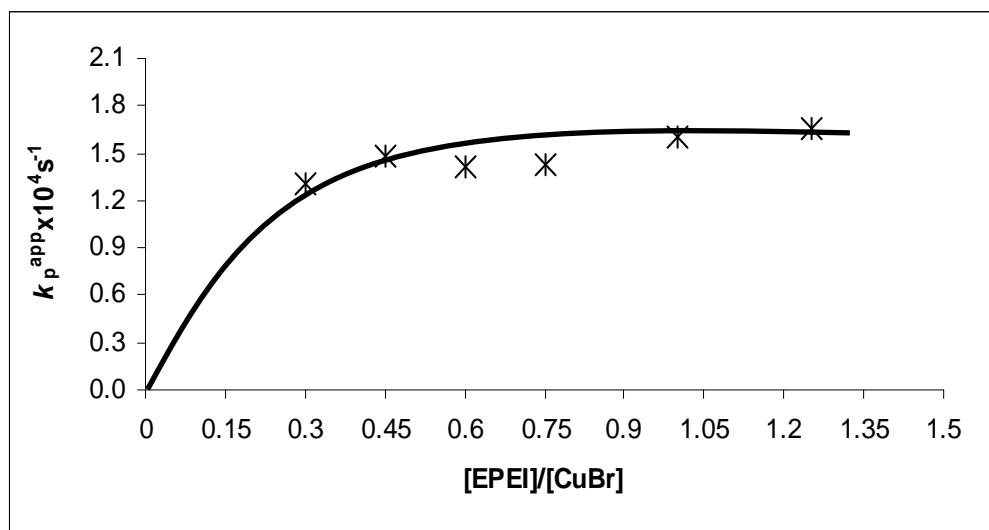


**Figure 4.6.**  $[EPEI]/[CuBr]$  versus  $k_p^{app}$  for ATRP of Styrene.  $[St]: 5.70 \text{ mol L}^{-1}$  in anisole at  $110^\circ\text{C}$ .  $[St]_0/[EBrP]_0/[CuBr]_0/[EPEI]_0 = 200/1/1/x$ .

**Table 4.1** ATRP of Styrene for Different Ligand (EPEI) Ratios<sup>a</sup>

Run	[EPEI]/[CuBr]	Time <sup>b</sup> (min)	Conv. <sup>b</sup> (%)	$M_{n,th}^b$ (g mol <sup>-1</sup> )	$M_{n,GPC}^b$ (g mol <sup>-1</sup> )	$M_w/M_n^b$	$k_p^{app}$ (10 <sup>-4</sup> s <sup>-1</sup> )
St1	0.30	300	93.6	19750	19300	1.18	1.30
St2	0.45	210	88.3	18570	15700	1.20	1.48
St3	0.60	240	87.2	18350	23900	1.28	1.42
St4	0.75	240	88.0	18510	29800	1.32	1.43
St5	1.00	240	86.6	18220	24600	1.38	1.60
St6	1.25	270	94.1	19780	67000	1.83	1.65

<sup>a</sup> [St]: 5.70 mol L<sup>-1</sup> in anisole at 110 °C. [St]<sub>0</sub>/[EBrP]<sub>0</sub>/[CuBr]<sub>0</sub>/[EPEI]<sub>0</sub>=200/1/1/x.

<sup>b</sup> Last point of kinetic datas. Molecular weights were measured by GPC using polystyrene as standards for calibration.

### 4.3.2 Using Butylated Poly(ethyleneimine) (BPEI)

The semi-logarithmic kinetic plots ( $\ln ([M]_0/ [M])$  versus time) of ATRP reaction of S are shown in Appendix A, (Figures A.7-A.14) for different (BPEI) ligand ratios. Where,  $\ln([M]_0/[M])$  are determined from the percentage conversion calculation of gravimetric and GC measurements, which can be calculated as follows;

$$\% \text{ Conversion} = (W/M) \times 100$$

Where,  $W (=M_o - M)$  is the weight of the formed polymer and  $M_o$  represents the mass of the feed monomer. For GC measurements, percentage conversion was calculated by the formula;

$$\% \text{ Conversion} = [1 - (M_t \times Sol_o / M_o \times Sol_t)] \times 100$$

Where,  $M_o$ ,  $M_t$ ,  $Sol_o$  and  $Sol_t$  are pick area of the monomer and solvent measured from GC at initial time and the time that sample is taken, respectively.

It is clearly seen that a straight line are observed, almost in all kinetic graphs, indicating that the first order kinetics with respect to the monomer concentration and demonstrates that active center concentration is constant during the polymerization. This result reveals that termination is negligible.

Molecular weight of polymer versus gravimetrically calculated conversion plots were shown in Appendix B, (Figures B.7-B.14) for different (BPEI) ligand ratios. It is seen from figures, linear relationship indicates that transfer reactions are absent or insignificant. Measured molecular weights of the polymer are found close to the theoretical ones. Theoretical molecular weights were calculated by the formula;

$$M_{n,th} = ([M]_0/[I]_0) \times (\% \text{ Conversion}/100) \times (M_w)_o + (M_w)_I$$

Where,  $(M_w)_o$  and  $(M_w)_I$  are the molecular weight of the monomer and initiator respectively,  $([M]_0/[I]_0)$  is the initial monomer, and initiator concentrations ratio.

Refractive index versus solvent elution plots in GPC traces shown in Appendix C, (Figures C.7-C.14) indicates that molecular weight increase by time.

The comparison of results of St polymerization for different BPEI ligand ratios are presented in Table 4.2. It is observed from Figure 4.7 that  $k_p^{\text{app}}$  is increasing by increase in  $[\text{BPEI}]/[\text{CuBr}]$  ratio, then reach plato value around  $[\text{BPEI}]/[\text{CuBr}] = 0.50$

ratio, which can be conclude two copper salt molecules are ligated per ligand molecule.

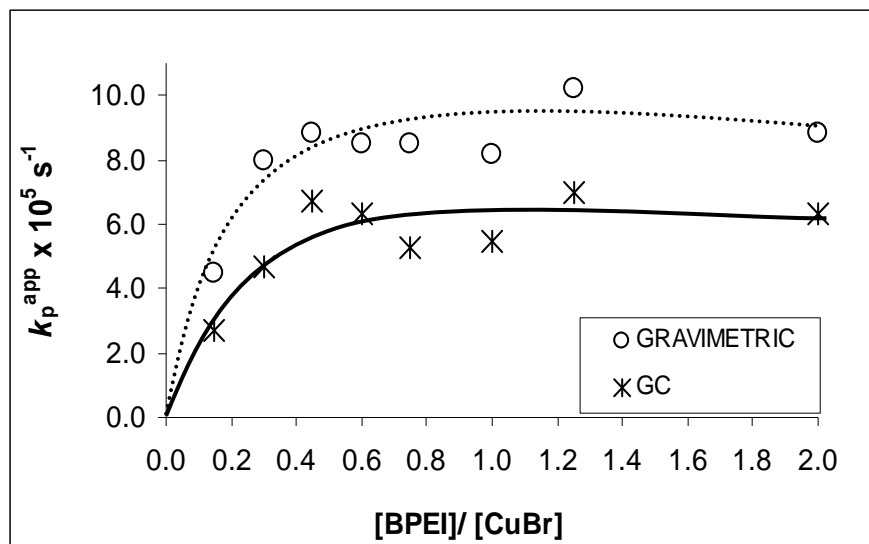


**Figure 4.7.**  $[\text{BPEI}]/[\text{CuBr}]$  versus  $k_p^{\text{app}}$  for ATRP of Styrene for different BPEI ligand ratios.  $[\text{St}]$ : 5.7 mol  $\text{l}^{-1}$  in toluene at 110 °C.  $[\text{St}]_0/[\text{EBrP}]_0/[\text{CuBr}]_0/[\text{BPEI}]_0 = 200/1/1/x$ .

The rate of polymerization depended on the nature of the nitrogen-binding site of the ligand. In order to compare the effect of APEIs with well known ATRP ligands, ATRPs of St carried out under the similar experimental conditions by using ALAL's, DiNBpy PMDETA, ME<sub>6</sub>Tren and BPy are listed in Table 4.3. All of the kinetic curves of these ligands show linearity. In these ATRP reactions of St, homogeneity was achieved by using PEDETA, PBDETA, PHDETA, HETETA, HBTETA, HHTETA, EPEI, BPEI, ME<sub>6</sub>-Tren and dNbpy ligands [47].

So that APEI have similar structure with PEDETA, PBDETA, PHDETA, HETETA, HBTETA and HHTETA. It is seen from the table that,  $k_p^{\text{app}}$  value is increasing by an increase in the number of coordinating sites, and decreasing by an increase in the number of linking carbon atoms. Even the concentrations values of monomers are less in polymerizations using APEI ligands then the others ALALs,  $k_p^{\text{app}}$  value of APEI would have the same place in the coordinating sites and linking carbon atoms order, by considering dilution parameter in the rate equation of controlled polymerization.

**Table 4.2** ATRP of Styrene for Different Ligand (BPEI) Ratios<sup>a</sup>

Run	[BPEI]/[CuBr]	Time <sup>b</sup> (min)	Conv. <sup>b</sup> (%)	$M_{n,\text{th}}^{\text{b}}$ (g mol <sup>-1</sup> )	$M_{n,\text{GPC}}^{\text{b}}$ (g mol <sup>-1</sup> )	$M_w/M_n^{\text{b}}$	$k_p^{\text{app}}$ (10 <sup>-5</sup> s <sup>-1</sup> ) <i>c</i>	<i>d</i>
St7	0.15	330	42.4	9010	15600	1.22	2.7	4.5
St8	0.30	270	55.6	11760	11300	1.22	4.7	8.0
St9	0.45	270	67.3	14180	13900	1.27	6.7	8.8
St10	0.60	270	68.2	14390	17200	1.36	6.3	8.5
St11	0.75	270	62.2	13180	14600	1.24	5.3	8.5
St12	1.00	270	59.1	12480	16700	1.27	5.5	8.2
St13	1.25	270	68.2	14400	15600	1.29	7.0	10.2
St14	2.00	270	65.7	13880	20200	1.4	6.3	8.8

<sup>a</sup> [St]<sub>o</sub>: 5.7 mol L<sup>-1</sup> in toluene at 110 °C. [St]<sub>o</sub>/[EBrP]<sub>o</sub>/[CuBr]<sub>o</sub>/[BPEI]<sub>o</sub> = 200/1/1/x.

<sup>b</sup> Last point of kinetic data from GC measurements. Molecular weights were measured by GPC using polystyrene standards.

<sup>c</sup> GC Measurements

<sup>d</sup> Gravimetric Measurements

**Table 4.3** ATRP of Styrene for Different Amine Ligand [47]

Entry	Ligand	Time (min)	Conv. <sup>d</sup> (%)	$M_{n,\text{th}}^d$	$M_n^d$	$M_w/M_n$	$k_p^{\text{app}} (10^{-4} \cdot \text{s}^{-1})$	Ini eff. (f)
1	PEDETA <sup>a</sup>	210	71	14800	17500	1.10	0.87	0.81
2	PBDETA <sup>a</sup>	210	53	11050	11500	1.20	0.58	0.96
3	PHDETA <sup>a</sup>	210	50	10400	14300	1.07	0.52	0.73
4	HETETA <sup>a</sup>	210	83	17300	19300	1.17	1.15	0.90
5	HBTETA <sup>a</sup>	210	73	15200	16500	1.19	0.87	0.92
6	HHTETA <sup>a</sup>	210	71	14800	14300	1.23	0.80	1.00
7	EPEI <sup>b</sup>	240	87	18220	24600	1.38	1.60	0.74
8	BPEI <sup>c</sup>	270	59	12480	16700	1.27	0.55	0.75
9	DiNBpy <sup>a</sup>	420	20	4150	2800	1.10	0.12	>1.00
10	ME <sub>6</sub> Tren <sup>a</sup>	210	54	13400	27000	1.03	0.78	0.49
11	PMDETA <sup>a</sup>	210	63	13100	12600	1.05	0.78	1.00
12	BPy <sup>a</sup>	300	24	5000	3200	1.21	0.15	>1.00

<sup>a</sup> [St]<sub>o</sub>: 7.91 mol L<sup>-1</sup> in anisole at 110 °C. [St]<sub>o</sub>/[EBrP]<sub>o</sub>/[CuBr]<sub>o</sub>/[Ligand]<sub>o</sub> = 200/1/1/1.<sup>b</sup> [St]<sub>o</sub>: 5.70 mol L<sup>-1</sup> in anisole at 110 °C. [St]<sub>o</sub>/[EBrP]<sub>o</sub>/[CuBr]<sub>o</sub>/[EPEI]<sub>o</sub> = 200/1/1/1.<sup>c</sup> [St]<sub>o</sub>: 5.70 mol L<sup>-1</sup> in toluene at 110 °C. [St]<sub>o</sub>/[EBrP]<sub>o</sub>/[CuBr]<sub>o</sub>/[BPEI]<sub>o</sub> = 200/1/1/1<sup>d</sup> Last point of the kinetic data.

#### 4.4 ATRP of Methyl Methacrylate for Different Ligand Ratio

ATRP of MMA was carried out with different ligand ratios under similar conditions which MMA (4.60 mol L<sup>-1</sup>) CuBr (5.3x10<sup>-2</sup> mol L<sup>-1</sup>), EBrIB (2.3x10<sup>-2</sup> mol L<sup>-1</sup>) in anisole (100 % v/v), and BPEI were used in these ATRP reactions (Figure 4.8). Polymerizations were carried out at 80°C and 400 rpm.

All the polymerization of MMA were homogeneous and light green color were observed during the polymerization, which signified that Cu(I) salt and ligand complex was dominated the reaction medium.

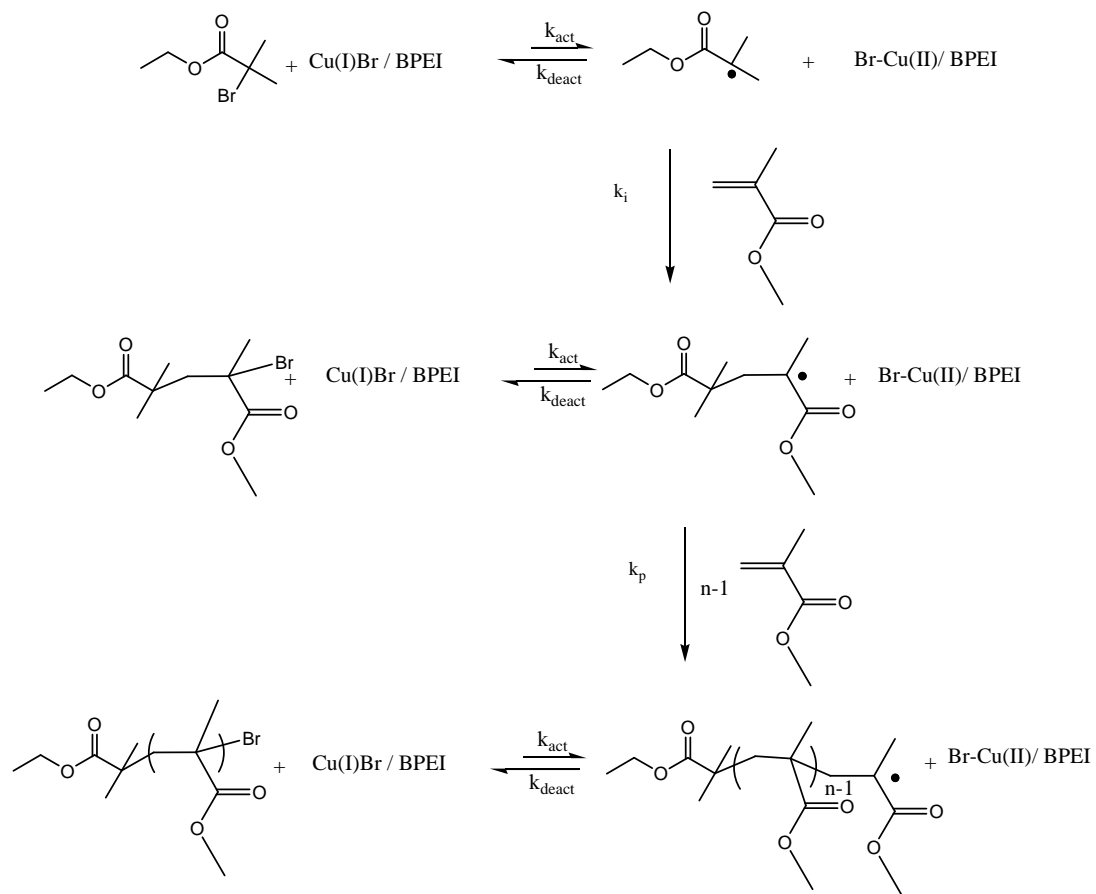


**Figure 4.8.** ATRP of Methyl Methacrylate by Using BPEI Ligand.

The semi-logarithmic kinetic plots ( $\ln([M]_0/[M])$  versus time) of ATRP reaction of MMA are shown in Appendix A, (Figures A.15-A.21) for different (BPEI) ligand ratios. Where,  $\ln([M]_0/[M])$  are determined from the conversion calculation of GC measurements, which can be calculated as follows;

$$\% \text{ Conversion} = [1 - (M_t \times \text{Sol}_0 / M_0 \times \text{Sol}_t)] \times 100$$

Where,  $M_o$ ,  $M_t$ ,  $Sol_o$  and  $Sol_t$  are pick area of the monomer and solvent measured from GC at initial time and the time that sample is taken, respectively.

It is clearly seen that a straight line is observed indicating that the first order kinetics with respect to the monomer concentration and demonstrates that active center concentration is constant during the polymerization. This result reveals that termination is absent or negligible.

Molecular weight of polymer versus conversion plots were shown in Appendix B, (Figures B.15-B.16) representatively for 0.30 and 1.00 [BPEI]/[CuBr] ratios. It is seen from figures, linear relationship indicates that transfer reactions are absent or insignificant. Measured molecular weights of the polymer are found close to the theoretical ones. Theoretical molecular weights were calculated as follows;

$$M_{n,th} = ([M]_o/[I]_o) \times (\% \text{ Conversion}/100) \times (Mw)_o + (Mw)_I$$

Where,  $(Mw)_o$  and  $(Mw)_I$  are the molecular weight of the monomer and initiator respectively,  $([M]_o/[I]_o)$  is the initial monomer, and initiator concentrations ratio.

Refractive index versus solvent elution plots in GPC traces shown in appendix C, (Figures C.15-C.16) as representatively for 0.30 and 1.00 ratios [BPEI]/[CuBr] indicates that molecular weight increases by time.

The comparison of results of MMA polymerization for different BPEI ligand ratios are presented in Table 3. It is observed from Figure 4.9 that  $k_p^{app}$  is increasing by increase in [BPEI]/[CuBr] ratio, then reach plato value around [BPEI]/[CuBr]=0.50 ratio, which can be concluded two copper salt molecules are ligated per ligand molecule.

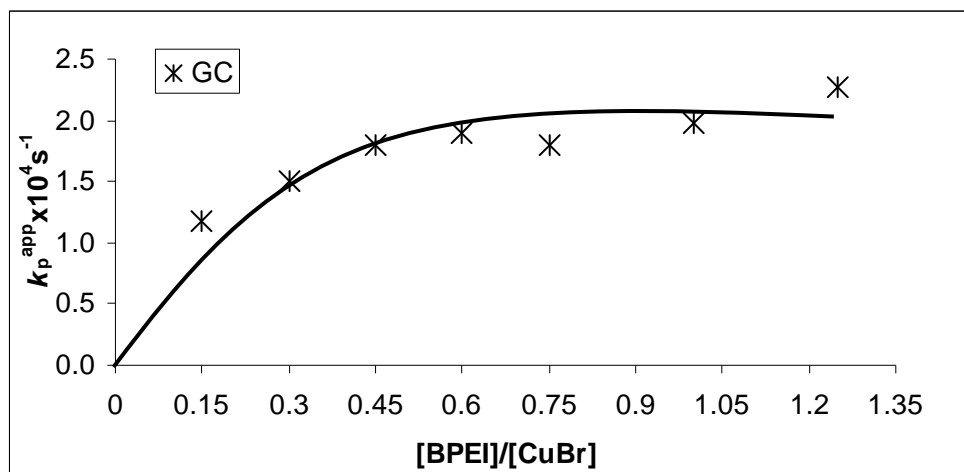


**Figure 4.9.**  $[\text{BPEI}]/[\text{CuBr}]$  versus  $k_p^{\text{app}}$  for ATRP of Methyl Methacrylate at  $80^\circ\text{C}$ .  $[\text{MMA}]_0: 4.60 \text{ mol L}^{-1}$  in anisole  $[\text{MMA}]_0/[\text{EBrIB}]_0/[\text{CuBr}]_0/[\text{BPEI}]_0 = 200/1/1/x$ .

The rate of polymerization depended on the nature of the nitrogen-binding site of the ligand. In order to compare the effect of APEIs with well known ATRP ligands, ATRPs of MMA, carried out under the similar experimental conditions, by using ALAL's, DiNBpy PMDETA, ME<sub>6</sub>Tren and BPy are listed in Table 4.3. All of the kinetic curves of these ligands show linearity. In these ATRP reactions of MMA, homogeneity was achieved by using PEDETA, PBDETA, PHDETA, HETETA, HBTETA, HHTETA, BPEI, ME<sub>6</sub>-Tren and dNbpy ligands [47].

So that BPEI have similar structure with PEDETA, PBDETA, PHDETA, HETETA, HBTETA and HHTETA. It is seen from the table that,  $k_p^{\text{app}}$  value of PBDETA, HBTETA and BPEI is decreasing respectively, which indicates that the number of coordinating sites in activity order is reverse for MMA compared to St.

**Table 4.4** ATRP of Methyl Methacrylate for Different Ligand (BPEI) Ratios<sup>a</sup>

Run	[EPEI]/[CuBr]	Time <sup>b</sup> (min)	Conv. <sup>b</sup> (%)	$M_{n,\text{th}}^{\text{b}}$ (g mol <sup>-1</sup> )	$M_{n,\text{GPC}}^{\text{b}}$ (g mol <sup>-1</sup> )	$M_w/M_n^{\text{b}}$	$k_p^{\text{app}}$ (10 <sup>-4</sup> s <sup>-1</sup> )
MMA1	0.15	100	49.8	9960	12200	1.28	1.18
MMA2	0.30	100	56.9	11390	18700	1.17	1.50
MMA3	0.45	100	66.0	13210	18980	1.18	1.80
MMA4	0.60	100	66.5	13320	18100	1.13	1.90
MMA5	0.75	100	70.5	14120	15400	1.18	1.80
MMA6	1.00	100	72.0	14340	15970	1.21	1.98
MMA7	1.25	100	75.3	15090	16390	1.19	2.27

<sup>a</sup> [MMA]<sub>0</sub>: 4.60 mol L<sup>-1</sup> in anisole at 80°C. [MMA]<sub>0</sub>/[EBrIB]<sub>0</sub>/[CuBr]<sub>0</sub>/[BPEI]<sub>0</sub>=200/1/1 /x.

<sup>b</sup> Last point of kinetic datas. Molecular weights were measured by GPC using poly(methyl methacrylate) standards.

**Table 4.5** ATRP of Methyl Methacrylate for Different Amine Ligands [47]

Entry	Ligand	Time (min)	Conv. <sup>c</sup> (%)	$M_{n,th}^c$	$M_n^c$	$M_w/M_n$	$k_p^{app}$ ( $10^4 \cdot s^{-1}$ )	Ini eff. (f)
1	PEDETA <sup>a</sup>	100	84	16800	23700	1.21	3.30	0.71
2	PBDETA <sup>a</sup>	100	82	16400	21400	1.15	2.85	0.72
3	PHDETA <sup>a</sup>	100	85	17000	23600	1.11	2.75	0.74
4	HETETA <sup>a</sup>	100	82	16400	22100	1.19	2.63	0.74
5	HBTTETA <sup>a</sup>	100	79	16800	22500	1.24	2.42	0.75
6	HHTETA <sup>a</sup>	100	76	16200	23800	1.10	2.17	0.68
7	BPEI <sup>b</sup>	100	72	14340	16000	1.21	1.98	0.90
8	DiNBpy <sup>a</sup>	360	51	10200	9900	1.20	0.42	1.00
9	ME <sub>6</sub> -Tren <sup>a</sup>	150	67	13400	27000	1.59	1.27	0.49
10	PMDETA <sup>a</sup>	100	71	14200	24000	1.11	2.30	0.60
11	BPy <sup>a</sup>	150	73	14600	16800	1.33	1.88	0.87

<sup>a</sup> [MMA]<sub>0</sub>: 6.09 mol L<sup>-1</sup> in anisole at 80 °C; [MMA]<sub>0</sub>/[EBrIB]<sub>0</sub>/[CuBr]<sub>0</sub>/[Ligand]<sub>0</sub> = 200/1/1/1.

<sup>b</sup> [MMA]<sub>0</sub>: 4.60 mol L<sup>-1</sup> in anisole at 80 °C. [MMA]<sub>0</sub>/[EBrIB]<sub>0</sub>/[CuBr]<sub>0</sub>/[BPEI]<sub>0</sub> = 200/1/1/1.

<sup>c</sup> Last point of the kinetic data.

## 5. CONCLUSION and RECOMMENDATIONS

In this study ethylated and butylated polydentate nitrogen ligands (alkylated polyethyleneimine) were synthesized by a simple reaction of alkylation of amines.. Both of APEIs were characterized by  $^1\text{H-NMR}$ . ATRP reaction of St and MMA were performed by using both of ethylated and butylated poly(ethyleneimine) ligands in the presence of CuBr as co-catalyst and EBrP and EBrIB as initiators.

Homogeneous reaction conditions and light green color were obtained by using APEI ligands for ATRP of St and MMA. It is concluded from concentration effects of ligands that  $k_p^{\text{app}}$  is increasing until the [APEI]/[CuBr] is around 0.5, than reach the plato value, which explain that each APEI molecule ligates two copper salt.

The simple synthesis of a new class of ligands, alkylated poly(ethyleneimine), (APEI), was demonstrated. The investigation of their concentration effect on ATRP might contribute an attraction in polymer research groups by providing homogenous polymerization reaction medium and relatively fast polymerization rates resulted well-defined polymers.

## 6. REFERENCES

- [1] **Matyjaszewski, K. and Xia, J.**, 2001. Atom Transfer Radical Polymerization, *ACS, Chem Rev.*, **101**, 2921–2990.
- [2] **Ding, S., Shen, Y., and Radosz, M.**, 2004. A New tetridentate ligand for atom transfer radical polymerization, *J. Polym. Sci., Part A: Polym. Chem.*, **42**, 3553–3562.
- [3] **Wang, J. S. and Matyjaszewski, K.**, 1995. Controlled living radical polymerization-halogen atom transfer radical polymerization promoted by a Cu(I)/Cu(II) redox process, *Macromolecules*, **28**, 7901–7910.
- [4] **Wang, J. S. and Matyjaszewski, K.**, 1995. Controlled living radical polymerization-ATRP in the presence of transition-metal complexes, *J. Am. Chem. Soc.*, **117**, 5614–5615.
- [5] **Percec, V. and Barboiu, B.**, 1995. “Living” radical polymerization of styrene initiated by arensulfonyl Chlorides and CuI(bpy)nCl, *Macromolecules*, **28**, 7970–7972.
- [6] **Matyjaszewski, K.**, 1998. Ed. Controlled Radical Polymerization, ACS Symposium Series No. 685, American Chemical Society: Washington, DC.
- [7] **Matyjaszewski, K.**, 2000. Ed. Controlled/Living Radical Polymerization. Progress in ATRP, NMP, and RAFT, ACS Symposium Series No. 768, American Chemical Society: Washington, DC.
- [8] **Patten, T. E. and Matyjaszewski, K.**, 1998. ATRP and synthesis of polymeric materials, *Adv. Mater.*, **10**, 901.
- [9] **Matyjaszewski, K.**, 1999. Transition metal analysis in controlled radical polymerization: ATRP, *Chem. Eur. J.*, **5**, 3095.
- [10] **Patten, T. E. and Matyjaszewski, K.**, 1999. Cu(I) catalyzed ATRP, *Acc. Chem. Res.*, **32**, 895–903.
- [11] **Kamigaito, M., Ando, T. and Sawamoto, M.**, 2001. Metal-catalyzed living radical polymerization, *Chem. Rev.*, **101**, 3689–3746.

[12] **Matyjaszewski, K. and Xia, J.**, 2002. In *Handbook of Radical Polymerization*, Matyjaszewski, K., Davis, T. P., Eds., p 602, Wiley: New York

[13] **Davis, K.A. and Matyjaszewski, K.**, 2000. ATRP of tert-butyl acrylate and preparation of block copolymers, *Macromolecules*, **33**, 4039.

[14] **Matyjaszewski, K.**, 2003. *Macromol.Symp.* **195**, 25-31.

[15] **Fischer, H.** 1999. The persistent radical effect in controlled radical polymerizations, *J. Polym. Sci., Part A: Polym. Chem.*, **37**, 1885.

[16] **Fischer, H.**, 1997. The persistent radical effect in "living" radical polymerization, *Macromolecules*, **30**, 5666.

[17] **Shipp, D. A. and Matyjaszewski, K.**, 2000. Kinetic analysis of controlled/"living" radical polymerizations by simulations. 2. apparent external orders of reactants in atom transfer radical polymerization, *Macromolecules*, **33**, 1553.

[18] **Matyjaszewski, K., Patten, T. E. and Xia, J.**, 1997. Controlled/living radical polymerization-kinetics of the homogeneous atom transfer radical polymerization of styrene, *J. Am. Chem. Soc.*, **119**, 674.

[19] **Davis, K., Paik, H.-j. and Matyjaszewski, K.**, 1999. Kinetic investigation of the atom transfer radical polymerization of methyl acrylate, *Macromolecules*, **32**, 1767.

[20] **Wang, J. L., Grimaud, T. and Matyjaszewski, K.**, 1997. Kinetic study of the homogeneous atom transfer radical polymerization of methyl methacrylate, *Macromolecules*, **30**, 6507–6512.

[21] **Percec, V., Barboiu, B. and Kim, H.-J.**, 1998. Arenesulfonyl halides: A universal class of functional initiators for metal-catalyzed "living" radical polymerization of styrene(s), methacrylates, and acrylates, *J. Am. Chem. Soc.*, **120**, 305.

[22] **Percec, V., Barboiu, B., Neumann, A. and Ronda, A.**, 1996. Metal-catalyzed "living" radical polymerization of styrene initiated with arenenesulfonyl chlorides. From heterogeneous to homogeneous catalysis, *Macromolecules*, **29**, 3665.

[23] **Levy, A. T., Olmstead, M. M. and Patten, T. E.**, 2000. Synthesis, characterization, and polymerization activity of [bis(4,4'-bis(neophyldimethylsilylmethyl)-2,2'-bipyridyl)copper(I)]<sup>+</sup>CuBr<sub>2</sub><sup>-</sup> and implications for copper(I) catalyst structures in atom transfer radical polymerization, *Inorg. Chem.*, **39**, 1628.

[24] **Hester A. J. F., Banerjee P., Won Y.-Y., Akthakul A., Acar M. H. and Mayes A. M.**, 2002. ATRP of amphiphilic graft copolymers based on PVDF and their use as membrane additives, *Macromolecules*, **35**, 7652.

[25] **Inceoglu S., Olugebefola S. C., Acar M. H. and Mayes A. M.**, 2004. Atom transfer radical polymerization using poly(vinylidenefluoride) as macroinitiator, *Designed Monomers and Polymers*, **7**, 181.

[26] **Xia, J. and Matyjaszewski, K.**, 1997. Controlled/"living" radical polymerization. Atom transfer radical polymerization using multidentate amine ligands, *Macromolecules*, **30**, 7697–7700.

[27] **Xia, J. H. and Matyjaszewski, K.**, 1997. Controlled/"living" radical polymerization. Homogeneous reverse atom transfer radical polymerization using AIBN as the initiator, *Macromolecules*, **30**, 7692–7696.

[28] **Kickelbick, G. and Matyjaszewski, K.**, 1999. 4,4",4"-Tris(5-nonyl)-2,2':6',2"-terpyridine as ligand in atom transfer radical polymerization (ATRP), *Macromol Rapid Commun*, **20**, 341–346.

[29] **Matyjaszewski, K., Goebelt, B., Paik, H.-J. and Horwitz, C. P.**, 2001. Tridentate nitrogen-based ligands in Cu-based ATRP: A structure-activity study, *Macromolecules*, **34**, 430–440.

[30] **Destarac, M., Bessiere, J.-M. and Boutevin, B.**, 1997. Transition metal catalyzed atom Transfer Radical Polymerization (ATRP): from heterogeneous to homogeneous catalysis using 1,10-phenanthroline and its derivatives as new copper(I) ligands, *Macromol Rapid Commun*, **18**, 967–974.

[31] **Xia, J. and Matyjaszewski, K.**, 1999. Homogeneous reverse ATRP of Styrene initiated by peroxides, *Macromolecules*, **32**, 2434–2437.

[32] **Haddleton, D. M., Jasieczek, C. B., Hannon, M. J. and Shooter, A. J.**, 1997. Atom transfer radical polymerization of methyl methacrylate initiated by alkyl bromide and 2-Pyridinecarbaldehyde imine copper(I) complexes, *Macromolecules*, **30**, 2190–2193.

[33] **Amass, A. J., Wyres, C. A., Colclough, E. and Hohn, I. M.**, 2000. N-alkyl-2-pyridinemethanimine mediated atom transfer radical polymerization of styrene: the transition from heterogeneous to homogeneous catalysis, *Polymer*, **41**, 1697–1702.

[34] **Haddleton, D. M., Crossman, M. C., Dana, B. H., Duncalf, D. J., Heming, A. M., Kukulj, D. and Shooter, A. J.**, 1999. Atom transfer polymerization of methyl methacrylate mediated by alkylpyridylmethanimine type ligands, copper(I)bromide, and alkyl halides in hydrocarbon solution, *Macromolecules*, **32**, 2110–2119.

[35] **Clark, A. J., Battle, G. M., Heming, A. M., Haddleton, D. M. and Bridge, A.**, 2001. Ligand electronic effects on rates of copper mediated atom transfer radical cyclization and polymerization, *Tetrahedron Lett*, **42**, 2003–2005.

[36] **Wang, X. S., Malet, F. L. G., Armes, S. P., Haddleton, D. M. and Perrier, S.**, 2001. Unexpected viability of pyridyl methanimine-based ligands for transition-metal-mediated living radical polymerization in aqueous media at ambient temperature, *Macromolecules*, **34**, 162–164.

[37] **Shen, Y., Zhu, S., Zeng, F. and Pelton, R. H.**, 2000. Atom transfer radical polymerization of alkyl methacrylates using T-triazine as ligand, *Macromol. Chem. Phys.*, **201**, 1169–1175.

[38] **Shen, Y., Zhu, S. and Pelton, R. H.**, 2001. Soluble and recoverable support for copper bromide-mediated living radical polymerization, *Macromolecules*, **34**, 3182–3185.

[39] **Shen, Y. and Zhu, S.**, 2001. Atom transfer radical polymerization of methyl methacrylate mediated by copper bromide-tetraethyldiethylenetriamine grafted on soluble and recoverable poly(ethylene-*b*-ethylene glycol) supports, *Macromolecules*, **34**, 8603–8609.

[40] **Xia, J., Gaynor, S. G. and Matyjaszewski, K.**, 1998. Controlled/living radical polymerization. ATRP of acrylates at ambient temperature, *Macromolecules*, **31**, 5958–5959.

[41] **Gromada, J. and Matyjaszewski, K.**, 2002. Polym. Prepr. (Am. Chem. Soc. Div. Polym. Chem.), **43**(2), 195–196.

[42] **Shen, Y. and Zhu, S.**, 2002. Continuous atom transfer radical block copolymerization of methacrylate, *A. I. Ch. E. J.*, **48**, 2609–2619.

[43] **Zeng, F., Shen, Y., Zhu, S. and Pelton, R.**, 2000. Synthesis and characterization of comb-branched polyelectrolytes. 1. Preparation of cationic macromonomer of 2-(dimethylamino)ethyl methacrylate by atom transfer radical polymerization, *Macromolecules*, **33**, 1628–1635.

[44] **Xia, J., Zhang, X. and Matyjaszewski, K.**, 2000. In *Transition Metal Macromolecular Design*, Boffa, L. S., Novak, B. M., Eds., ACS Symposium Series 760, American Chemical Society: Washington, DC, pp 207–223.

[45] **Acar M. H. and Bicak N.**, 2003. Synthesis of hexylated triethylenetetramine: New ligand for homogeneous Atom Transfer Radical Polymerization, *J. Polym. Sci.-A-Polym. Chem.*, **41**, 1677.

[46] **Acar M.H., Becer C. R., Ondur H. A. and Inceoglu S.**, 2005. Synthesis of alkylated linear amine ligands and their effect on homogeneous atrp, *Polym. Prep.*, **46**, 433.

[47] **Acar M. H., Becer C. R., Ondur H. A. and Inceoglu S.**, 2006. Alkylated Linear Amine Ligands for Homogeneous AtomTransfer Radical Polymerization, Matyjaszewski, K., Ed, In *Controlled/ Living Radical Polymerization: From Synthesis to Materials*, ACS Symposium Series No. 994; American Chemical Society: Washington, DC, 97-110.

[48] **Gunnar N., and Walter H.**, 1998. Amphiphilic poly(ethyleneimine) based on long-chain alkyl bromides, *Macromol. Chem. and Phys.*, **199**, 1637.

[49] **Faucher S., Okrutny P., and Zhu S.**, 2006. Facile and effective purification of polymers produces by atom transfer radical polymerization via simple catalyst precipitation and microfiltration, *Macromolecules*, **39**, 3.

## APPENDIX A.

### SEMI-LOGARITHMIC KINETIC PLOTS

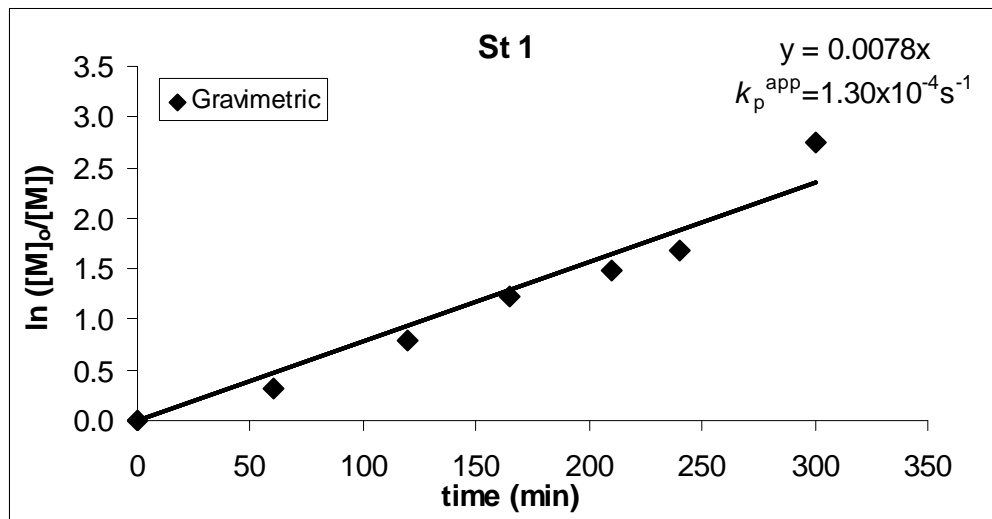


**Figure A.1.** Kinetic plot of St by ATRP using EPEI at 110 °C. [St]: 5.7 mol L<sup>-1</sup> in anisole [St]<sub>0</sub>/[EBrP]<sub>0</sub>/[CuBr]<sub>0</sub>/[EPEI]<sub>0</sub>=200/1/1/0.30

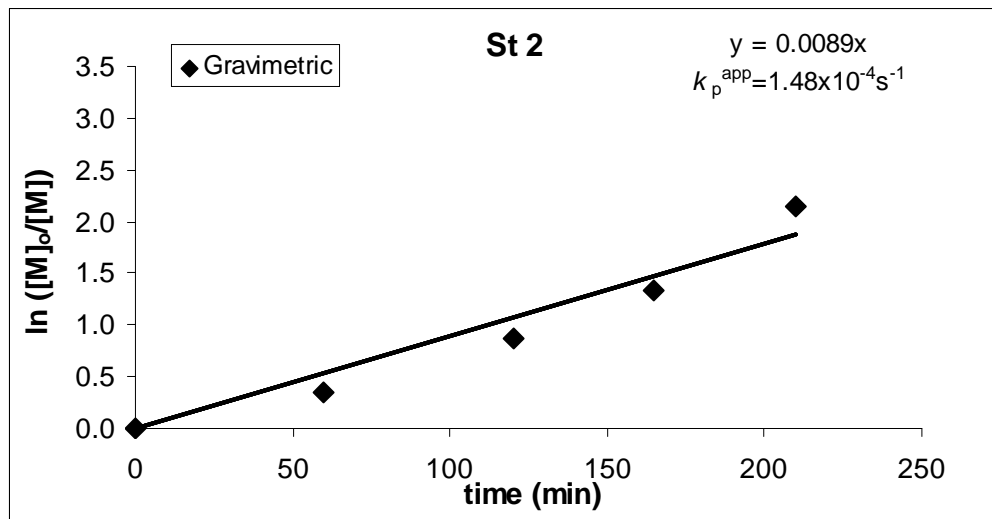


**Figure A.2.** Kinetic plot of St by ATRP using EPEI at 110 °C. [St]: 5.7 mol L<sup>-1</sup> in anisole [St]<sub>0</sub>/[EBrP]<sub>0</sub>/[CuBr]<sub>0</sub>/[EPEI]<sub>0</sub>=200/1/1/0.45

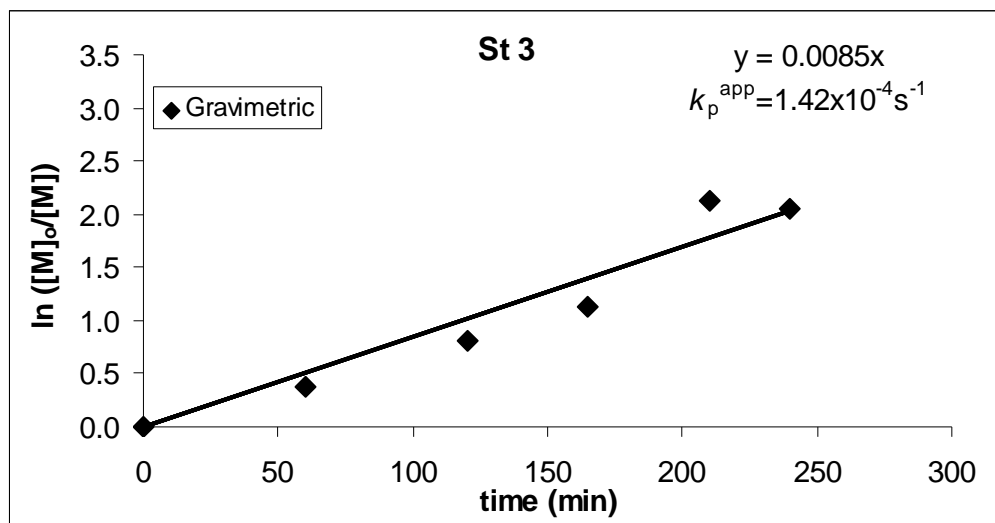


**Figure A.3.** Kinetic plot of St by ATRP using EPEI at 110 °C. [St]: 5.7 mol L<sup>-1</sup> in anisole [St]<sub>0</sub>/[EBrP]<sub>0</sub>/[CuBr]<sub>0</sub>/[EPEI]<sub>0</sub>=200/1/1/0.60

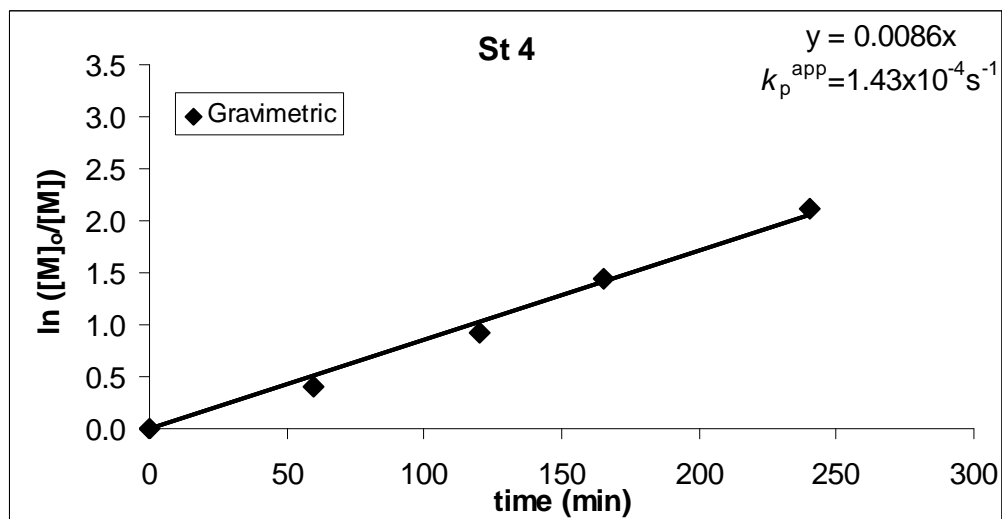


**Figure A.4.** Kinetic plot of St by ATRP using EPEI at 110 °C. [St]: 5.7 mol L<sup>-1</sup> in anisole [St]<sub>0</sub>/[EBrP]<sub>0</sub>/[CuBr]<sub>0</sub>/[EPEI]<sub>0</sub>=200/1/1/0.75

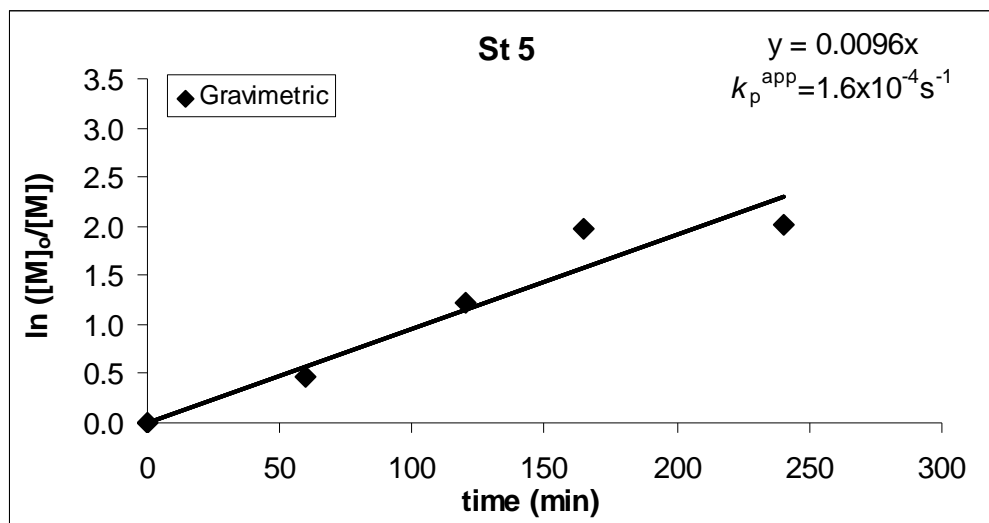


**Figure A.5.** Kinetic plot of St by ATRP using EPEI at 110 °C. [St]: 5.7 mol L<sup>-1</sup> in anisole [St]<sub>0</sub>/[EBrP]<sub>0</sub>/[CuBr]<sub>0</sub>/[EPEI]<sub>0</sub>=200/1/1/1.00

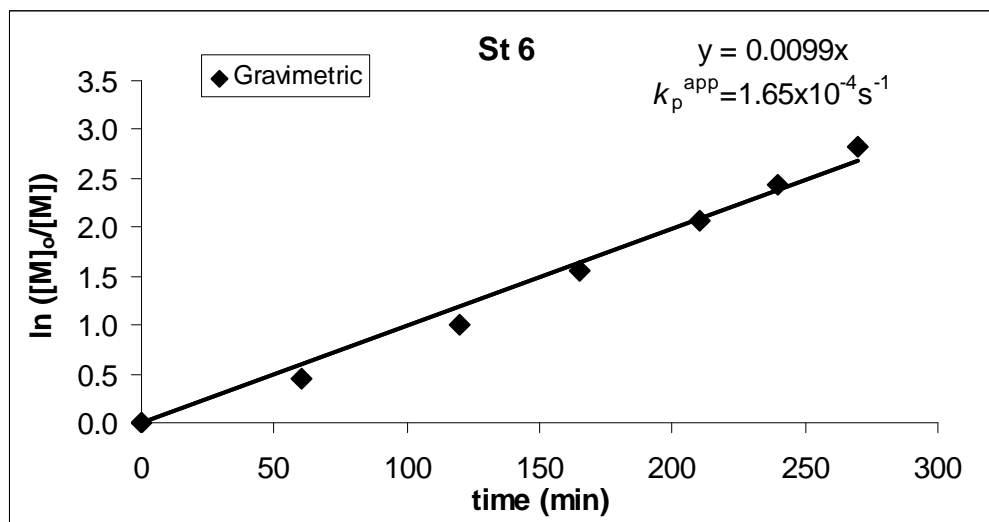


**Figure A.6.** Kinetic plot of St by ATRP using EPEI at 110 °C. [St]: 5.7 mol L<sup>-1</sup> in anisole [St]<sub>0</sub>/[EBrP]<sub>0</sub>/[CuBr]<sub>0</sub>/[EPEI]<sub>0</sub>=200/1/1/1.25

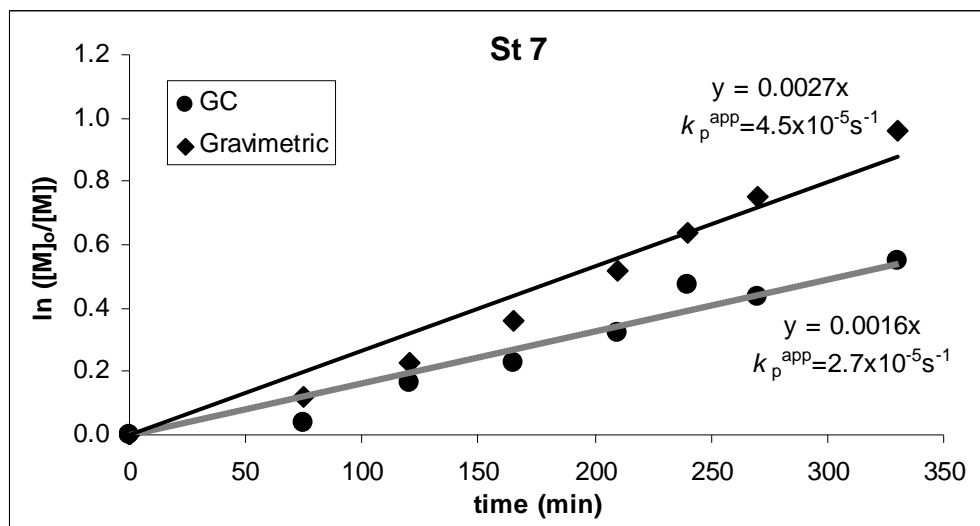


**Figure A.7.** Kinetic plot of St by ATRP using BPEI at 110 °C. [St]: 5.7 mol L<sup>-1</sup> in toluene [St]<sub>0</sub>/[EBrP]<sub>0</sub>/[CuBr]<sub>0</sub>/[BPEI]<sub>0</sub>=200/1/1/0.15

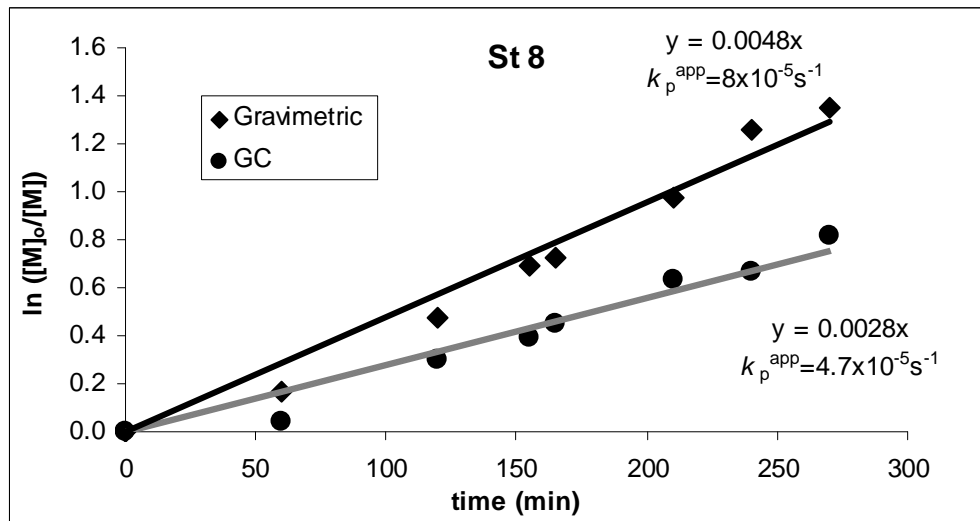


**Figure A.8.** Kinetic plot of St by ATRP using BPEI at 110 °C. [St]: 5.7 mol L<sup>-1</sup> in toluene [St]<sub>0</sub>/[EBrP]<sub>0</sub>/[CuBr]<sub>0</sub>/[BPEI]<sub>0</sub>=200/1/1/0.30

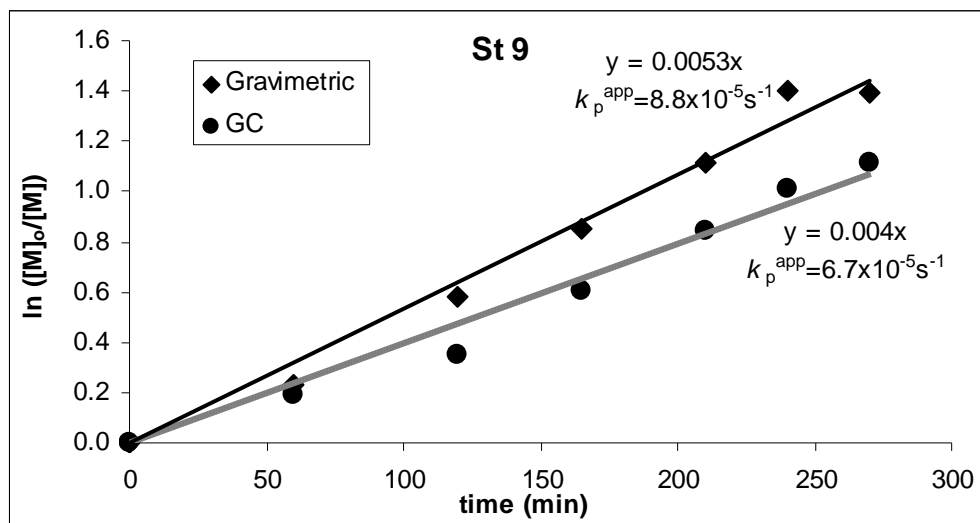


**Figure A.9.** Kinetic plot of St by ATRP using BPEI at 110 °C. [St]: 5.7 mol L<sup>-1</sup> in toluene [St]<sub>0</sub>/[EBrP]<sub>0</sub>/[CuBr]<sub>0</sub>/[BPEI]<sub>0</sub>=200/1/1/0.45

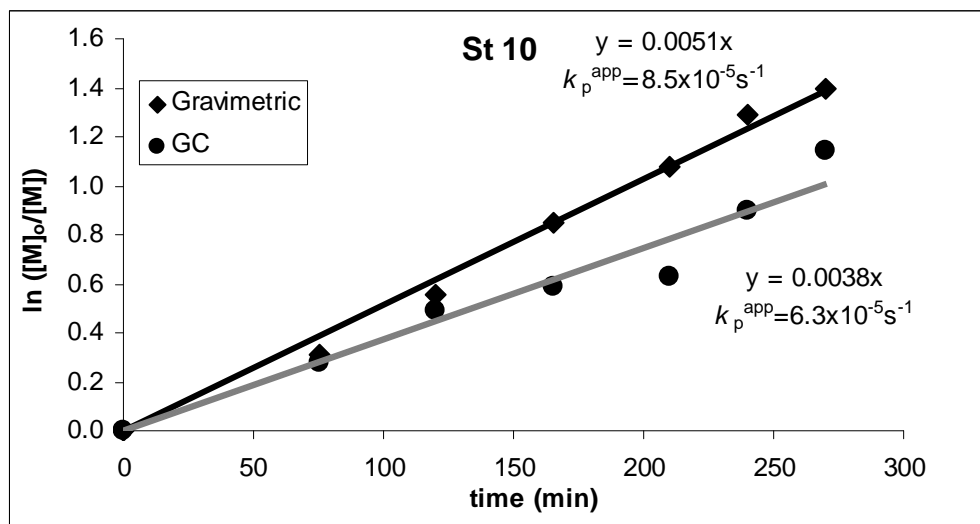


**Figure A.10.** Kinetic plot of St by ATRP using BPEI at 110 °C. [St]: 5.7 mol L<sup>-1</sup> in toluene [St]<sub>0</sub>/[EBrP]<sub>0</sub>/[CuBr]<sub>0</sub>/[BPEI]<sub>0</sub>=200/1/1/0.60

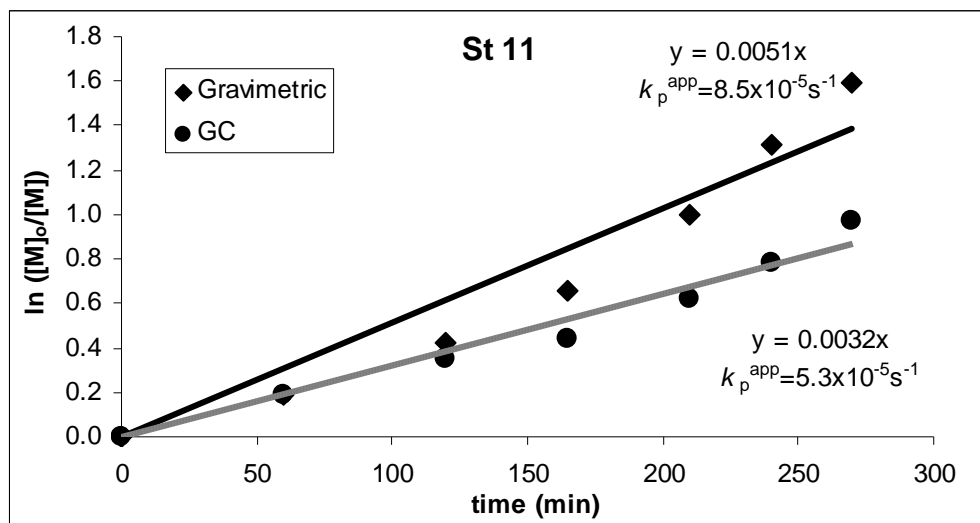


**Figure A.11.** Kinetic plot of St by ATRP using BPEI at 110 °C. [St]: 5.7 mol L<sup>-1</sup> in toluene [St]<sub>0</sub>/[EBrP]<sub>0</sub>/[CuBr]<sub>0</sub>/[BPEI]<sub>0</sub>=200/1/1/0.75

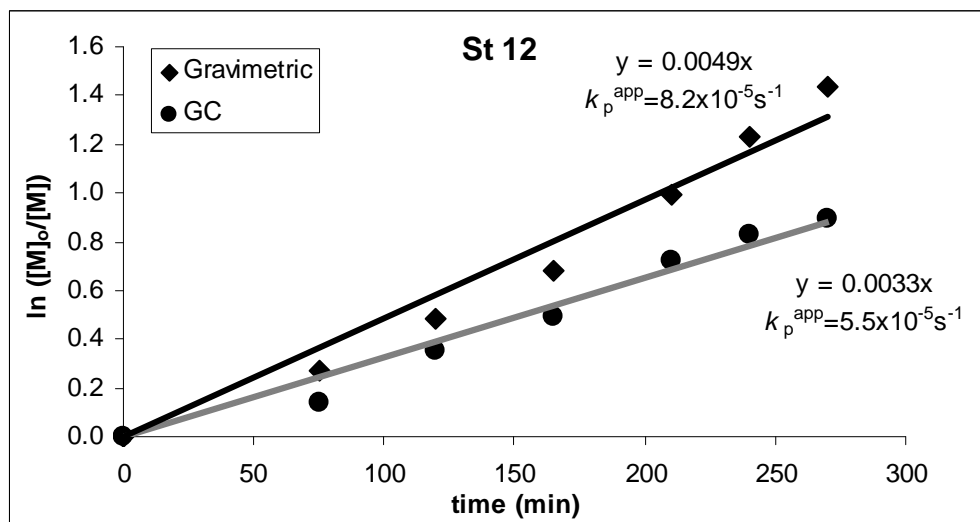


**Figure A.12.** Kinetic plot of St by ATRP using BPEI at 110 °C. [St]: 5.7 mol L<sup>-1</sup> in toluene [St]<sub>0</sub>/[EBrP]<sub>0</sub>/[CuBr]<sub>0</sub>/[BPEI]<sub>0</sub>=200/1/1/1.00

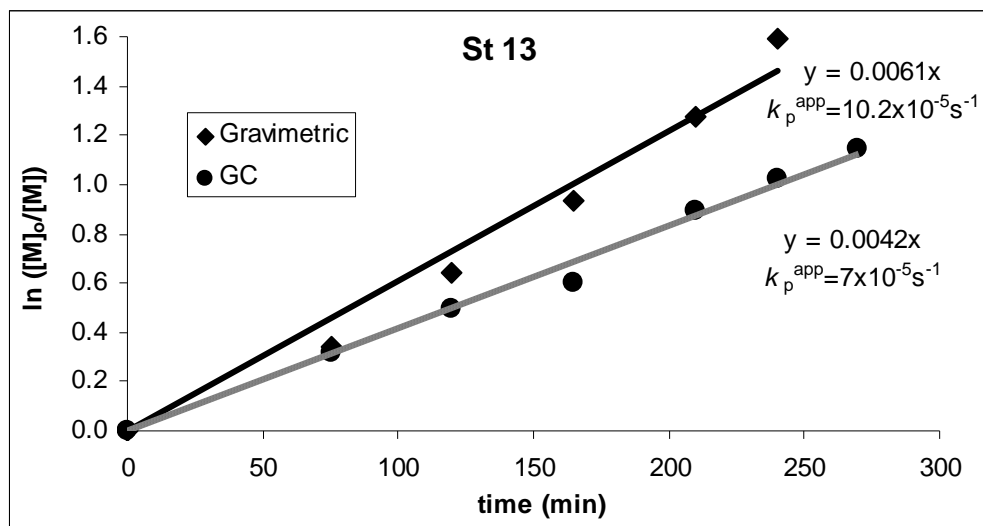


**Figure A.13.** Kinetic plot of St by ATRP using BPEI at 110 °C. [St]: 5.7 mol L<sup>-1</sup> in toluene [St]<sub>0</sub>/[EBrP]<sub>0</sub>/[CuBr]<sub>0</sub>/[BPEI]<sub>0</sub>=200/1/1/1.25

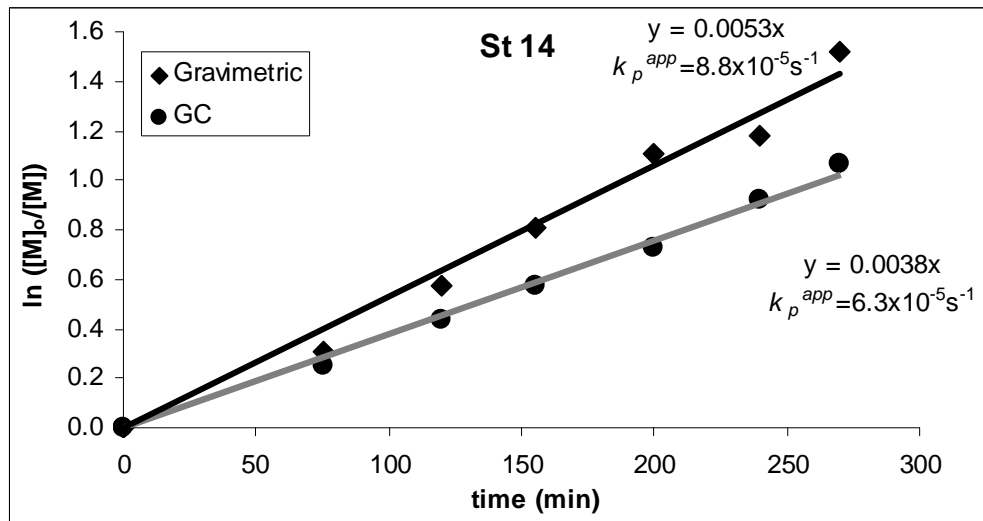


**Figure A.14.** Kinetic plot of St by ATRP using BPEI at 110 °C. [St]: 5.7 mol L<sup>-1</sup> in toluene [St]<sub>0</sub>/[EBrP]<sub>0</sub>/[CuBr]<sub>0</sub>/[BPEI]<sub>0</sub>=200/1/1/2.00

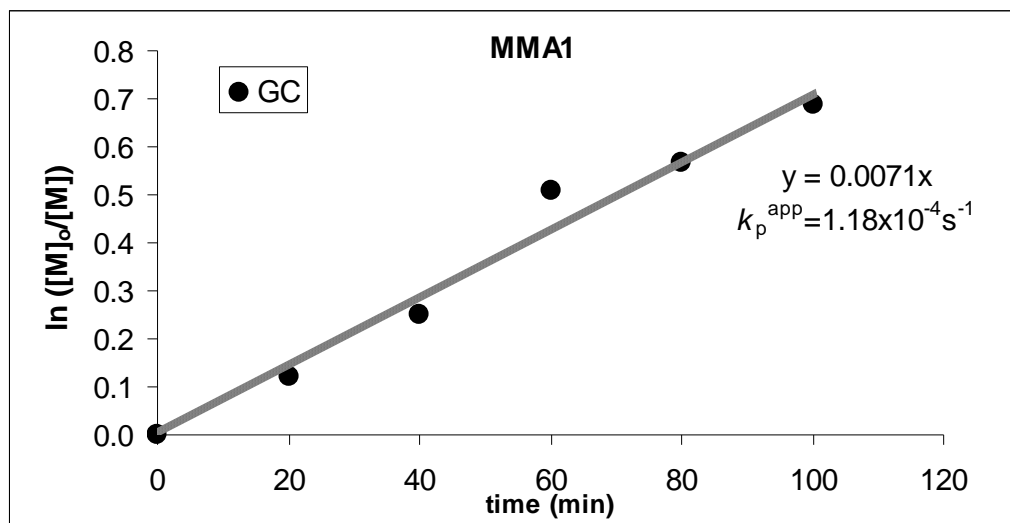


**Figure A.15.** Kinetic plot of MMA by ATRP using BPEI at 80 °C.  
 $[\text{MMA}]_0/[\text{EBrIB}]_0/[\text{CuBr}]_0/[\text{BPEI}]_0 = 200/1/1/0.15$   $[\text{MMA}]$ :4.60 mol L<sup>-1</sup> in anisole

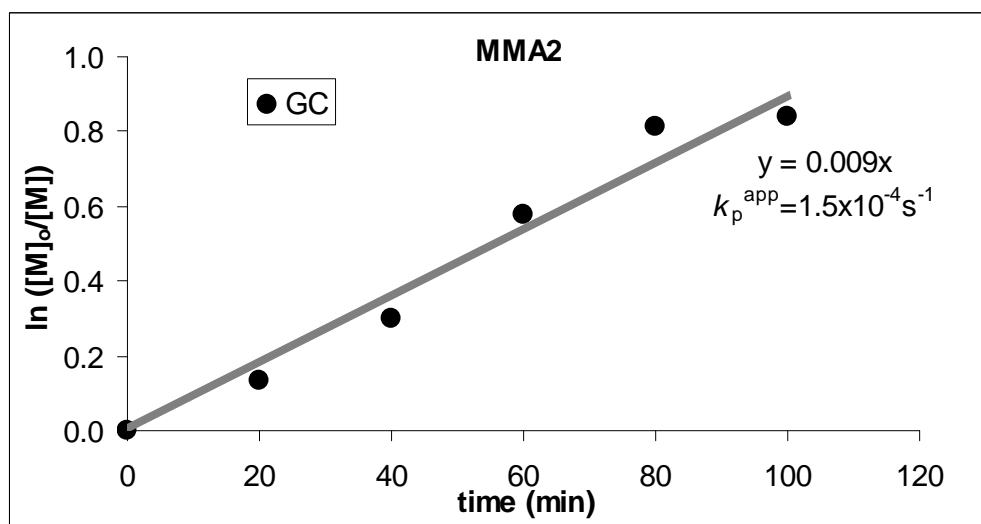


**Figure A.16.** Kinetic plot of MMA by ATRP using BPEI at 80 °C.  
 $[\text{MMA}]_0/[\text{EBrIB}]_0/[\text{CuBr}]_0/[\text{BPEI}]_0 = 200/1/1/0.30$   $[\text{MMA}]$ :4.60 mol L<sup>-1</sup> in anisole

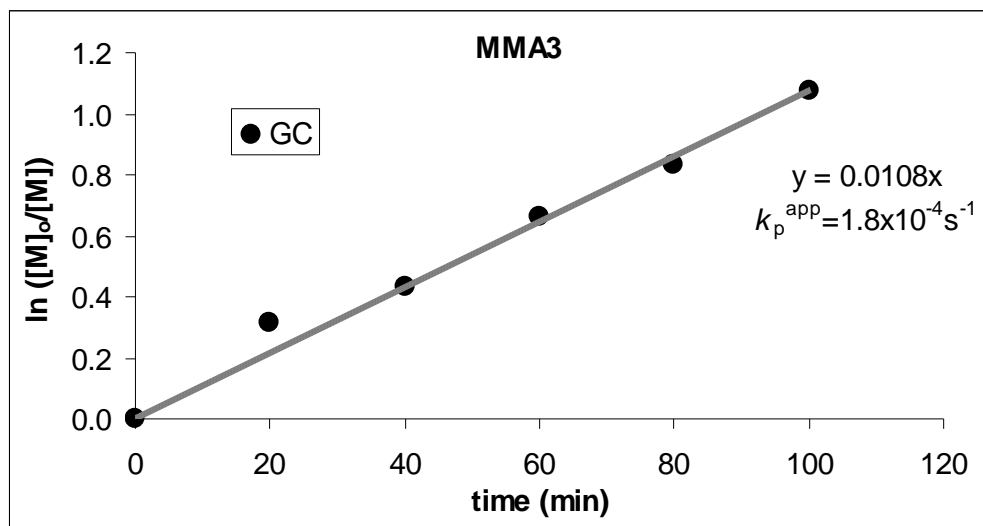


**Figure A.17.** Kinetic plot of MMA by ATRP using BPEI at 80 °C.  
 $[\text{MMA}]_0/[\text{EBrIB}]_0/[\text{CuBr}]_0/[\text{BPEI}]_0 = 200/1/1/0.45$   $[\text{MMA}]$ : 4.60 mol L<sup>-1</sup> in anisole

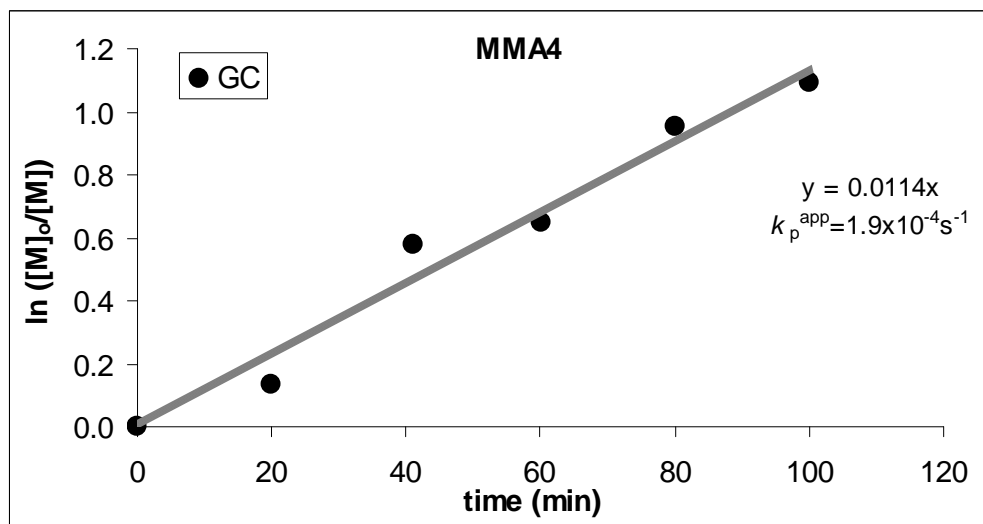


**Figure A.18.** Kinetic plot of MMA by ATRP using BPEI at 80 °C.  
 $[\text{MMA}]_0/[\text{EBrIB}]_0/[\text{CuBr}]_0/[\text{BPEI}]_0 = 200/1/1/0.60$   $[\text{MMA}]$ : 4.60 mol L<sup>-1</sup> in anisole

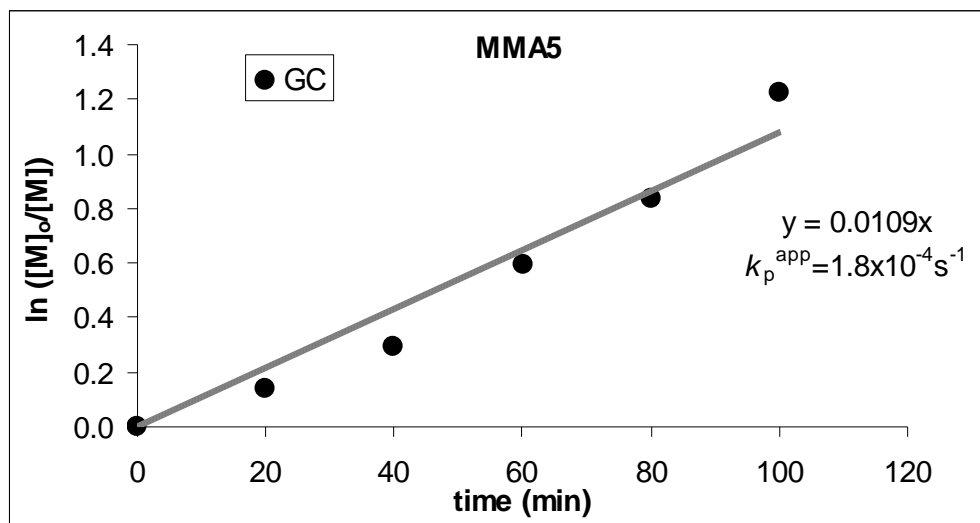


**Figure A.19.** Kinetic plot of MMA by ATRP using BPEI at 80 °C.  
 $[\text{MMA}]_0/[\text{EBrIB}]_0/[\text{CuBr}]_0/[\text{BPEI}]_0 = 200/1/1/0.75$   $[\text{MMA}] = 4.60 \text{ mol L}^{-1}$  in anisole

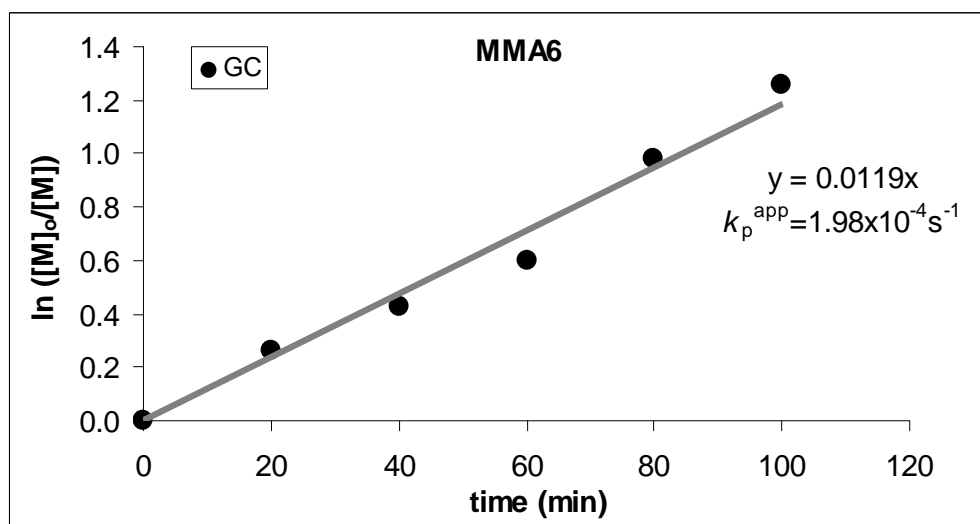


**Figure A.20.** Kinetic plot of MMA by ATRP using BPEI at 80 °C.  
 $[\text{MMA}]_0/[\text{EBrIB}]_0/[\text{CuBr}]_0/[\text{BPEI}]_0 = 200/1/1/1.00$   $[\text{MMA}] = 4.60 \text{ mol L}^{-1}$  in anisole

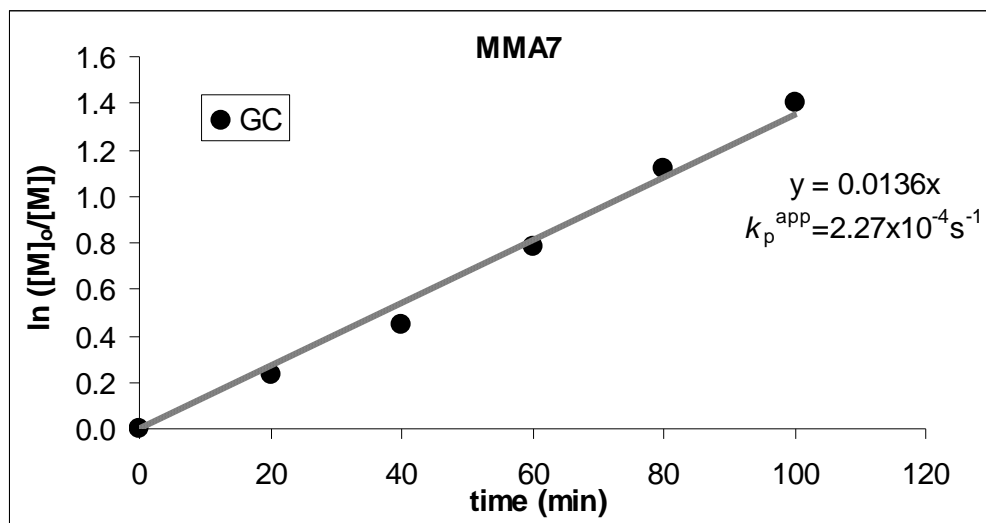


**Figure A.21.** Kinetic plot of MMA by ATRP using BPEI at 80 °C.  
 $[\text{MMA}]_0/[\text{EBrIB}]_0/[\text{CuBr}]_0/[\text{BPEI}]_0 = 200/1/1/1.25$   $[\text{MMA}] = 4.60 \text{ mol L}^{-1}$  in anisole

## APPENDIX B.

### MOLECULAR WEIGHT, MOLECULAR WEIGHT DISTRIBUTION VERSUS CONVERSION PLOTS

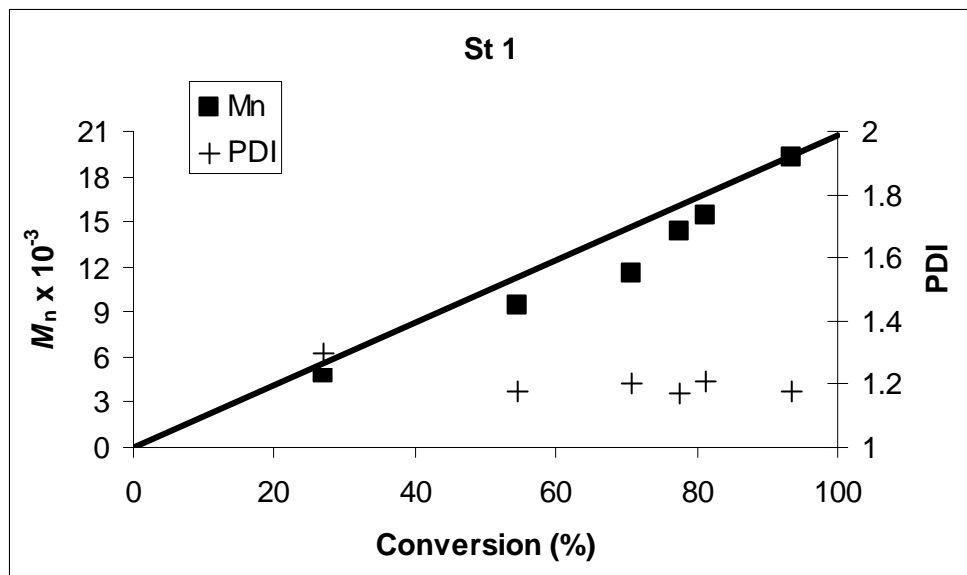


**Figure B.1.**  $M_n$  versus conversion plot of St by ATRP using EPEI at 110 °C.  $[St]_0/[EBrP]_0/[CuBr]_0/[EPEI]_0=200/1/1/0.30$   $[St]: 5.7 \text{ mol L}^{-1}$  in anisole.

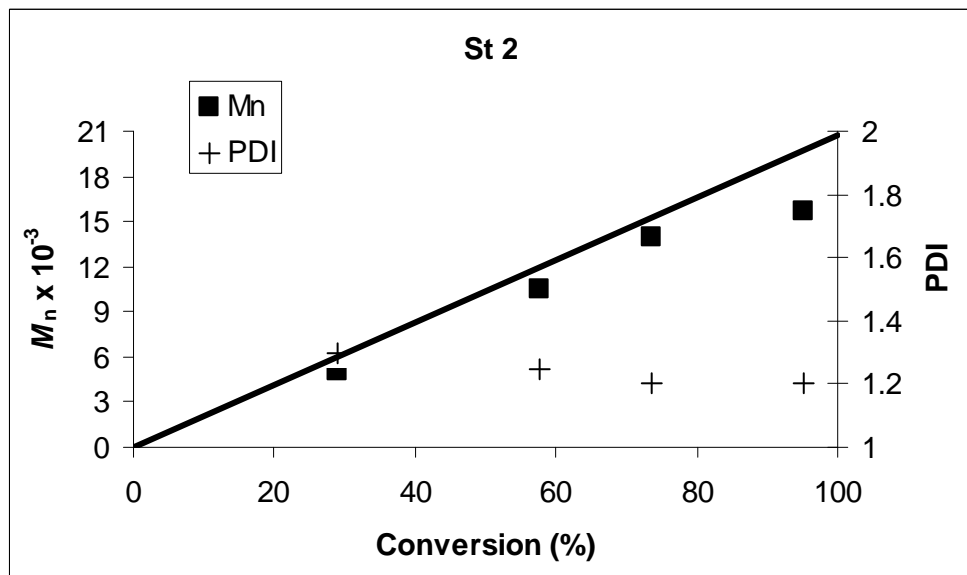


**Figure B.2.**  $M_n$  versus conversion plot of St by ATRP using EPEI at 110 °C.  $[St]_0/[EBrP]_0/[CuBr]_0/[EPEI]_0=200/1/1/0.45$   $[St]: 5.7 \text{ mol L}^{-1}$  in anisole

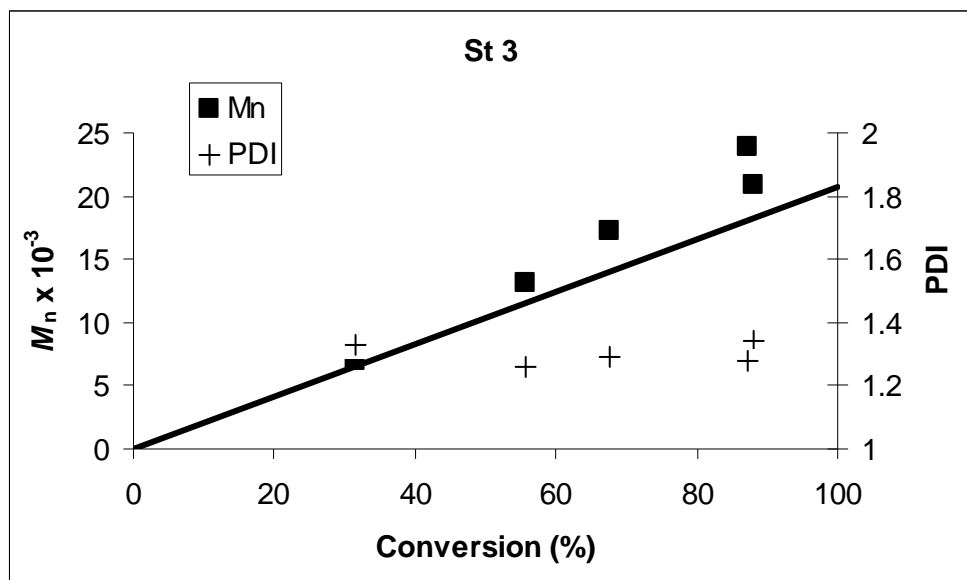


**Figure B.3.**  $M_n$  versus conversion plot of St by ATRP using EPEI at 110 °C.  
 $[St]_o/[EBrP]_o/[CuBr]_o/[EPEI]_o=200/1/1/0.60$  [St]: 5.7 mol L<sup>-1</sup> in anisole

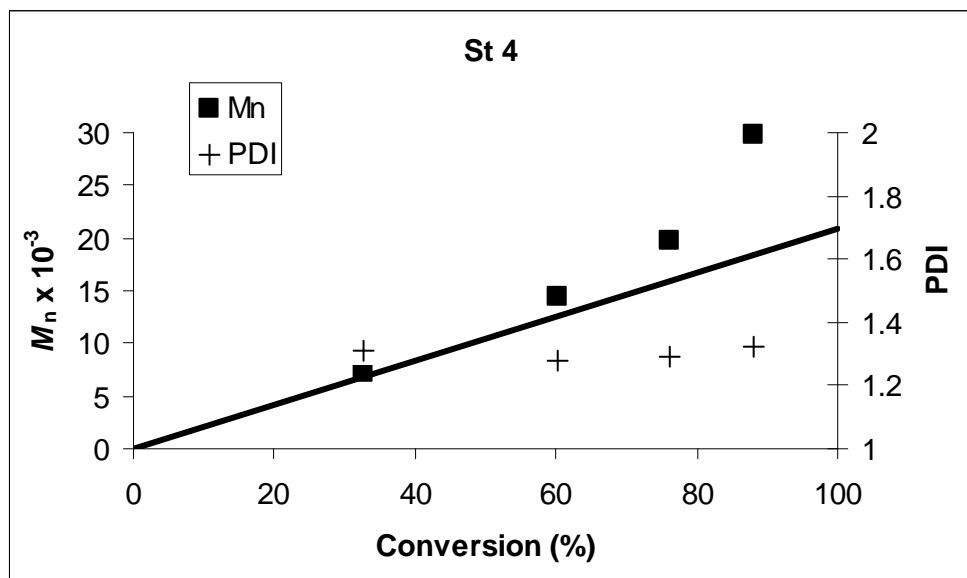


**Figure B.4.**  $M_n$  versus conversion plot of St by ATRP using EPEI at 110 °C.  
 $[St]_o/[EBrP]_o/[CuBr]_o/[EPEI]_o=200/1/1/0.75$  [St]: 5.7 mol L<sup>-1</sup> in anisole

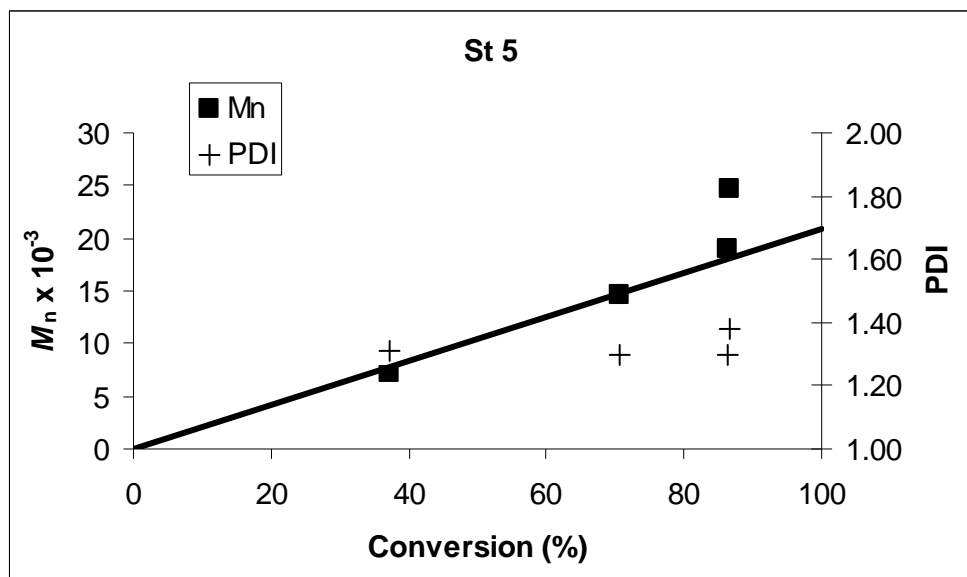


**Figure B.5.**  $M_n$  versus conversion plot of St by ATRP using EPEI at 110 °C.  
 $[St]_o/[EBrP]_o/[CuBr]_o/[EPEI]_o=200/1/1/1.00$   $[St]: 5.7 \text{ mol L}^{-1}$  in anisole

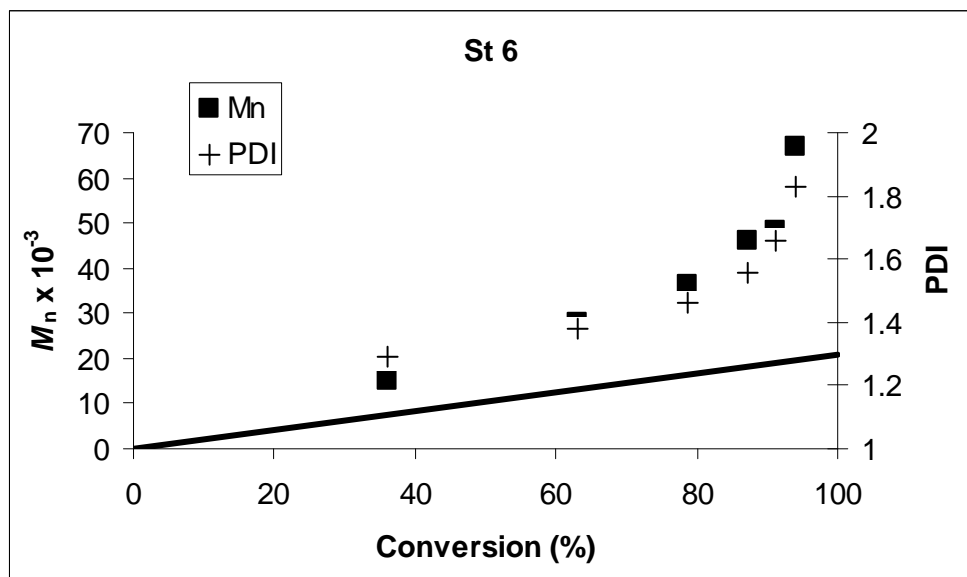


**Figure B.6.**  $M_n$  versus conversion plot of St by ATRP using EPEI at 110 °C.  
 $[St]_o/[EBrP]_o/[CuBr]_o/[EPEI]_o=200/1/1/1.25$   $[St]: 5.7 \text{ mol L}^{-1}$  in anisole

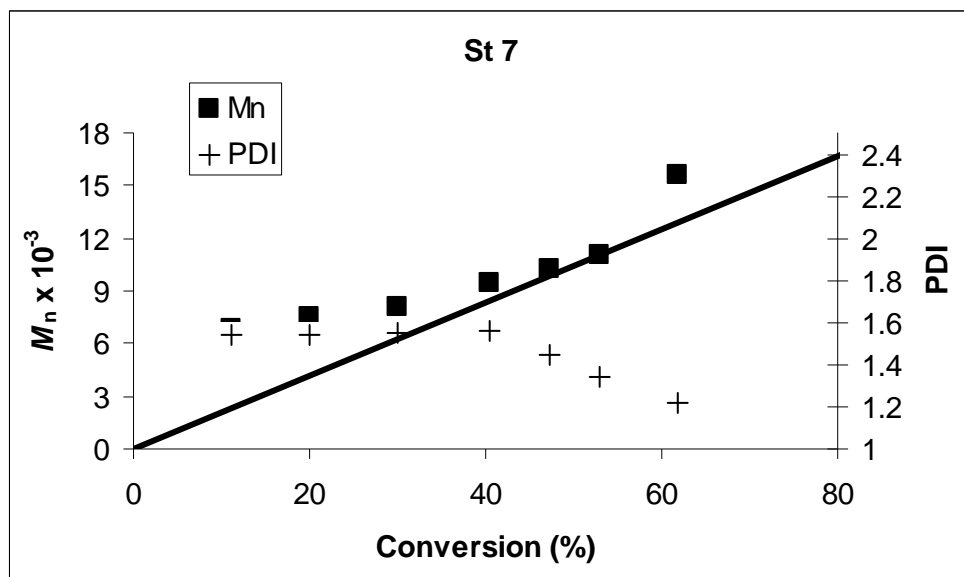


**Figure B.7.**  $M_n$  versus conversion plot of St by ATRP using BPEI at 110 °C.  
 $[St]_o/[EBrP]_o/[CuBr]_o/[EPEI]_o=200/1/1/0.15$   $[St]$ : 5.7 mol L<sup>-1</sup> in toluene

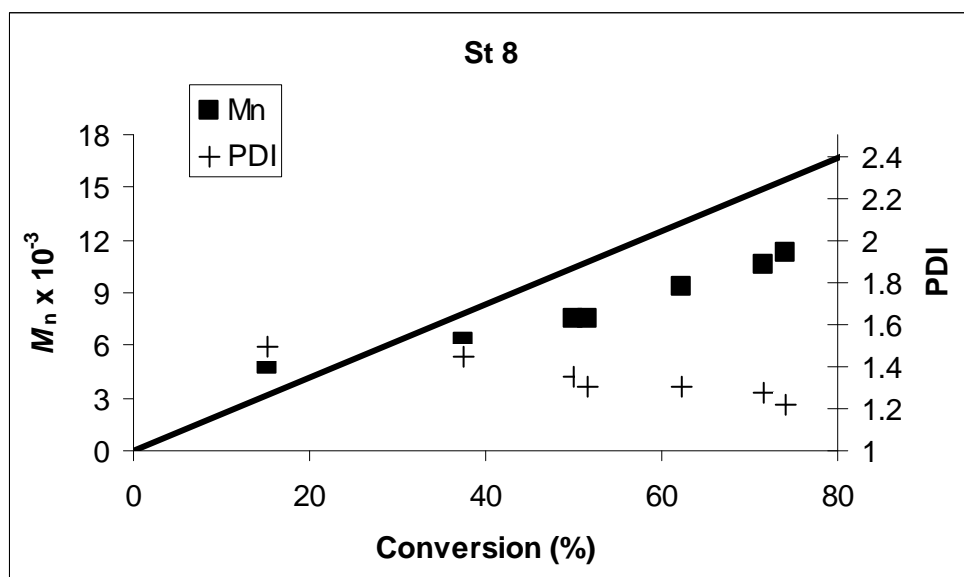


**Figure B.8.**  $M_n$  versus conversion plot of St by ATRP using BPEI at 110 °C.  
 $[St]_o/[EBrP]_o/[CuBr]_o/[EPEI]_o=200/1/1/0.30$   $[St]$ : 5.7 mol L<sup>-1</sup> in toluene

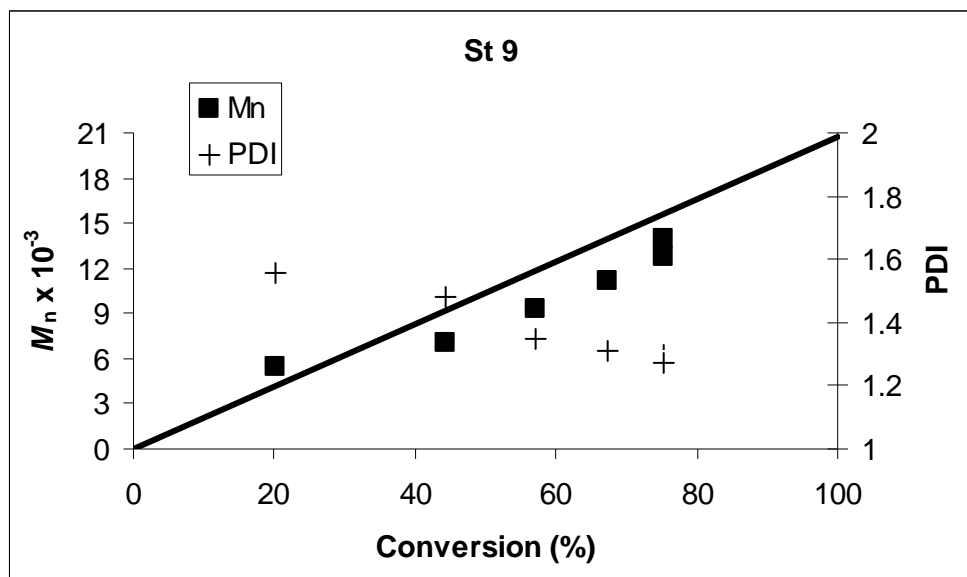


**Figure B.9.**  $M_n$  versus conversion plot of St by ATRP using BPEI at 110 °C.  $[St]_o/[EBrP]_o/[CuBr]_o/[EPEI]_o=200/1/1/0.45$   $[St]: 5.7 \text{ mol L}^{-1}$  in toluene

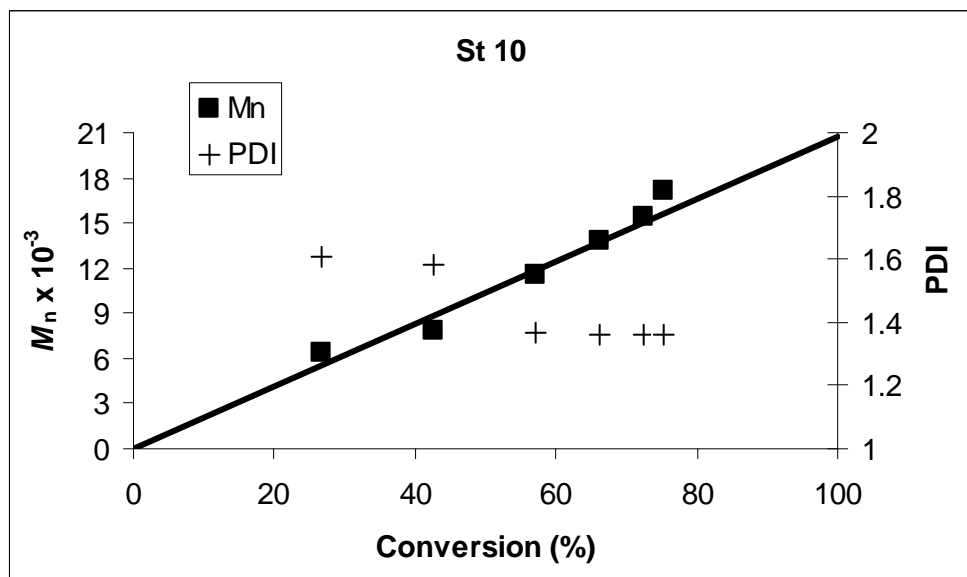


**Figure B.10.**  $M_n$  versus conversion plot of St by ATRP using BPEI at 110 °C.  $[St]_o/[EBrP]_o/[CuBr]_o/[EPEI]_o=200/1/1/0.60$   $[St]: 5.7 \text{ mol L}^{-1}$  in toluene

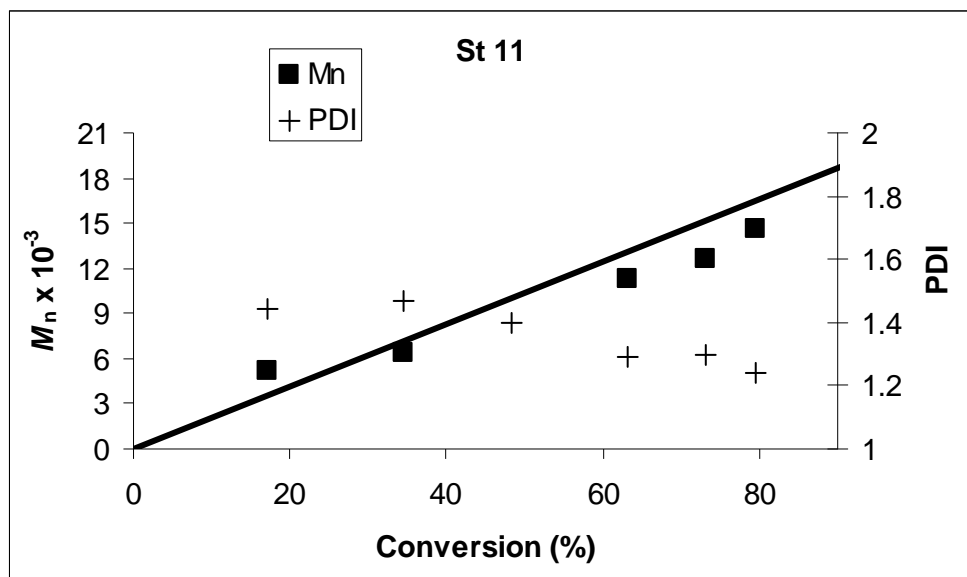


**Figure B.11.**  $M_n$  versus conversion plot of St by ATRP using BPEI at 110 °C.  
 $[St]_o/[EBrP]_o/[CuBr]_o/[EPEI]_o=200/1/1/0.75$   $[St]: 5.7 \text{ mol L}^{-1}$  in toluene

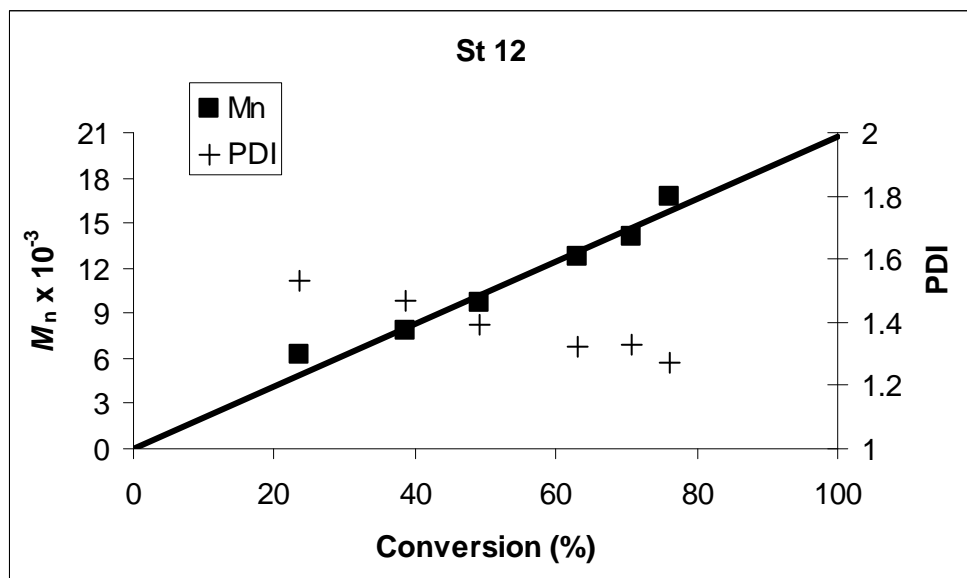


**Figure B.12.**  $M_n$  versus conversion plot of St by ATRP using BPEI at 110 °C.  
 $[St]_o/[EBrP]_o/[CuBr]_o/[EPEI]_o=200/1/1/1.00$   $[St]: 5.7 \text{ mol L}^{-1}$  in toluene

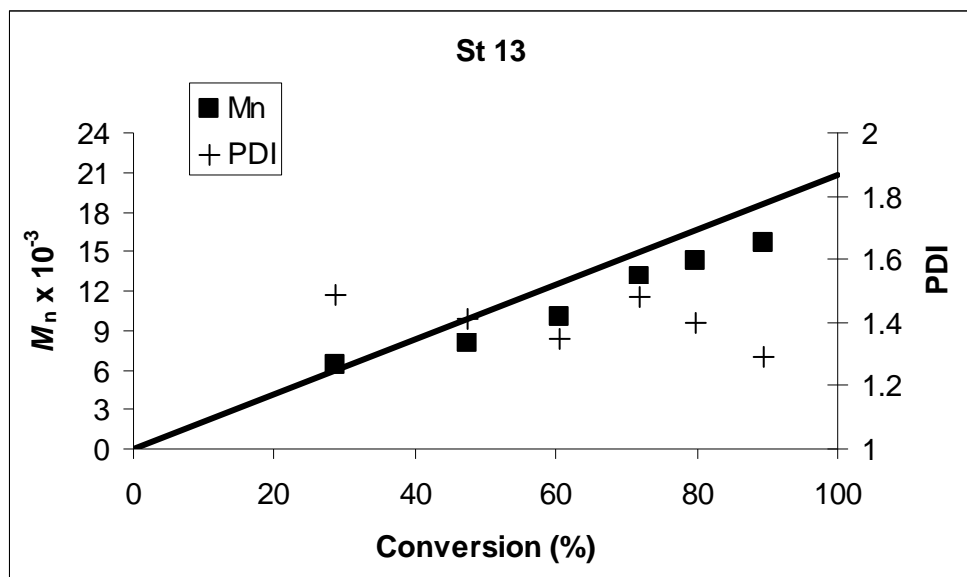


**Figure B.13.**  $M_n$  versus conversion plot of St by ATRP using BPEI at 110 °C.  
 $[St]_o/[EBrP]_o/[CuBr]_o/[EPEI]_o=200/1/1/1.25$  [St]: 5.7 mol L<sup>-1</sup> in toluene

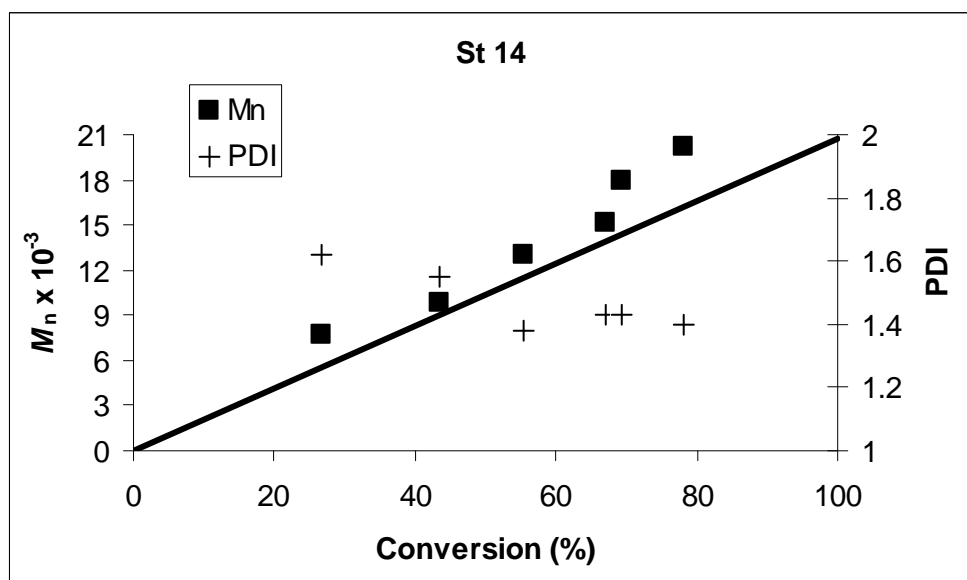


**Figure B.14.**  $M_n$  versus conversion plot of St by ATRP using BPEI at 110 °C.  
 $[St]_o/[EBrP]_o/[CuBr]_o/[EPEI]_o=200/1/1/2.00$  [St]: 5.7 mol L<sup>-1</sup> in toluene

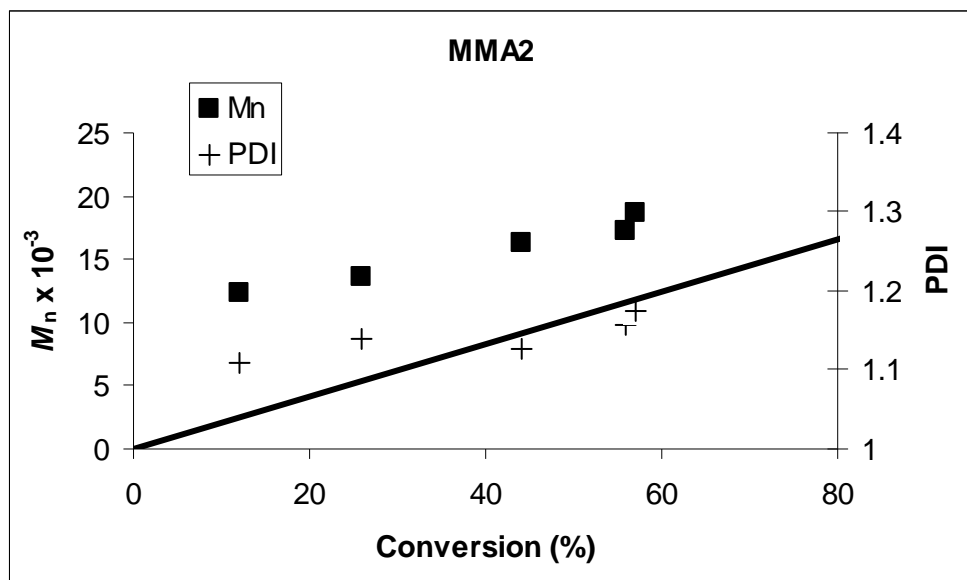


**Figure B.15.**  $M_n$  versus conversion plot of MMA by ATRP using BPEI at 110 °C.  $[MMA]_0/[EBrIB]_0/[CuBr]_0/[BPEI]_0=200/1/1/0.30$   $[MMA]: 4.6 \text{ mol L}^{-1}$  in anisole.

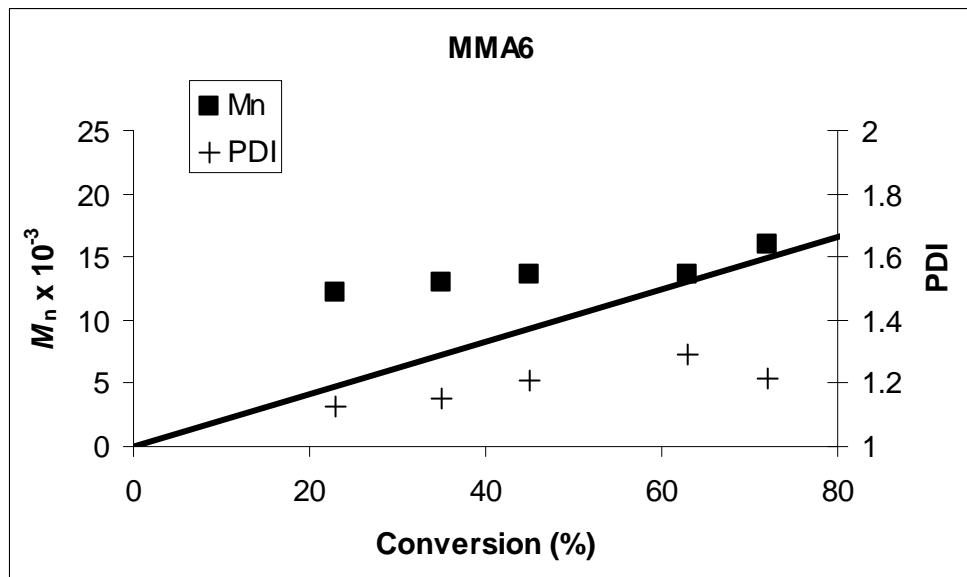


**Figure B.16.**  $M_n$  versus conversion plot of MMA by ATRP using BPEI at 110 °C.  $[MMA]_0/[EBrIB]_0/[CuBr]_0/[BPEI]_0=200/1/1/1.00$   $[MMA]: 4.6 \text{ mol L}^{-1}$  in anisole.

## APPENDIX C.

### GPC TRACES

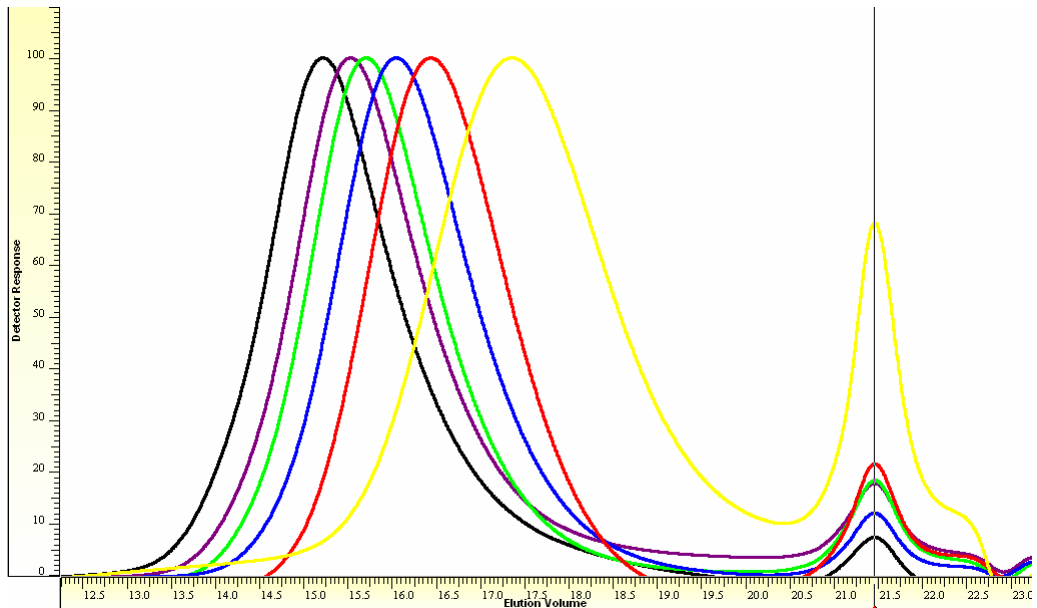


**Figure C.1.** GPC traces of St by ATRP using EPEI at 110 °C. [St]: 5.7 mol L<sup>-1</sup> in anisole [St]<sub>0</sub>/[EBrP]<sub>0</sub>/[CuBr]<sub>0</sub>/[EPEI]<sub>0</sub>=200/1/1/0.30

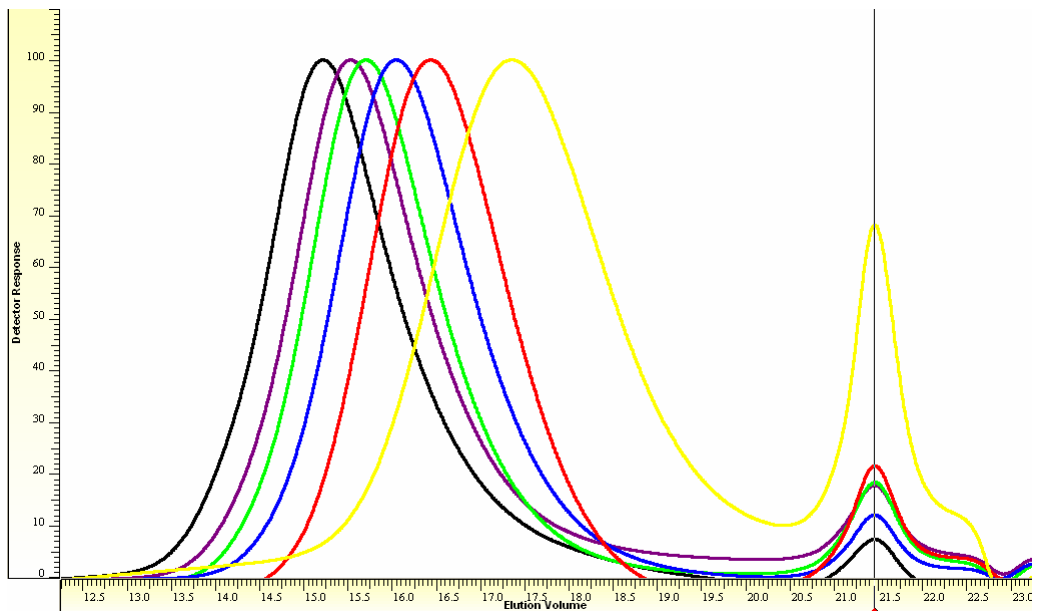


**Figure C.2.** GPC traces of St by ATRP using EPEI at 110 °C. [St]: 5.7 mol L<sup>-1</sup> in anisole [St]<sub>0</sub>/[EBrP]<sub>0</sub>/[CuBr]<sub>0</sub>/[EPEI]<sub>0</sub>=200/1/1/0.45

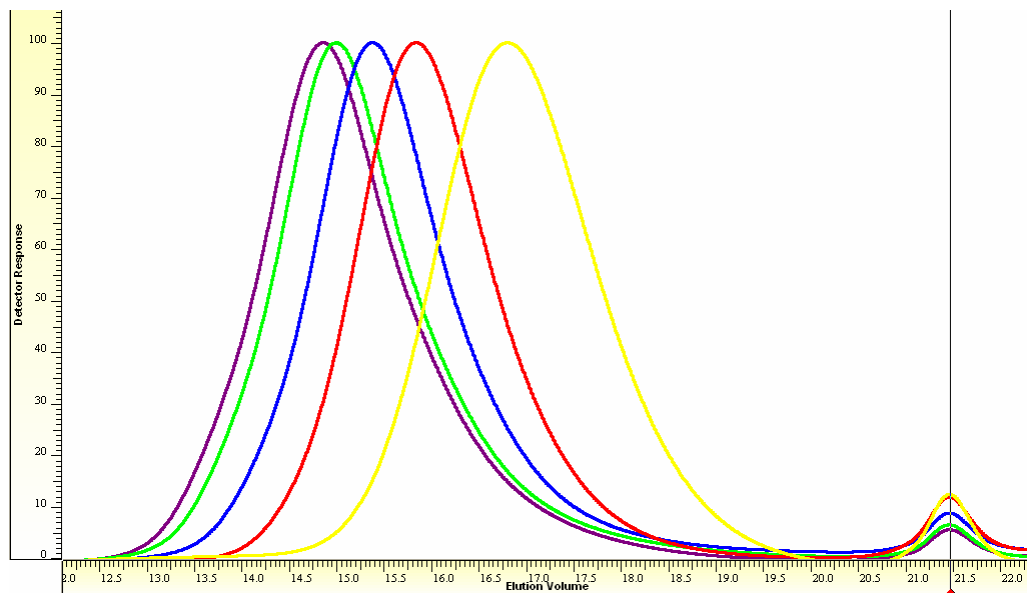


**Figure C.3.** GPC traces of St by ATRP using EPEI at 110 °C. [St]: 5.7 mol L<sup>-1</sup> in anisole [St]<sub>0</sub>/[EBrP]<sub>0</sub>/[CuBr]<sub>0</sub>/[EPEI]<sub>0</sub>=200/1/1/0.60

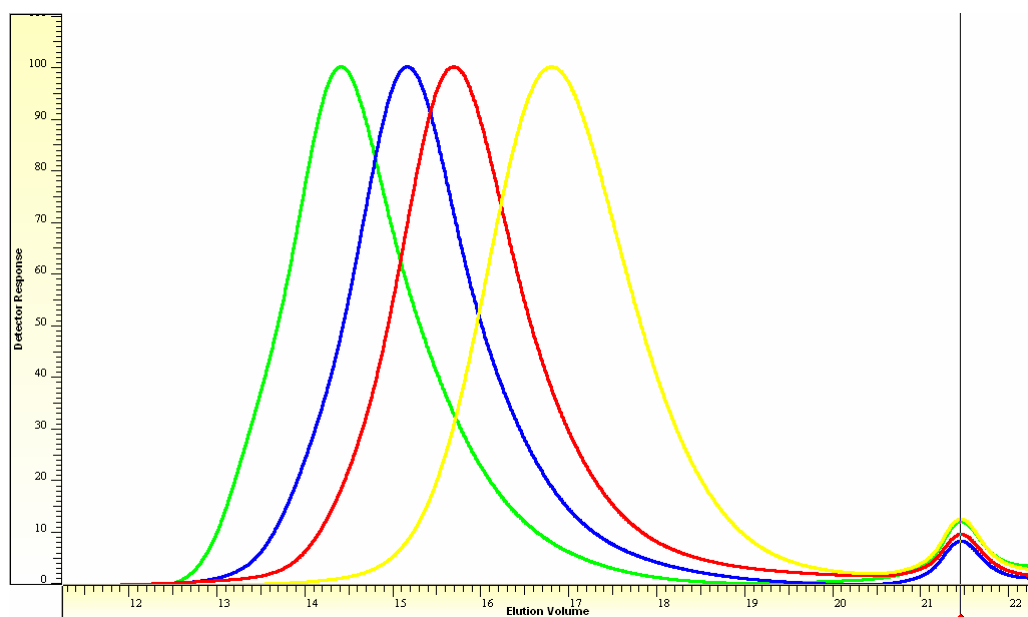


**Figure C.4.** GPC traces of St by ATRP using EPEI at 110 °C. [St]: 5.7 mol L<sup>-1</sup> in anisole [St]<sub>0</sub>/[EBrP]<sub>0</sub>/[CuBr]<sub>0</sub>/[EPEI]<sub>0</sub>=200/1/1/0.75

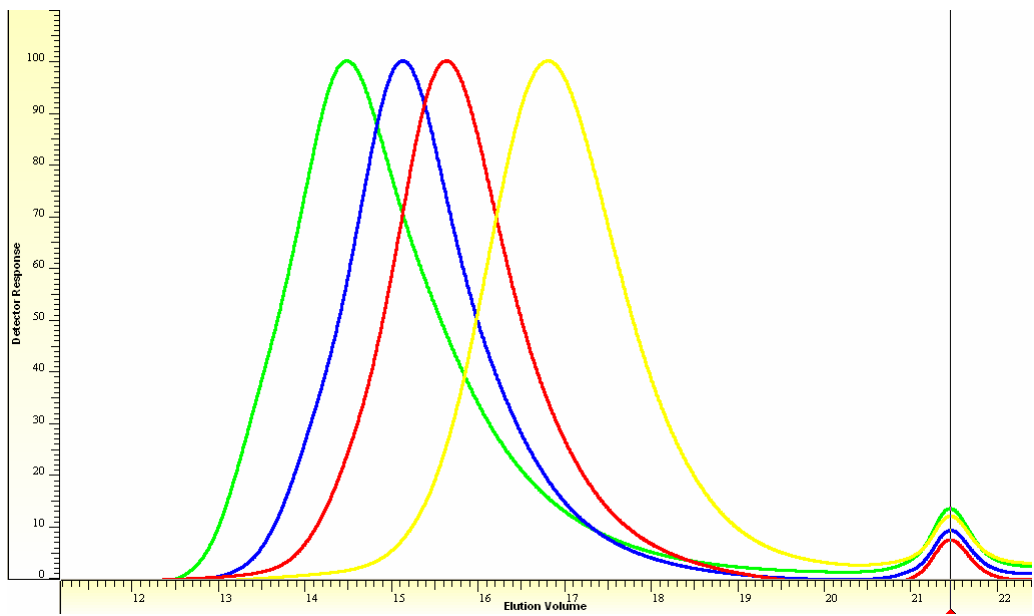


**Figure C.5.** GPC traces of St by ATRP using EPEI at 110 °C. [St]: 5.7 mol L<sup>-1</sup> in anisole [St]<sub>0</sub>/[EBrP]<sub>0</sub>/[CuBr]<sub>0</sub>/[EPEI]<sub>0</sub>=200/1/1/1.00

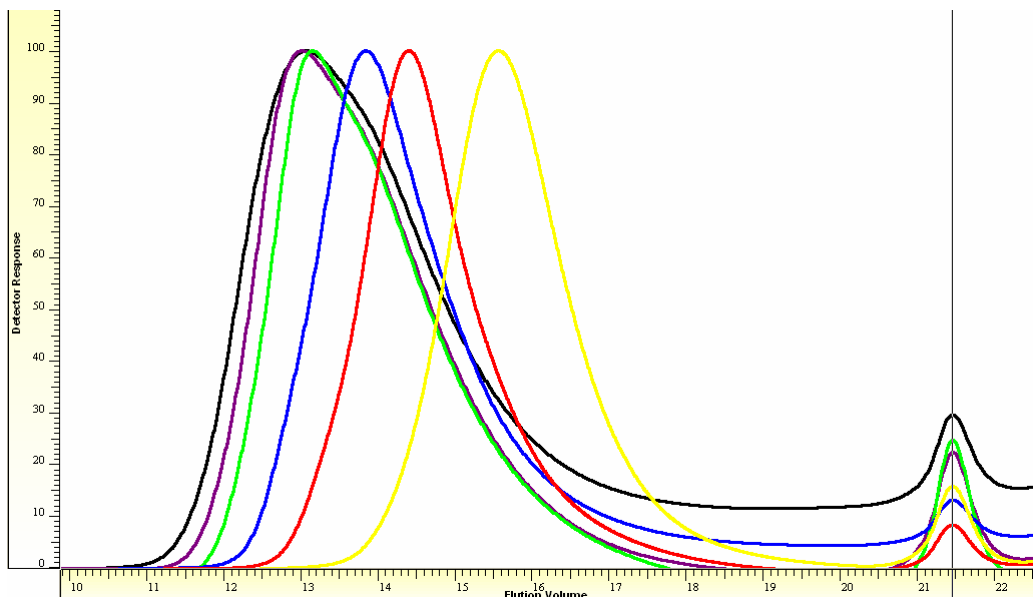


**Figure C.6.** GPC traces of St by ATRP using EPEI at 110 °C. [St]: 5.7 mol L<sup>-1</sup> in anisole [St]<sub>0</sub>/[EBrP]<sub>0</sub>/[CuBr]<sub>0</sub>/[EPEI]<sub>0</sub>=200/1/1/1.25

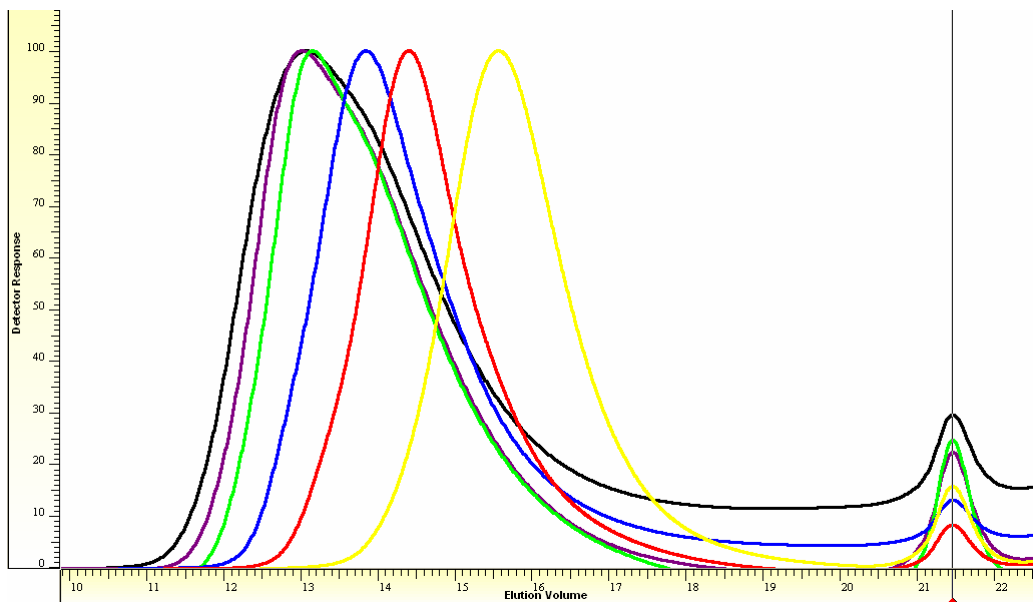


**Figure C.7.** GPC traces of St by ATRP using BPEI at 110 °C. [St]: 5.7 mol L<sup>-1</sup> in toluene [St]<sub>0</sub>/[EBrP]<sub>0</sub>/[CuBr]<sub>0</sub>/[BPEI]<sub>0</sub>=200/1/1/0.15

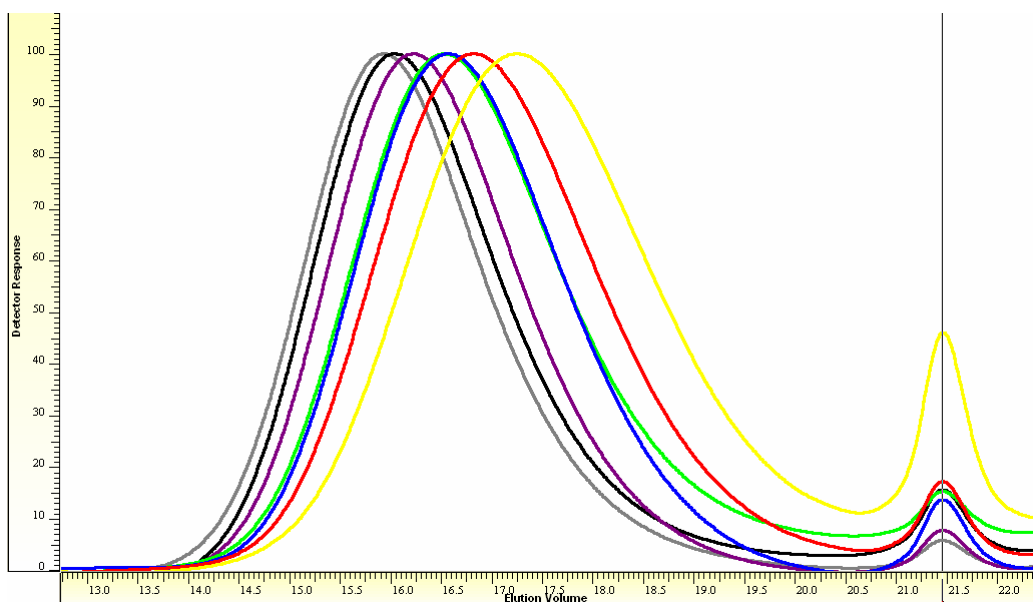


**Figure C.8.** GPC traces of St by ATRP using BPEI at 110 °C. [St]: 5.7 mol L<sup>-1</sup> in toluene [St]<sub>0</sub>/[EBrP]<sub>0</sub>/[CuBr]<sub>0</sub>/[BPEI]<sub>0</sub>=200/1/1/0.30

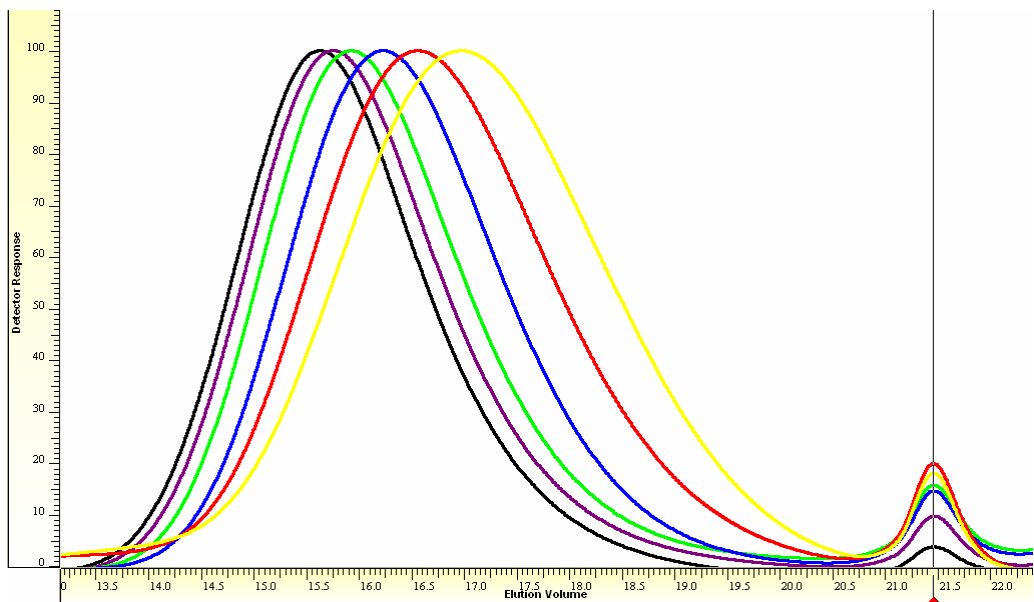


**Figure C.9.** GPC traces of St by ATRP using BPEI at 110 °C. [St]: 5.7 mol L<sup>-1</sup> in toluene [St]<sub>0</sub>/[EBrP]<sub>0</sub>/[CuBr]<sub>0</sub>/[BPEI]<sub>0</sub>=200/1/1/0.45

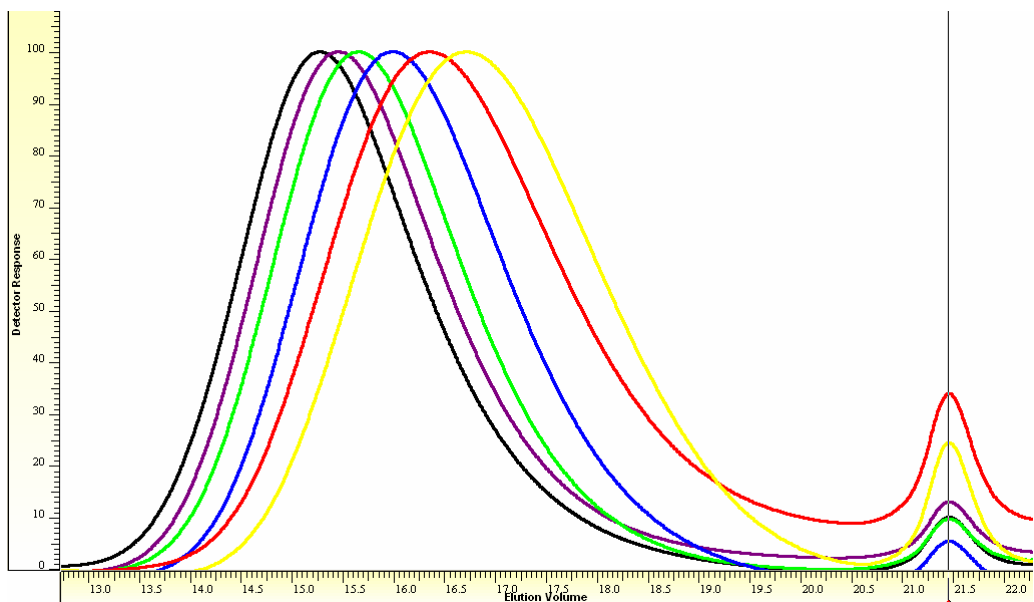


**Figure C.10.** GPC traces of St by ATRP using BPEI at 110 °C. [St]: 5.7 mol L<sup>-1</sup> in toluene [St]<sub>0</sub>/[EBrP]<sub>0</sub>/[CuBr]<sub>0</sub>/[BPEI]<sub>0</sub>=200/1/1/0.60

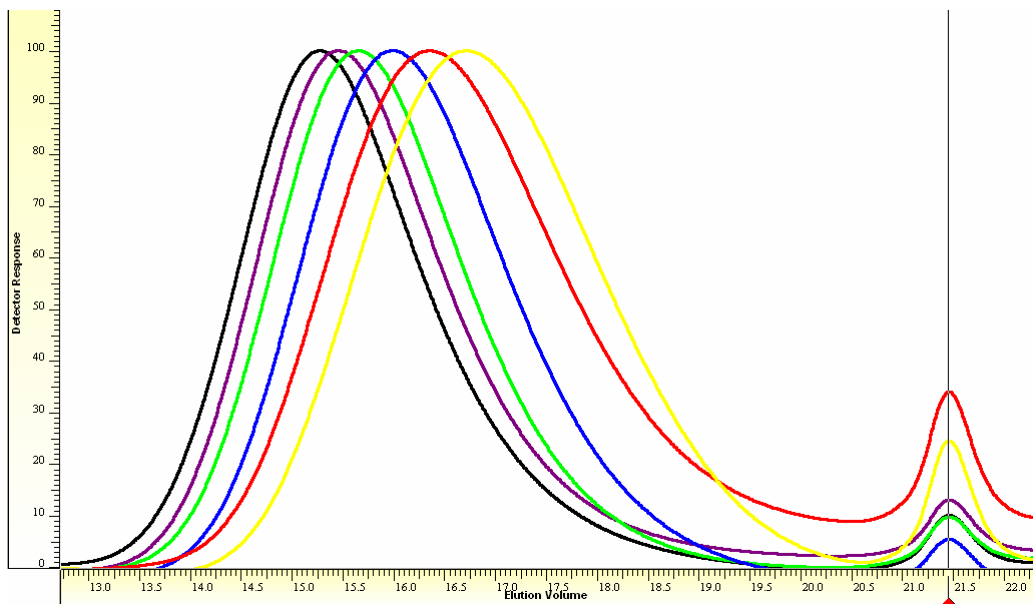


**Figure C.11.** GPC traces of St by ATRP using BPEI at 110 °C. [St]: 5.7 mol L<sup>-1</sup> in toluene [St]<sub>0</sub>/[EBrP]<sub>0</sub>/[CuBr]<sub>0</sub>/[BPEI]<sub>0</sub>=200/1/1/0.75

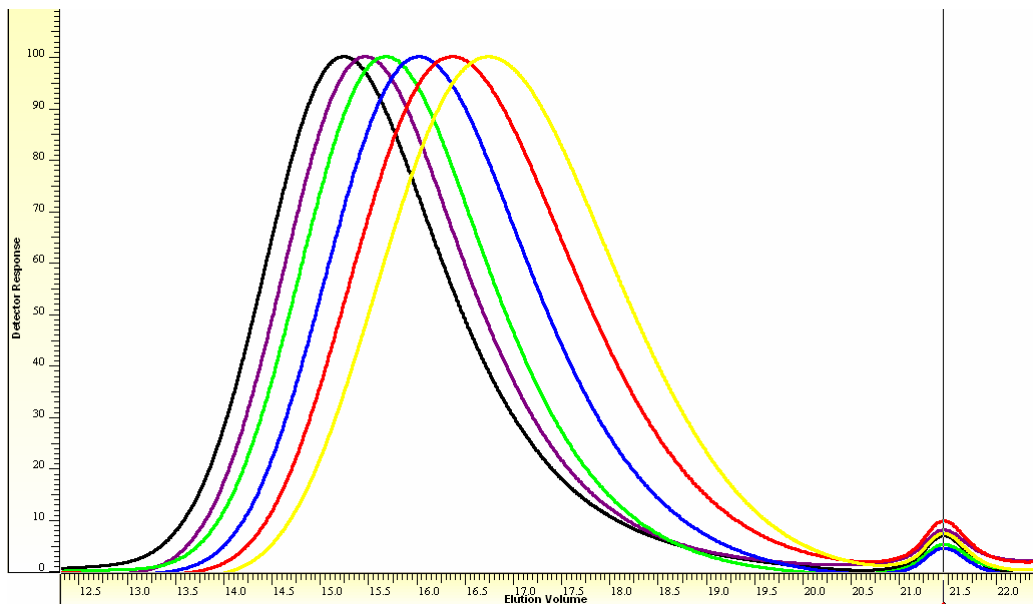


**Figure C.12.** GPC traces of St by ATRP using BPEI at 110 °C. [St]: 5.7 mol L<sup>-1</sup> in toluene [St]<sub>0</sub>/[EBrP]<sub>0</sub>/[CuBr]<sub>0</sub>/[BPEI]<sub>0</sub>=200/1/1/1.00

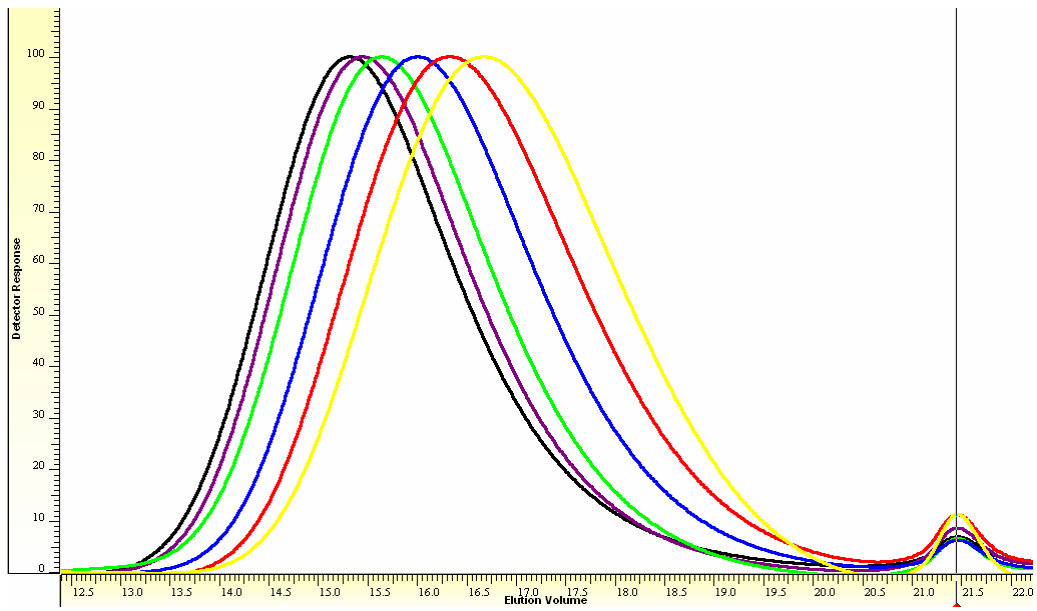


**Figure C.13.** GPC traces of St by ATRP using BPEI at 110 °C. [St]: 5.7 mol L<sup>-1</sup> in toluene [St]<sub>0</sub>/[EBrP]<sub>0</sub>/[CuBr]<sub>0</sub>/[BPEI]<sub>0</sub>=200/1/1/1.25

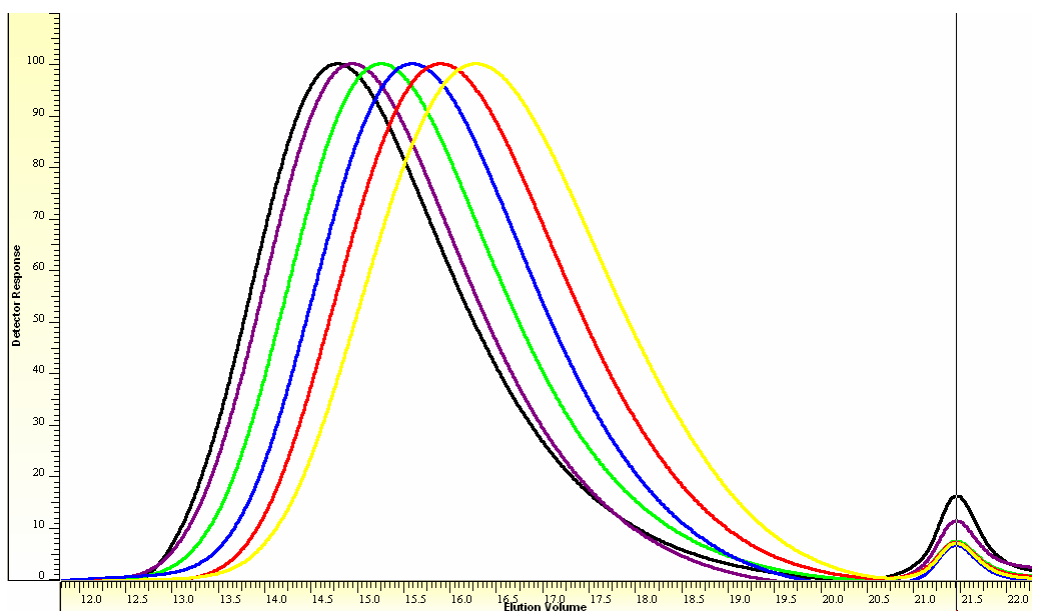


**Figure C.14.** GPC traces of St by ATRP using BPEI at 110 °C. [St]: 5.7 mol L<sup>-1</sup> in toluene [St]<sub>0</sub>/[EBrP]<sub>0</sub>/[CuBr]<sub>0</sub>/[BPEI]<sub>0</sub>=200/1/1/2.00

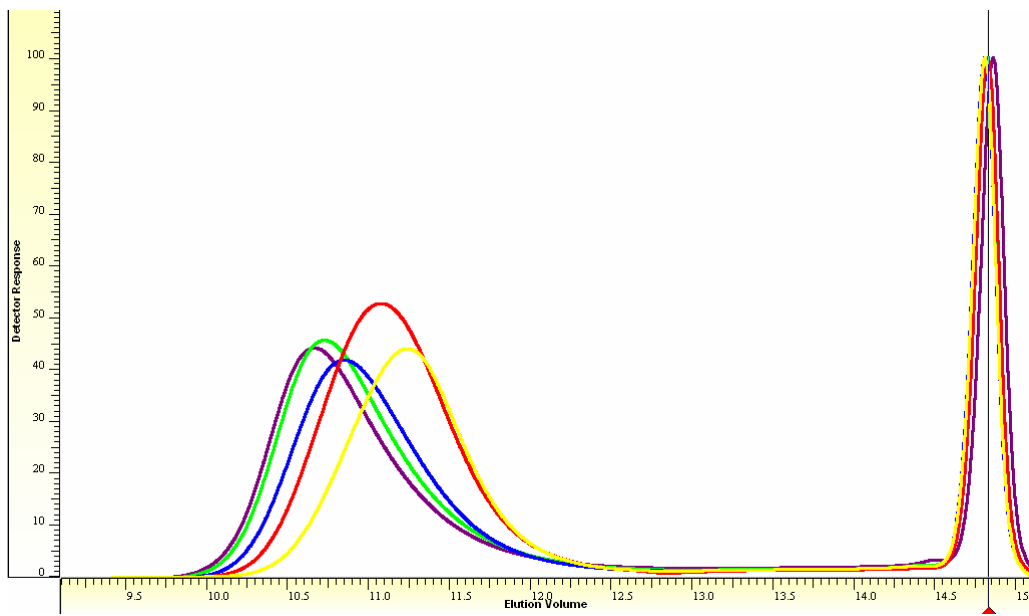


**Figure C.15.** GPC traces of MMA by ATRP using BPEI at 80 °C. [MMA]: 4.60 mol L<sup>-1</sup> in anisole [MMA]<sub>0</sub>/[EBrIB]<sub>0</sub>/[CuBr]<sub>0</sub>/[BPEI]<sub>0</sub>=200/1/1 /0.30

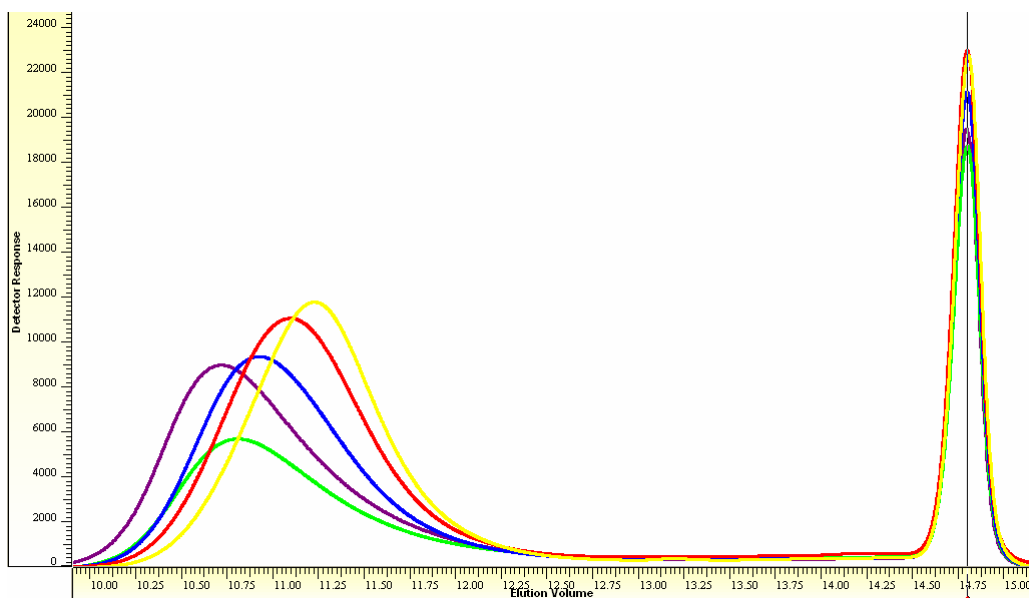


**Figure C.16.** GPC traces of MMA by ATRP using BPEI at 80 °C. [MMA]:4.60 mol L<sup>-1</sup> in anisole [MMA]<sub>0</sub>/[EBrIB]<sub>0</sub>/[CuBr]<sub>0</sub>/[BPEI]<sub>0</sub>=200/1/1 /1.00

## **AUTOBIOGRAPHY**

He was born in 1983 in Istanbul. In 2001, he was graduated from Saint Michel French High School and attended to the Chemistry Department of Istanbul Technical University in same year.

After graduating from Istanbul Technical University in 2006, he was registered as a M.Sc. student to Istanbul Technical University, Polymer Science and Technology Department of the Institute of Science and Technology in 2006.

In 2006-2007 he started to work as a research assistant in Prof. M. H. Acar's, surface active and thermoplastic block copolymer synthesis project associated with Henkel KGaA Germany, in polymer laboratory of Istanbul Technical University.